U.PORTO

DOUTORAMENTO EM CIÊNCIAS BIOMÉDICAS

Modulation of drug efflux at the blood-brain barrier through targeted siRNA delivery *via* nanoparticles

Maria João Bidarra Tavares Gomes

D
2017

U.PORTO

Maria João Bidarra Tavares Gomes
Modulation of drug efflux at the blood-brain barrier through targeted siRNA delivery ***via*** nanoparticles

Modulation of drug efflux at the blood-brain barrier through targeted siRNA delivery *via* nanoparticles
Maria João Bidarra Tavares Gomes

INSTITUTO DE CIÊNCIAS BIOMÉDICAS ABEL SALAZAR

D.ICBAS **2017**

Maria João Bidarra Tavares Gomes

Modulation of drug efflux at the blood-brain barrier through targeted siRNA delivery *via* nanoparticles

Tese de Candidatura ao grau de Doutor em Ciências Biomédicas submetida ao Instituto de Ciências Biomédicas Abel Salazar da Universidade do Porto

Orientador:
Doutor Bruno Filipe Carmelino Cardoso Sarmento
Categoria – Investigador Auxiliar/Professor Auxiliar
Afiliação – i3S - Instituto de Investigação e Inovação em Saúde, INEB - Instituto de Engenharia Biomédica, Universidade do Porto & IUCS - Instituto Universitário de Ciências da Saúde

Co-orientadora:
Doutora Susana Amélia Marques Martins
Categoria – Pós-doutorada
Afiliação – Departamento de Física, Química e Farmácia da Universidade do Sul da Dinamarca

Tutor:
Doutor Pedro Lopes Granja
Categoria – Investigador Principal/Professor Associado
Afiliação – i3S - Instituto de Investigação e Inovação em Saúde, INEB - Instituto de Engenharia Biomédica & ICBAS - Instituto de Ciências Biomédicas Abel Salazar, Universidade do Porto

A todos os que torcem por mim.

The work presented in this thesis was developed at:

Biomaterials for Multistage Drug & Cell Delivery Group
i3S - Instituto de Investigação e Inovação em Saúde and
INEB - Instituto de Engenharia Biomédica
Universidade do Porto, Porto, Portugal
Rua Alfredo Allen, 208
4200-135 Porto, Portugal
www.i3s.up.pt | www.ineb.up.pt

and

Department of Physics, Chemistry and Pharmacy
University of Southern Denmark, Odense, Denmark
Campusvej 55, DK-5230
www.sdu.dk

Financial support

Maria João Gomes was supported by a national PhD grant (SFRH/BD/90404/2012) from Fundação para a Ciência e Tecnologia (FCT).

This work was financed by FEDER - Fundo Europeu de Desenvolvimento Regional funds through the COMPETE 2020 - Operational Programme for Competitiveness and Internationalisation (POCI), Portugal 2020, and by Portuguese funds through FCT/Ministério da Ciência, Tecnologia e Inovação in the framework of the project "Institute for Research and Innovation in Health Sciences" (POCI-01-0145-FEDER-007274).

PUBLICATIONS

Ao abrigo do disposto do nº 2, alínea a) do artigo 31º do Decreto-Lei n.º 115/2013 de 7 de Agosto, fazem parte integrante desta tese de doutoramento os seguintes trabalhos já publicados ou submetidos para publicação:

- **Gomes, M.J.**, Kennedy, P.J., Martins, S. and Sarmento, B. 2017. Delivery of siRNA silencing P-glycoprotein in peptide-functionalized nanoparticles causes efflux modulation at a human blood-brain barrier model. Submitted.

- **Gomes, M.J.**, Fernandes, C., Martins, S., Borges, F. and Sarmento, B. 2016. Tailoring lipid and polymeric nanoparticles as siRNA carriers towards the blood-brain barrier - from targeting to safe administration. J Neuroimmune Pharmacol., in press doi: 10.1007/s11481-016-9685-6.

- **Gomes, M.J.**, Dreier, J., Brewer, J., Martins, S., Brandl, M. and Sarmento, B. 2016. A new approach for a blood-brain barrier model based on phospholipid vesicles: membrane development and siRNA-loaded nanoparticles permeability. J Membrane Sci. 503: 8-15.

- **Gomes, M.J.**, Martins, S. and Sarmento, B. 2015. siRNA as a tool to improve the treatment of brain diseases: mechanism, targets and delivery. Ageing Res Rev. 21: 43-54.

- **Gomes, M.J.**, Mendes, B., Martins, S. and Sarmento, B. 2016. Cell-based *in vitro* models for studying blood-brain barrier (BBB) permeability. In Concepts and models for drug permeability studies: cell and tissue based *in vitro* culture models, Bruno Sarmento, ed. (Elsevier). ISBN:978-0-08-100094-6, Pages 169-188.

- **Gomes, M.J.**, Mendes, B., Martins, S. and Sarmento, B. 2016. Nanoparticle functionalization for brain targeting drug delivery and diagnostic. In Handbook of nanoparticles: synthesis, functionalization and surface treatment, Mahmood Aliofkhazraei, ed. (Springer). ISBN:978-3-319-15337-7, Pages 941-959.

ACKNOWLEDGEMENTS

From the beginning of this adventure I heard that "science is to be discussed in English". However, what is deep inside my heart is undoubtedly Portuguese. Thus, the following words are written in my mother tongue, except on necessary occasions, depending on whom they are addressed to.

É com alívio, uma lágrima escondida, e de coração grande, mas apertado, que recordo cada um de vocês.

Antes de todos, as palavras irão sempre para o professor Bruno Sarmento, o meu orientador. Por me ter inserido no seu grupo de investigação, ter puxado por mim, e me ter feito crescer cientificamente. Admiro-o muito pela sua persistência e trabalho incansáveis que felizmente têm gerado merecidos, inegáveis e invejados frutos. Obrigada por me compreender e apoiar em todas as minhas decisões, pessoais e profissionais. Por me ajudar a realizar sonhos e ambições, mesmo quando isso implica ter de me afastar. Por me aconselhar e defender, a mim e aos meus interesses. Por me ter apadrinhado, cá dentro e lá fora, um obrigado não chega, mas tenta resumir.

Agradeço também à Susana Martins, a minha co-orientadora, a ponte que fez a ligação entre este ciclo e o anterior. Por me ter dado a possibilidade de ir para outro grupo de investigação, por me ter recebido tão bem e me ter feito sentir em casa, o meu obrigado. Obrigada também por todas as discussões científicas e por todos os momentos de descontração vividos longe dos meus.

Ao professor Pedro Granja agradeço por me ter chamado e aberto as portas do INEB, sem esta deixa, muito provavelmente, o desfecho desta história seria outro. Obrigada pela oportunidade e por todas as palavras encorajantes.

I would like to thank Dr. Martin Brandl, from the University of Southern Denmark, for the opportunity to go to a different lab in a different country. I would like to thank him for the warm welcoming in his lab and his group. It was a great experience from which I learned a lot.

I would like to truly acknowledge Dr. Martin Brandl's research group, present and former elements, for receiving me so well, for sharing knowledge, for their fellowship and all

the help. I would like to emphasize Camilla Tullesen, Hanady Ajine, Sara Munk Hedegård and Ulla Trettenes for making me feel at home.

I would also like to thank Jes Dreier and Dr. Jonathan Brewer for the help and support in some experiments.

À professora Salette Reis agradeço a minha entrada no mundo científico e das nanopartículas, todo o seu carinho e palavras reconfortantes.

Não posso esquecer pessoas chave no meu crescimento académico que agora conclui mais uma etapa. Professores que me transmitiram conhecimentos de forma leve, fácil e motivante, que me incutiram hábitos e gostos que se revelam hoje grande parte de mim. Obrigada aos professores António Rangel, Idalina Amorim, Idalina Santos e Nuno Oliveira.

Obrigada ao Carlos Fernandes e à professora Fernanda Borges, da Faculdade de Ciências da Universidade do Porto, pela disponibilidade e ajuda nalgumas experiências necessárias ao desenvolvimento deste trabalho.

À Ana Isabel Oliveira, da Escola Superior de Saúde do Politécnico do Porto, para além de agradecer toda a disponibilidade, o apoio e a ajuda, realço também a animação contagiante.

Obrigada aos meus colegas e amigos INEBianos, a todos, sem excepção, por todos os pequenos grandes pormenores do dia-a-dia, pelas ajudas em tudo, desde uma apresentação ou uma experiência, até um login num computador ou uma gargalhada ao almoço.

Em particular aos colegas e amigos do grupo Biocarrier, obrigada pela proximidade, por todas as discussões científicas, pelos eventos de grupo (quase) eternamente adiados, pelas ajudas em todas as dúvidas e alíquotas. Um especial agradecimento à Ana Luísa Torres pelas cantorias, partilhas de câmara e boa disposição; ao Rúben Pereira pela amizade, compreensão e companhia fora de horas; e ao Tiago Santos pelo modo relax e descomplicado.

Sem esquecer o grupo criado não pela ciência mas pelo espaço que ela ocupa, agradeço com carinho à Cristina Martins e suas meninas.

Aos meus colegas e amigos da minha equipa de trabalho com quem partilhei orientador, obrigada por todos os conselhos e sugestões. Uma palavra especial para a Ana

Costa, o José das Neves, o Patrick Kennedy e o Pedro Fonte, por todas as vezes que me ajudaram, por todos os problemas existenciais resolvidos e por resolver, e por todas as discussões científicas com as quais aprendi. Por tudo isto e ainda pela companhia e devaneios fora de horas, à Rute Nunes e à sua "Francisca Janete".

Obrigada aos meus pequeninos: à Cláudia Martins, pela companhia durante as derradeiras experiências; ao João Pedro Martins, pelos momentos de riso e piadas sem piada; e à Patrícia Henriques, pela amizade e enorme doçura a todos os níveis.

Obrigada às minhas lufadas de ar fresco, Ana Filipa Lourenço, Bianca Lourenço e Francisca Araújo, por todos os abraços e desabafos, por todos os dias me fazerem ver o que de bom um doutoramento pode sempre trazer. À Ana Filipa Lourenço, pela animação, pelas palhaçadas, pelos cozinhados e pela amizade que se construiu sem darmos conta. À Bianca Lourenço, por ter estado presente desde o dia 1, pelas conversas no cantinho do *Shark*, por ser minha confidente e por genuinamente torcer por mim - o teu sucesso é o meu também. À Francisca Araújo, pela partilha de todos os momentos, por estar sempre por perto mesmo quando fisicamente não esteve, pelas maratonas de biotério, pelas memórias de amizade espalhadas pelo Porto, por Copenhaga, por Seattle e guardadas no coração.

Obrigada aos meus amigos de sempre e para sempre, Ana Lúcia Mota, Ana Sofia Alves, André Sarmento, Cláudia Ferreirinha, Mariana Cardoso, Nuno Braga e Sara Santos, por todos os minutinhos em que houve tempo para partilhar a vida, por todas as sobremesas, por todos os aniversários, pelo ombro amigo e o colo mimado, por todos os momentos em que me enchem o coração.

Obrigada à minha família, à minha base de tudo.

Ao meu pai, Vítor Gomes, por me ter possibilitado chegar onde cheguei da forma como cheguei.

À minha prima, Teresa Tavares, por me motivar sem me fazer esquecer do que é mais importante.

À minha avó, Maria Aldegundes Bidarra, por todo o carinho e preocupação, por achar que tenho o mundo aos meus pés, por se certificar que eu já comi, estou a comer, e vou comer em breve. Ao meu avô, Urbano Tavares, por todo o mimo, mesmo que ausente há tanto tempo, e porque sei que estaria a delirar com este meu momento que é dele também. Aos dois, por terem feito crescer a mãe maravilhosa que tenho.

ACKNOWLEDGEMENTS

À minha irmã, Ana Gomes, a pequenina da mana, por todo o apoio (a mim e aos meus), por todas as tentativas nem sempre bem-sucedidas de perceber o que faço e os meus horários, por mesmo quando não foram bem-sucedidas continuar a estar lá. Por todas as brincadeiras e momentos leves, por dividir tristezas e multiplicar alegrias. Por acreditar em mim e me dar um valor enorme.

À minha querida mãe, Idalina Tavares, por tudo, por estar sempre incondicionalmente presente e fazer de mim quem sou, por todo o amor, preocupação, cuidado e mimo, pelos braços sempre abertos, por ter aceitado e compreendido todas as distâncias e todas as ausências mesmo quando não traduzidas em quilómetros, por torcer por mim e me ajudar como pode e como não pode.

Ao Lourenço Castro, o meu Lourenço, por felizmente ter surgido no início disto tudo, por me ouvir e apoiar todos os dias, mesmo quando a distância física se fez sentir, por me incentivar e encorajar, pela partilha diária, por entender o que é e como tem de ser, por ainda assim me alertar quando ultrapasso os limites do razoável, por ser o meu maior amigo, por todas as ajudas de todas as formas, por todo o amor e compreensão nos (muitos) dias que pareciam impossíveis e inacabáveis - teria sido ainda mais difícil sem ti.

"Shoot for the moon. Even if you miss you'll land among the stars."

Les Brown

TABLE OF CONTENTS

ABSTRACT

Central nervous system (CNS) disorders are increasing over the last years as a consequence of a continuously aged population growth. Despite scientific advances, current therapeutics are often not thrived, which raises the increasing need for successful ways to reach CNS and achieve fruitful treatments. Additionally, the blood-brain barrier (BBB) is a unique membrane involving the brain, able to create such restrict CNS environment. Therefore, regarding CNS disorders incidence, failing therapeutics and BBB-related responsibility, the development of *in vitro* BBB models that mimic the physiologic BBB is a key factor for the study of newly developed drug/gene delivery systems, namely their interaction with BBB and permeability. Simultaneously, the production of effective platforms to circumvent BBB protective functions is leading this research field.

Drug efflux pumps at the BBB interface, as P-glycoprotein (P-gp), act as a noteworthy barrier that prevents the effectiveness of CNS disorders treatments, due to their ability to strongly limit the perfusion of compounds into the brain. Over the past decades, new approaches towards overcoming the BBB and its efflux transporters have been proposed, with limited degree of success. Small interfering RNA (siRNA) has been taking place in this topic as consequence of its targeting competence to specifically silence a protein of interest in a post-transcriptional way. Therefore, siRNA is used as a promising approach to selectively silent target proteins, improving the ability of drugs to reach the brain.

As important as the efficient protein silence is the transport of siRNA to its anatomical site of action. Nanotechnology and bioengineering joined to carry siRNA to the desired location, protecting the oligonucleotide circulation, directing its transport, and promoting intracellular delivery. Recent research on functionalization strategies offers distinct chemical tools to bind specific ligands to the surface of nanosystems, enabling them to obtain targeted functions. The selection of proper ligands is promoting the BBB surpassing likelihood of siRNA-loaded systems.

Gathering these previous ideas, the main aim of this thesis was to develop targeted and safe nanosystems, able to modulate the drug efflux at the BBB *via* siRNA against P-gp. The first part of this approach was focused on the development of a non-cellular based BBB model where permeability experiments could be performed in a simple and fast way, obtaining a high throughput screening tool, also used for *in vivo* permeability prediction. Phospholipid vesicle-based permeability assay (PVPA) method was used to produce such model, and then, to assess passive transcellular-like permeability of siRNA, free and loaded into nanoparticles. Both polymeric poly(lactic-co-glycolic acid) (PLGA) and lipid (solid lipid

nanoparticles, SLN) nanoparticles encapsulating siRNA were developed. Slightly negative (-10 mV) and monodisperse populations around 140 nm were obtained and their effect on siRNA permeability through the BBB-PVPA model was assessed. The permeability of siRNA has increased from 3.7×10^{-6} cm s^{-1} (free siRNA) to 5.5×10^{-6} cm s^{-1} and 6.9×10^{-6} cm s^{-1} after encapsulation into polymeric and lipid nanoparticles, respectively.

Then, the nanoparticulate-based systems were improved through the assessment of several materials and functionalization techniques. A PLGA-based polymer and a lipid, both amine terminated, were added to the previously formulation systems in order to improve their surface functionalization through carbodiimide and maleimide chemical approaches. Concurrently, the surfactant previously used, poly(vinyl alcohol), was replaced for Tween80, as this last one was easier to remove from nanoparticles surface, enhancing the functional groups availability and therefore exhibiting their mainly negative charge. Therefore, polymeric PLGA nanoparticles presented mean size around 115 nm, negatively charged surface (-30 mV) and 50% of siRNA association efficiency, while SLN, also negatively charged (up to -21 mV), presented 150 nm of mean size and association efficiency up to 52%. The release profile of siRNA from nanoparticles was sustained, reaching around 60% of released siRNA after 24h in physiological conditions. As well, the safety of nanoparticles was demonstrated assessing the metabolic activity of brain endothelial cells, found to be generally above 80%, up to 24h of incubation. To enhance transcellular permeability, nanoparticles were functionalized on the surface with a peptide-binding transferrin receptor (TfR), in a site-oriented manner, obtaining mean sizes between 321 and 506 nm and surface charge within the range -10 to -40 mV. Such modification was confirmed by ^{1}H nuclear magnetic resonance (^{1}H NMR), and their targeting ability against human brain endothelial cells was demonstrated by fluorescence microscopy and flow cytometry. The interaction of TfR-targeted nanoparticles with brain endothelial cells increased 3- and 4-fold compared to non-modified SLN and PLGA nanoparticles, respectively.

While the interaction with endothelial cells of functionalized and non-functionalized PLGA nanoparticles were evident and detected through fluorescence microscopy, minor differences were found between functionalized and non-functionalized SLN. These data may indicate an inefficient SLN functionalization, either due to a low yield binding chemistry process itself, or due to the lack of correct peptide availability for its receptor. Therefore, polymeric systems seemed to be more benefic that lipid ones, which justifies the selection of PLGA-based nanoparticles for the next project step.

Finally, the functionality of TfR-targeted PLGA nanoparticles *via* different peptide linkage bridges (carbodiimide and maleimide) was assessed on a human BBB cell-based model. Beyond their ability to improve siRNA permeability through the BBB by 2-fold, it was shown that, 96h post transfection, TfR-peptide functionalized PLGA nanoparticles *via*

maleimide chemistry successfully induced reduction of P-gp messenger RNA (mRNA) expression up to 52%, compared to non-functionalized systems. Subsequently, the permeability of rhodamine 123, as a P-gp substrate, through the human BBB model, was determined upon the treatment of endothelial cells with siRNA-loaded TfR-peptide functionalized PLGA systems, resulting in an increase up to 27% in permeability in three hours of assay. This suggested a positive and marked biologic effect of the siRNA-induced P-gp down-regulation.

Overall, a BBB-targeted polymeric nanosystem was developed for delivery of siRNA against P-gp. Functionalized siRNA-loaded PLGA nanoparticles showed to be successful in silencing P-gp as a BBB efflux transporter and, consequently, in enhancing the blood-to-brain *in vitro* permeability of a P-gp substrate. Hence, drug efflux modulation at the BBB level was attained, bringing hope to CNS disorders treatments, since drugs could reach brain in higher and therapeutic concentrations. Additionally, being P-gp commonly over expressed at tumor cells, this polymeric system has the potential to be applied to cancer when properly functionalized to those cells.

RESUMO

Com o contínuo envelhecimento da população, as perturbações relacionadas com o sistema nervoso central (CNS) têm vindo a aumentar ao longo dos anos. Apesar dos avanços científicos, as terapias existentes até à data não são suficientemente eficazes para travar o avanço das doenças relacionadas com o CNS, o que gera uma necessidade de desenvolver tratamentos mais dirigidos e eficientes. Adicionalmente, a barreira hemato-encefálica (BBB) é uma membrana única que envolve o cérebro e cria o ambiente restrito característico do CNS. Assim, tendo em conta a incidência das perturbações do CNS, os insucessos terapêuticos e a responsabilidade relacionada com a BBB, o desenvolvimento de modelos *in vitro* da BBB que mimetizem esta barreira fisiológica torna-se preponderante no desenvolvimento de novos sistemas de entrega de fármacos/genes, nomeadamente na sua interação com a BBB e permeabilidade. Simultaneamente, esta área de investigação tem sido liderada pela produção de formas eficazes de contornar as funções protetoras da BBB.

As bombas de efluxo de fármacos existentes na BBB, tal como a glicoproteína-P (P-gp), são barreiras bioquímicas que previnem a eficácia dos tratamentos de distúrbios do CNS, devido à sua forte capacidade de limitar a perfusão de compostos para o interior do cérebro. Ao longo das últimas décadas, foram propostas novas abordagens no sentido de modular a passagem de fármacos pela BBB e controlar os seus transportadores de efluxo, embora com sucesso limitado. Como consequência das propriedades relacionadas com o específico silenciamento de proteínas de interesse ao nível da pós-transcrição, o RNA de interferência (siRNA) tem assumido uma especial preponderância nesta área da investigação. Desta forma, o siRNA é usado como uma abordagem promissora para silenciar seletivamente proteínas alvo, aumentando a probabilidade dos fármacos alcançarem o cérebro.

Tão importante quanto o eficaz silenciamento proteico é o transporte do siRNA para o seu local de ação pretendido. Assim, a nanotecnologia e bioengenharia uniram-se, protegendo a circulação sanguínea dos oligonucleótidos, conduzindo o seu transporte para os locais-alvo e promovendo a entrega intracelular. Os recentes estudos relacionados com estratégias de funcionalização oferecem várias ferramentas químicas para conjugar ligandos moleculares específicos à superfície de nanossitemas, o que possibilita o seu direcionamento ativo. Desta forma, a seleção dos ligandos apropriados promove a probabilidade de sistemas transportadores de siRNA atravessarem a BBB.

Reunindo as ideias anteriores, o principal objetivo desta tese consistiu no desenvolvimento de nanossistemas para encapsular siRNA, seguros e direcionados, capazes de modular o efluxo de fármacos na BBB através de siRNA contra a P-gp. Inicialmente procedeu-se ao desenvolvimento de um modelo não celular de BBB. Os objetivos deste modelo prendiam-se com a possibilidade de testar, de um modo simples e rápido, a permeabilidade de compostos. Assim, uma ferramenta de rastreio e avaliação, também usada para a previsão da permeabilidade *in vivo*, foi obtida. Este modelo de permeabilidade baseado em vesículas fosfolipídicas (PVPA) foi otimizado e posteriormente testado para avaliar a permeabilidade passiva transcelular de siRNA, tanto livre como encapsulado. Foram desenvolvidas nanopartículas poliméricas de ácido poli(lático-co-glicólico) (PLGA) e lipídicas (nanopartículas lipídicas sólidas, SLN) com siRNA encapsulado. O efeito das nanopartículas desenvolvidas, ligeiramente negativas (-10 mV) e com populações monodispersas de cerca de 140 nm, na permeabilidade do siRNA através do modelo BBB-PVPA foi avaliado. Detetou-se um aumento na permeabilidade do siRNA, desde 3.7×10^{-6} cm s^{-1} (siRNA livre) até 5.5×10^{-6} cm s^{-1} e 6.9×10^{-6} cm s^{-1} após encapsulação em nanopartículas poliméricas e lipídicas, respetivamente.

De seguida, o sistema baseado em nanopartículas foi melhorado através do teste de vários materiais e técnicas de funcionalização. Componentes matriciais das nanopartículas modificados com grupos amina terminal foram adicionados aos sistemas já produzidos, de forma a promover a funcionalização da sua superfície através de duas abordagens químicas distintas, tanto por cardodiimida como maleimida. Simultaneamente, o surfactante previamente usado foi substituído por Tween80, caracterizado por ser mais facilmente removido da superfície das nanopartículas, promovendo a disponibilidade dos grupos funcionais, que assim expõem as suas cargas substancialmente negativas. Consequentemente, as nanopartículas poliméricas apresentaram tamanho médio de cerca de 115 nm, com superfície negativamente carregada (-30 mV) e com 50% de eficiência de associação de siRNA, enquanto as SLN, também carregadas negativamente (até -21 mV), apresentaram 150 nm de tamanho médio e eficiência de associação até aos 52%. A libertação controlada do siRNA foi verificada, alcançando cerca de 60% de libertação das nanopartículas após 24h em condições fisiológicas. Mais ainda, a segurança das nanopartículas foi garantida, uma vez que a atividade metabólica de células endoteliais cerebrais, quando em contacto com todas as nanopartículas em concentrações crescentes, esteve geralmente acima dos 80%, até 24h de incubação. Com vista a melhorar a permeabilidade transcelular, as nanopartículas foram funcionalizadas com um péptido que se liga ao recetor da transferrina (TfR), atingindo tamanhos médios entre 321 e 506 nm, e cargas de superfície entre -10 e -40 mV. Ensaios de ressonância magnética nuclear ^{1}H (^{1}H NMR) confirmaram esta modificação de superfície, e a capacidade das nanopartículas se

direcionarem para células da BBB humana foi demonstrada por microscopia de fluorescência e citometria de fluxo. A interação entre os sistemas funcionalizados e as células aumentou 3- e 4-vezes quando comparado aos mesmos sistemas não funcionalizados de SLN e PLGA, respetivamente.

Apesar das diferenças de interação com as células endoteliais entre as nanopartículas de PLGA funcionalizadas e não funcionalizadas terem sido notórias através de microscopia de fluorescência, o mesmo não aconteceu relativamente às SLN. Estes resultados indicam a possível ineficácia na funcionalização das SLN, que poderá estar relacionado com o baixo rendimento do processo de ligação química, ou dever-se à falta de péptido, espacial e corretamente disponível, para o seu recetor. Deste modo, os sistemas poliméricos pareceram ser mais benéficos que os lipídicos, razão pela qual foram selecionados para prosseguir no desenvolvimento do projeto de tese.

Por fim, as nanopartículas funcionalizadas com o péptido anti-TfR, através da implementação da ligação carbodiimida ou maleimida, foram avaliadas num modelo celular de BBB humana. Para além da sua capacidade de duplicar a permeabilidade do siRNA através da barreira, foi evidenciado que, 96h após a transfeção, as nanopartículas funcionalizadas *via* maleimida induziram eficazmente a redução da expressão do RNA mensageiro (mRNA) da P-gp até 52%, em relação aos sistemas não funcionalizados. Subsequentemente, a permeabilidade da rodamina 123, como substrato da P-gp, foi determinada através do modelo de BBB humana, após incubação das células endoteliais com as nanopartículas de PLGA funcionalizadas. No final de três horas de ensaio, a permeabilidade da rodamina 123 aumentou até 27%, o que sugere a existência de um efeito biológico positivo e notável, através da regulação negativa da P-gp induzida por siRNA.

De uma forma geral, foram desenvolvidos nanossitemas poliméricos, direcionados para a BBB, para a entrega de siRNA anti-P-gp. As nanopartículas funcionalizadas e carregadas com siRNA mostraram conseguir silenciar a P-gp como um transportador de efluxo da BBB e, consequentemente, potenciar a permeabilidade sangue-cérebro de um substrato da P-gp. Desta forma, foi alcançada a modulação do efluxo de fármacos ao nível da BBB, o que traz esperança para o tratamento das perturbações do CNS, já que os fármacos poderão alcançar o cérebro em concentrações mais elevadas e potencialmente terapêuticas. Visto que a P-gp é comummente sobre expressa em células cancerígenas, o sistema polimérico desenvolvido poderá ser aplicado a condições tumorais, desde que adequadamente funcionalizado para essas mesmas células.

ACRONYMS AND ABBREVIATIONS LIST

ABC transporter	ATP-binding cassette transporter
AE	Association efficiency
ANOVA	One-way analysis of variance
ApoE	Apolipoprotein E
Arg	Arginine
BBB	Blood-brain barrier
BCEC	Brain capillary endothelial cell line
BCRP	Breast cancer resistance protein
BCS	Biopharmaceutics classification system
BCSF	Blood cerebrospinal fluid barrier
bFGF	Basic fibroblast growth factor
Cav-1	Caveolin-1
CD	Cyclodextrin
CHO	Cholesterol
CNS	Central nervous system
CPP	Cell-penetrating peptide
CTX	Chlorotoxin
Cys	Cysteine
C6	Rat glioma cell line
DAPI	4',6-diamidino-2-phenylindole dihydrochloride
DHPE	Dihexadecanoyl-sn-glycero-3-phosphoethanolamine
DIV	Dynamic *in vitro*
DMSO	Dimethyl sulfoxide
DNA	Deoxyribonucleic acid
EBM-2	Endothelial basal medium-2
ECS	Extracellular space
EDC	1-ethyl-3-(3-dimethylaminopropyl)carbodiimide

EDS	Electronic data system
EDTA	Ethylenediamine tetraacetic acid
em.	Emission
ex.	Excitation
e.g.	*Exempli gratia*
FACS	Fluorescence-activated cell sorting
FBS	Fetal bovine serum
FITC	Fluorescein isothiocyanate
FLZ	Synthetic squamosamide derivative
g	G force
GFP	Green fluorescent protein
GSH	Glutathione
HBSS	Hanks' balanced salt solution
hCMEC/D3	Immortalized human cerebral microvascular endothelial cell line
HEPES	4-(2-hydroxyethyl)-1-piperazineethanesulfonic acid
His	Histidine
HTT	Huntingtin
i.e.	*Id est*
LDL	Low density lipoprotein
Mdr	Multi-drug resistance
MES	2-(N-morpholino)ethanesulfonic acid
Met	Methionine
MicroBBB	Microfluidic-Blood-brain barrier
mRNA	Messenger RNA
Mrp	Multi-drug resistance related protein
MTT	3-[4,5-dimethylthiazol-2-yl]-2,5-diphenyltetrazolium bromide
MWCO	Molecular weight cut off
NHS	N-hydroxysuccinimide
NH_2	Amine group
NMR	Nuclear magnetic resonance

NP(s)	Nanoparticle(s)
NS	Non-silencing
Oatp2	Organic anion transporting polypeptide
Oat3	Organic anion transporter
OCTN2	Organic cation/carnitine transporter
O/W	Octanol/water
PAMPA	Parallel artificial membrane permeation assay
Papp	Apparent permeability
PB	Phosphate buffer
PBS	Phosphate buffered saline
PC	Phosphatidylcholine
PD	Parkinson's disease
PdI	Polydispersity index
PE	Phosphatidylethanolamine
PEG	Polyethylene glycol
pept	Peptide Thr-His-Arg-Pro-Pro-Met-Trp-Ser-Pro-Val-Trp-Pro
pept-Cys	Peptide Thr-His-Arg-Pro-Pro-Met-Trp-Ser-Pro-Val-Trp-Pro-Cys
PET	Polyethylene terephthalate
PFA	Paraformaldehyde
PLGA	Poly(lactic-co-glycolic acid)
PLL	Poly L-lysine
ppm	Parts per million
Pro	Proline
PS	Phosphatidylserine
PVA	Poly(vinyl alcohol)
PVPA	Phospholipid vesicle-based permeability assay
P-gp	P-glycoprotein
qRT-PCR	Quantitative reverse transcription polymerase chain reaction
RISC	RNA induced silencing complex
RNA	Ribonucleic acid

rpm	Rotation per minute
SEM	Scanning electron microscopy
Ser	Serine
siRNA	Small interfering RNA
SLN	Solid lipid nanoparticle
SMCC	Succinimidyl 4-(N-maleimidomethyl)cyclohexane-1-carboxylate
SM(PEG)$_{24}$	PEGylated SMCC crosslinker
SS	Shear stress
TAT	Trans-activator protein
TEER	Transendothelial electrical resistance
Tf	Transferrin
TfR	Transferrin receptor
Thr	Threonine
TJ(s)	Tight junction(s)
TMS	Tetramethylsilane
Trp	Tryptophan
UV/Vis	Ultraviolet/Visible
Val	Valine
w	Week(s)
WGA	Wheat germ agglutinin
WT	Wild-type
w/o	Water-in-oil
w/o/w	Water-in-oil-in-water
YWHAZ	Tyrosine 3-monooxygenase/tryptophan 5-monooxygenase activation protein zeta gene
3D	Three-dimensional

CHAPTER I

Literature review

This chapter was based on the following published paper and book chapters:

- **Gomes, M.J.**, Martins, S. and Sarmento, B. 2015. siRNA as a tool to improve the treatment of brain diseases: mechanism, targets and delivery. Ageing Res Rev. 21: 43-54.
- **Gomes, M.J.**, Mendes, B., Martins, S. and Sarmento, B. 2016. Cell-based *in vitro* models for studying blood-brain barrier (BBB) permeability. In Concepts and models for drug permeability studies: cell and tissue based *in vitro* culture models, Bruno Sarmento, ed. (Elsevier). ISBN:978-0-08-100094-6, Pages 169-188.
- **Gomes, M.J.**, Mendes, B., Martins, S. and Sarmento, B. 2016. Nanoparticle functionalization for brain targeting drug delivery and diagnostic. In Handbook of nanoparticles: synthesis, functionalization and surface treatment, Mahmood Aliofkhazraei, ed. (Springer). ISBN:978-3-319-15337-7, Pages 941-959.

1. Central nervous system disorders

The number of people aged 60 years and over has tripled since 1950, reaching 600 million in 2000 and surpassing 700 million in 2006. It is projected that the combined senior and geriatric population will reach 2.1 billion by 2050 (United Nations, 2007). As the effects of ageing on the brain and cognition are widespread and have multiple etiologies, the increasing incidence of brain disorders is real and expected. The World Health Organization has indicated that central nervous system (CNS) disorders are the major medical challenge of the 21st Century (Research And Markets, 2007). Disorders of the CNS are numerous, diverse, frequently severe, and affect a large portion of the world population. These diseases can debilitate conditions that significantly affect the morbidity and mortality of modern society. Neurodegenerative diseases including Alzheimer's diseases, Parkinson's diseases and amyotrophic lateral sclerosis – which symptoms are related to loss of movement, memory, and dementia due to the gradual loss of neurons – are constantly and rapidly increasing as population ages. As well, brain tumors constitute a severe and unsolved clinical condition and are a common cause of cancer-related death.

Longer life expectancy should be followed by better quality of life, however, current therapies to CNS disorders (which are mainly incident on old-age population) do not positively correspond to their expectations (Bhaskar *et al.*, 2010). Neurodegenerative diseases, deeply associated with aging, are usually linked to a loss of brain and spinal cord cells. As examples, in Alzheimer's and Parkinson's diseases the neuronal damage occur due to abnormal protein processing and accumulation, which results in gradual cognitive and motor deterioration (Gilmore *et al.*, 2008).

According to Brain Tumor Research website statistics (Farm, 2014), brain tumors kill more children and adults under the age of 40 than any other cancer, and only 18.8% of those diagnosed with brain tumor survive beyond five years, compared to 50% average survival prognostic for all cancers. Moreover, the incidence of brain metastases has increased over the last decade mainly due to improved treatment of primary peripheral cancers resulting in increased patient survival, as well as due to the development of newer tools to image and diagnostic tumors of the CNS (Agarwal *et al.*, 2011). Among the different ways to treat cancer, such as surgery and radiotherapy (which uses high-energy particles or waves to destroy or damage cancer cells, that arise the possibility to damage also normal cells, reason why this treatment must be carefully planned to minimize side effects), tumor therapy is usually based on the interplay between chemotherapeutic and antiangiogenic agents

(Murthy, 2007). In general, treatment of many aging disorders and tumors require drugs acting on the CNS, highlighting the need and importance to reach CNS on a therapeutic concentration. Simultaneously, the field of nanomedicine is rapidly expanding and promises revolutionary advances to the diagnosis and treatment of devastating human diseases (Gilmore *et al.*, 2008).

2. Obstacles to brain diseases treatment

Drug delivery to the CNS represents a challenge in developing effective treatments for neurodegenerative diseases and brain tumors due to the unique and complicated environment imposed by the CNS itself. There are protective barriers which restrict the passage of foreign substances into the brain, namely the blood-brain barrier (BBB), the blood cerebrospinal fluid barrier (BCSF), and other specialized CNS barriers as the arachnoid barrier (Abbott *et al.*, 2010; Bhaskar *et al.*, 2010). Therefore, an important part of this CNS challenge is overcoming the natural tendency of the BBB to block drug transport. This barrier, a tightly packed layer of endothelial cells surrounding the brain (Bhaskar *et al.*, 2010), is designed to protect and prevent high-molecular weight molecules in blood from entering the brain by filter harmful compounds from the brain back to the bloodstream. As so, since the BBB cannot recognize therapeutic compounds, high doses must be administered to have a drug therapeutic concentration at the brain, with increased risks of adverse side effects (Murthy, 2007).

Due to the difficulty of physically active molecules overcome BBB and reach CNS, it becomes crucial to understand the structural composition as well as how the factors that regulate permeability of the substances across the BBB act. Morphologically, the BBB is mainly constituted by brain endothelial cells, which form the cerebral microvascular endothelium, paving the luminal side (the blood capillary side). This cell layer is in close association with basement membrane and neighboring cell types, which include pericytes, astrocytes, neurons and microglia in the abluminal membrane. Together, these various cell types form the neurovascular unit that is essential for the health and function of the CNS (**Figure 1.1**). Endothelial cells release a number of diffusible factors that are able to affect neural precursors and to promote stem-cell renewal (Cardoso *et al.*, 2010). On the other hand, pericytes play an important role on the integration of endothelial cells and astrocytes functions at the neurovascular unit (Armulik *et al.*, 2010; Fisher, 2009); and astrocytes are crucial on the induction of BBB integrity and functions, namely by the secretion of factors

such as basic fibroblast growth factor (Abbott *et al.*, 2006). Moreover, neurons are a key factor on BBB cerebral flow and vessel dynamics (Cardoso *et al.*, 2010; Choi and Kim, 2008a; Weiss *et al.*, 2009). Lastly, the exact mechanisms of how microglia influences BBB properties are still unknown, however it is clear that they are playing an important role in immune response of the CNS and consequently in the BBB integrity (Choi and Kim, 2008b).

Besides this cellular network, several molecular and receptor structures are present on the surface of the endothelial cells (**Figure 1.2**), able to mediate the transport of solutes and other substances including drugs in and out of the brain. Therefore, BBB is also responsible for leukocyte migration and maintenance of brain microenvironment homeostasis, which is crucial for neuronal activity and proper functioning of CNS. The transport of solutes and other substances across BBB is also dependent on intercellular junctions affecting the paracellular permeability (Wilhelm and Krizbai, 2014). Tight junctions (TJs) consist of an extreme complex of integral proteins spanning the intercellular cleft, junctional adhesion molecules and cytoplasmic accessory proteins bound to the actin cytoskeleton. Specifically, claudins form the primary seal of TJ, determining TJ integrity. Occludins are the dynamic regulatory proteins responsible for TJ regulation and subsequent transendothelial electrical resistance (TEER) enhancement, and paracellular permeability restriction. Together, claudins and occludins form the extracellular component of TJs (Abbott *et al.*, 2006). Furthermore, adherent junctions are located near the basolateral side of endothelial cells, holding them together and giving the tissue structural support (Abbott *et al.*, 2010). Besides junctions, as special characteristics of BBB that limit drug uptake, there is also a lack of fenestrations, low endogenous pinocytotic activity and metabolic barriers (enzymes and diverse transport systems) (Ballabh *et al.*, 2004). Other important characteristic of *in vivo* BBB is the shear stress over the surface of the cells, which is a tangential force generated by the blood flow. Shear stress (SS) promotes the differentiation process and maintenance of BBB phenotype (Cucullo *et al.*, 2011).

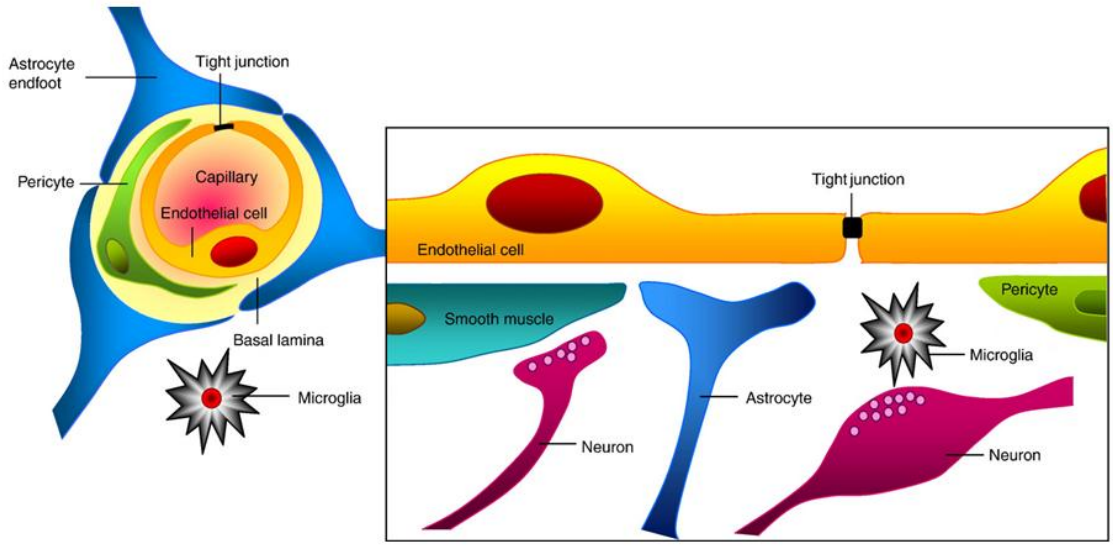

Figure 1.1. Blood-brain barrier cellular structure and morphology. The neurovascular unit is a complex cellular system that includes highly specialized endothelial cells, a high concentration of pericytes embedded in the endothelial cell basement membrane; astrocytic endfeet associated to the parenchymal basement membrane, neurons and immune cells. Adapted from Abbott, 2013.

Next to the BBB, BCSF is the second important feature of the CNS, formed by the epithelial cells of the choroid plexus. BCSF mainly regulates the exchange of molecules between the blood and cerebrospinal fluid, controlling the penetration within the interstitial fluid of the brain parenchyma (Bhaskar *et al.*, 2010; Gilmore *et al.*, 2008; Mahringer *et al.*, 2011). Moreover, another interface, the avascular arachnoid epithelium, has a relatively small surface that is the main reason why it is not a significant surface for exchange between blood and CNS (Abbott *et al.*, 2010). Some other CNS barriers, like blood tumor barrier and blood retina barrier, may also play a role in drug transport (Bhaskar *et al.*, 2010).

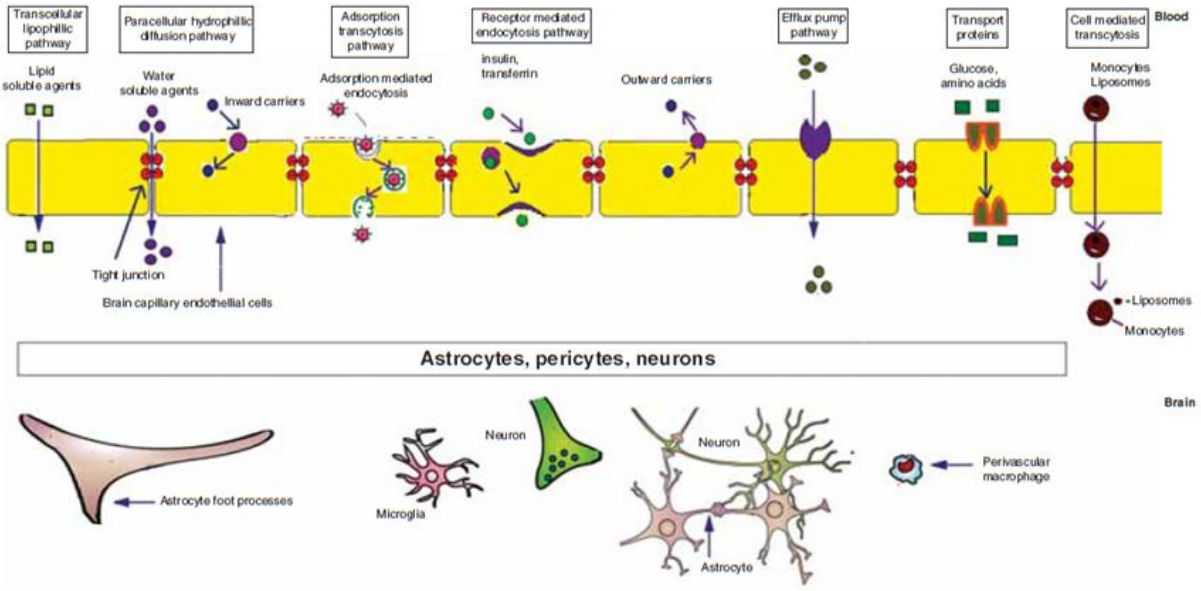

Figure 1.2. Mechanisms present at the BBB that mediate the transport from blood to brain (Nagpal *et al.*, 2013).

3. Blood-brain barrier and drug efflux

As already mentioned, BBB is an endothelial dynamic interface that shields the CNS from exposure to circulating toxins and potentially harmful chemicals (Hawkins and Davis, 2005). This protective barrier controls the influx and efflux of a wide variety of substances, excluding therapeutic drugs from entering the brain, and thus, at the same time, maintains a favorable environment for the CNS and becomes an obstacle for drugs intended to treat CNS diseases (Agarwal *et al.*, 2011; Bhaskar *et al.*, 2010). The ability of a substance to penetrate the BBB or be transported across BBB is dependent on its physiochemical properties, as small size, liposolubility and customizable surface, which are examples of favorable properties. The cerebral pharmacological efficacy of any drug depends on its CNS uptake which, in turn, depends on a combination of factors, including CNS physical barriers and the affinity of the substrate for specific transport systems located at both sides of these interfaces. In this context, efflux transporters present at the BBB are one of the main limitations of brain penetration as well as the main responsible for intra- and extra-cellular distribution of a variety of endogenous and exogenous compounds. Active efflux transport or carrier mediated efflux involve extrusion of drugs from the brain in the presence of efflux

transporters. This type of transport causes the active efflux of drugs from brain back to blood (Bhaskar *et al.*, 2010). Therefore, one strategy to improve the efficacy of CNS drugs would be the modulation of transport proteins mainly responsible for the drug efflux, being responsible for their improved passage across the BBB (Mahringer *et al.*, 2011).

3.1. Drug efflux transporters

A key element of the BBB function is the expression of ATP-binding cassette (ABC) drug efflux transporters in the luminal membrane of brain microvessel endothelial cells, which besides restrict the entry of many compounds into the brain, also plays a major role on the maintenance of brain homeostasis and detoxification. Among these ABC transporters, are the P-glycoprotein (multi-drug resistance 1 (Mdr1) gene product, P-gp), breast cancer resistance protein (BCRP), and members of the multi-drug resistance related proteins (Mrp1, 2, 4 and 5). These proteins collectively hamper brain uptake of a huge variety of lipophilic xenobiotics, potentially toxic metabolites and also drugs. Several other transport proteins and receptors are expressed at the BBB, such as the non-ABC transporters Oat3 (organic anion transporter) and Oatp2 (organic anion transporting polypeptide that handles steroid and drug conjugates, certain opioid peptides, and the cardiac glycoside, digoxin) that, when coupled to the appropriate ion gradients, are capable of driving organic anions into the endothelial cells (Agarwal *et al.*, 2011; Bauer *et al.*, 2005; Hermann and Patak, 2011; Mahringer *et al.*, 2011).

A deeply studied export pump is P-gp, a 170 kDa phosphorylated glycoprotein expressed in multiple cell types within the brain parenchyma, including astrocytes and microglia. Its highest activities seem to be in the luminal plasma membrane of the capillary endothelium (Mahringer *et al.*, 2011). Mdr1 is often over expressed in tumor cells, which contributes to the multi-drug resistant phenotype commonly seen in cancer (Fisher *et al.*, 2007). The fact that Mdr1 messenger RNA (mRNA) and P-gp are highly expressed in multi-drug resistant cells, while P-gp has a long turnover time, make this target very attractive to inhibit with antisense or small interference RNA (siRNA) oligonucleotides (Fisher *et al.*, 2007). Moreover, *in vivo* dosing studies in Mdr1-knockout mice show greatly increased plasma-to-brain ratios (5-fold to 50-fold) for a large number of drugs that are P-gp substrates (Schinkel *et al.*, 1996), which indicates the relevance of P-gp efflux system (Bauer *et al.*, 2005).

Another example that highlights P-gp efflux mechanism, by decreasing the effect of drugs which are its substrates, was studied by using morphine on rats-induced peripheral inflammatory pain (Sanchez-Covarrubias *et al.*, 2014). This condition results in increased expression and activity of P-gp and, consequently, there is a significant reduction in CNS uptake of morphine (since morphine is a P-gp substrate) and reduced morphine analgesic efficacy. Considering this, researchers induced peripheral inflammatory pain and examined the administration of diclofenac on BBB transport of morphine *via* P-gp, as well as on its analgesic and anti-inflammatory efficacy. Diclofenac, a non-steroidal anti-inflammatory drug, is commonly administered in conjunction with opioids (i.e. morphine) during pain therapy, and have been reported to modulate P-gp (Akanuma *et al.*, 2010). Authors observed a significant decrease in brain morphine uptake in injured animals. Moreover, in situ brain perfusion studies showed that not only pain induction but also diclofenac treatment alone increased P-gp efflux activity which results in decreased morphine brain uptake (Sanchez-Covarrubias *et al.*, 2014). Robillard and colleagues investigated *in vivo* the tissue distribution of the human immunodeficiency virus protease inhibitor atazanavir in wild-type (WT) mice and P-gp/BCRP-knockout mice. In this study, some WT mice were pre-treated with a P-gp/BCRP inhibitor, elacridar. In P-gp and Bcrp knockout mice, authors demonstrated a significant increase in atazanavir brain concentration of 5.4-fold compared to those in WT mice ($p < 0.05$). Moreover, elacridar-treated WT mice showed a significant increase in atazanavir brain concentration of 12.3-fold compared to those in vehicle-treated WT mice. These *in vivo* results show how P-gp (as well as BCRP) is involved in limiting the ability of atazanavir to permeate mice brain (Robillard *et al.*, 2014). Also Liu and co-workers studied P-gp consequences as an efflux transporter. A novel anti-Parkinson's disease (PD) candidate drug, which is a synthetic squamosamide derivative (FLZ), has shown poor BBB penetration, but the main reason for that (if caused by P-gp and/or BCRP) was still unclear. Therefore, *in vitro* permeability experiments of FLZ were carried out on BBB models (one mimicking physiological, and other PD pathological-related BBB properties). In PD models, both expressions of P-gp and BCRP were significantly greater, which is associated with the lower BBB permeability of FLZ in pathological model, compared with physiological model. Transport studies were also performed, and obtained data have shown that only P-gp blocker effectively inhibited the efflux of FLZ. Thus, from this study it is possible to conclude that P-gp is the main responsible for poor brain penetration of FLZ and low BBB permeability (Liu *et al.*, 2014).

The BCRP (72 kDa (Paturi *et al.*, 2010)) mainly transports sulphated conjugates of drugs and sterols (Hori *et al.*, 2005), which largely corresponds to cationic and uncharged substrates (Bauer *et al.*, 2005). Its function is regulated by steroid hormones, particularly

estrogens. In brain capillaries from male and female rats and mice, BCRP-mediated transport was rapidly and reversibly reduced after short term exposure to nanomolar concentrations of 17β-estradiol (Mahringer *et al.*, 2011).

Multi-drug resistance related protein 4 (Mrp4; 150 kDa (Sauna *et al.*, 2004)) shares many features with P-gp and BCRP, including broad substrate affinity and expression at the BBB (Lin *et al.*, 2013). Regarding the difficulty to evaluate the role of Mrp4 at the BBB (since most drugs are also substrates of P-gp and/or BCRP), Lin and co-workers created a mouse strain in which all these alleles were inactivated. Hence, they used these animals to assess inactivated alleles impact on brain delivery of camptothecin analogues (as gimatecan and itinotecan active metabolite SN-38), an important class of antitumor agents, substrates of these transporters. They were able to observe that additional deficiency of Mrp4 in P-gp;BCRP-/- mice significantly increased the brain concentration of all camptothecin analogues by 1.2-fold (gimatecan) and 5.8-fold (SN-38). The presence of P-gp or Mrp4 alone was sufficient to reduce the brain concentration of SN-38 to the level in WT mice. From this study, it is possible to conclude that Mrp4 limits the brain penetration of camptothecin analogues and teams up with P-gp and BCRP to form a robust cooperative drug efflux system. This intensive action limits the usefulness of selective ABC transport inhibitors to enhance drug entry for treatment of intracranial diseases (Lin *et al.*, 2013).

Regarding BBB composition features, namely these drug efflux transporters, only a small class of drugs or small molecules (molecular mass of < 400-500 Da) with high lipid solubility are actually able to across the BBB (Bhaskar *et al.*, 2010). Thus, conventional pharmacological drugs or chemotherapeutic agents are incapable to pass through the barrier.

4. Blood-brain barrier *in vitro* models

BBB represents a critical obstacle in the treatment of the neurological disorders as preventing most of the pharmaceutical solutions being successful (Nagpal *et al.*, 2013). Therefore, nowadays, there is a huge interest on the development of effective solutions to overcome this barrier and treat brain diseases. Thus, the development of a close *in vitro* system is an important step for the evaluation of new drugs and drug delivery systems to cross the BBB. However, as a unique environment, BBB is very difficult to mimic. Considering that a single factor could be enough to change BBB fundamental properties, so far no *in vitro* model can faithfully reproduce all the properties and characteristics of the *in*

vivo BBB (Cardoso *et al.*, 2010). Nonetheless, improve existing BBB models and/or creating new ones is a challenging aim to several researches groups.

Several options could be selected in order to mimic BBB, from non-cellular to cell-based models. Distinct type of apparatus (static or dynamic) could be established, as well as used with cells from different origins (as endothelial cells, astrocytes, neurons), as primary cells or immortalized cell lines, in monoculture or co-culture. Usually, the final purpose needs and the available facilities, time and resources determine which kind of model researchers select to reproduce.

4.1. Non-cellular based models

There exists an increasing demand for *in vitro* models. However, so far, there is no such thing as a perfect model; all of them have some drawbacks and deficiencies. Complexity, time-consuming, high costs, absence of some *in vivo* features or lack of accuracy are just a few examples. Investigators continue to explore the membrane model world, searching for a more reliable but still cost effective bio-relevant model approach. Usually, cell-based models are relatively costly to maintain and time-consuming, mainly due to culturing times. Therefore, models based on non-cellular membranes arise as attractive alternatives. Artificial membranes based on parallel artificial membrane permeability assay (PAMPA) and phospholipid vesicle-based permeation assay (PVPA) constitute effective models for passive and transcellular-like permeability (Buckley *et al.*, 2012). These models are particularly interest for poorly soluble drugs permeability studies, since they are transported through the evaluated transcellular route. Generally, non-cellular based models are relatively cheap and offer the opportunity for high throughput analysis, where a fast screening of large numbers of compounds could be performed (Buckley *et al.*, 2012).

PAMPA, a membrane model based on lipids, was first developed to predict transcellular absorption of drug in the intestine, but its potential was rapidly underlined and several variants with different lipid compositions have been generated (Buckley *et al.*, 2012), including the BBB-PAMPA (Wohnsland and Faller, 2001). Nonetheless, PVPA membranes are prepared through the deposition of liposomes on a porous filter, reaching a tight barrier comprised of phospholipid bilayers sandwiches (Buckley *et al.*, 2012). This is a more recently developed intestinal artificial model, which has already demonstrated a good correlation with *in vivo* data for drugs transported by passive diffusion (Flaten *et al.*, 2006). Although it is

most suitable for passive permeability studies, it can be applied for the prediction of the extent of oral drug absorption for new entities in early drug development. Interestingly, electrical resistance and permeability of a model drug (calcein) were used to confirm barrier integrity, as cellular-based models usually do (Flaten *et al.*, 2008). Moreover, the possibility to change the lipid composition and adapt the protocol in order to mimic different barriers was already executed for skin (Engesland *et al.*, 2013), leaving the opportunity and an open gap for other desired barriers.

4.2. Cell-based models

In the last decades, most of the current successful cell-based BBB *in vitro* models were based on primary cell cultures due to their high TEER values and low cellular passage. However, there may be a limitation on the availability of the primary cells resulting from animals' low accessibility, while these cells are also more susceptible to internal and external contaminations than immortalized cell lines. In addition, this approach has high costs and requires time-consuming and special skills for the cellular isolation (Wilhelm and Krizbai, 2014). On the other hand, immortalized cell lines offer a considerable number of advantages. They are reliable (using trusted well-established sources), consistent (cell source is controlled), long-lasting (it is important that cell features do not disappear over time), accessible (cells are available to be purchased at any time) and preparation time and cost are reduced (Zhang *et al.*, 2011). Despite lacking certain BBB features and having lower TEER, there is no doubt that immortalized cell lines are an emergent solution to reproduce the *in vitro* BBB models (Cardoso *et al.*, 2010).

Until current ages, mouse and rat brain endothelial cell lines are the most common to use (Cardoso *et al.*, 2010; Li *et al.*, 2010). Less studied but still used are porcine and bovine origins (Wilhelm and Krizbai, 2014). Human brain endothelial cells became available during the early 1980s and were revealed as crucial for the study of the BBB developmental and pathophysiological processes. The best characterized human cell line in this field is the cerebral microvascular endothelial cell line (hCMEC/D3) which has been shown to retain important BBB characteristics at least until the 35^{th} passage. Briefly, hCMEC/D3 shows a stable phenotype, the expression of endothelial cell markers and ABC-transporters. Human specimens are undoubtedly the best model, since they are the only ones that faithfully reproduce the human BBB characteristics (Wilhelm and Krizbai, 2014).

As mentioned previously, brain endothelial cells are the main component of BBB; nonetheless, other cell types also play an important role both in the function and regulation of BBB characteristics. Therefore, *in vitro* models could be improved and have an increased complexity when other cell types as astrocytes/glial cells, pericytes, and even neurons are included. To study the BBB models efficiency, several barrier properties should be analyzed, such as TEER and permeability of certain molecules (Wilhelm *et al.*, 2011).

4.2.1. Monoculture models

Semi-permeable membranes devices as Transwell® (further discussed in the **Figure 1.4 A**) enable the study of BBB cell culture models. Using this approach, different properties can be assessed within the same device, as drug permeability and TEER. However, some disadvantages include cell adhesion with a random pattern at semi-permeable membranes, which provokes the so-called "edge effect" with the possible subsequent TJ absence (Naik and Cucullo, 2012; Santaguida *et al.*, 2006).

A simplified view of the BBB, as monolayer of highly specialized brain microvascular endothelial cells on a Transwell® apparatus, is the most used idea for a BBB model. For this monoculture system, cells from various sources (bovine, rodent, porcine, non-human primate, and human) are seeded on the upper (luminal) surface of the membrane, immersed in their specific growth media. Transwell® apparatus have a microporous membrane interface that allows for nutrient exchange and the passage of cell-derived and exogenous substances, but does not allow cell movement across the two compartments, upper and lower (Naik and Cucullo, 2012). Brain endothelial cells from rat (as RBE4 (Vilas-Boas *et al.*, 2014; Wilhelm *et al.*, 2011) and GP8 (Demeuse *et al.*, 2004)) and mouse (b.End3 (Shi *et al.*, 2014)) are extensively cultured on monolayers as BBB plain models. Besides these non-human cell lines, the already mentioned hCMEC/D3 has been of growing importance (Abbott, 2013; Wilhelm *et al.*, 2011).

However, monoculture is a basic reconstruction of the BBB which therefore lacks several vital features necessary for the development of real BBB properties *in vitro*. These type of models do not have natural physiological stimuli as cell-to-cell interaction with perivascular astrocytes and other parenchymal cells (e.g. neurons), intraluminal SS, and circulating blood cells. These lacking properties significantly limit the vascular endothelium capability to develop and/or maintain the *in vivo* intrinsic BBB properties and functions. Moreover, besides these limitations, this disadvantage could also accelerate endothelial dedifferentiation, promoting the consequent loss of BBB characteristics (Naik and Cucullo,

2012). All of these lead to the development of more complex BBB models, incorporating different type of cells in order to reproduce more closely the neurovascular unit (Abbott, 2013).

4.2.2. Co-culture models

All previous described cells can be used in combination to obtain different and improved co-cultures models (**Figure 1.3**). From these, generally, the ones that better mimic *in vivo* BBB anatomical conditions bring into play brain endothelial cells with astrocytes and/or pericytes.

Different cells could need different medium composition. Hence, if co-culture is intended, determine how different media or their combination affect cell morphology and culture consistency is crucial.

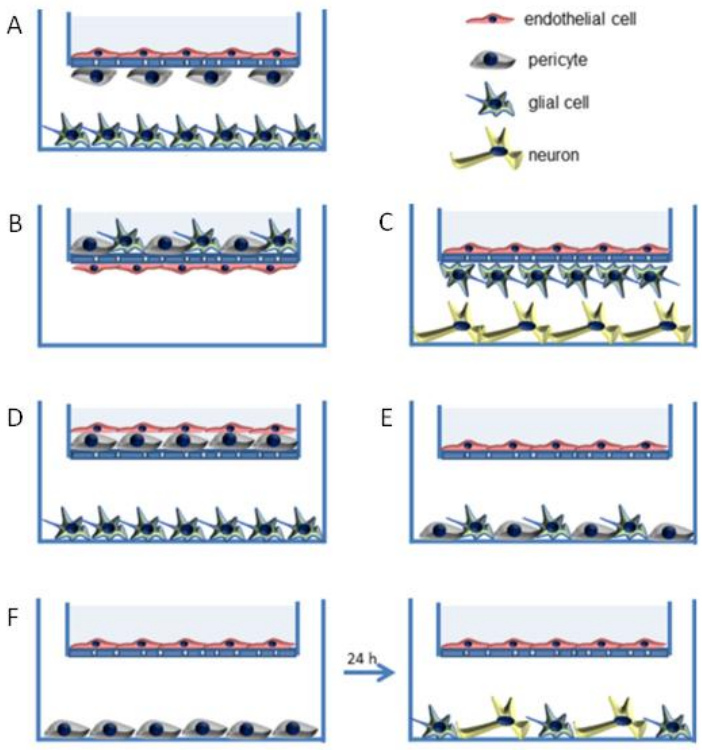

Figure 1.3. *In vitro* cell-based co-cultured BBB models using three types of cells (endothelial cells, pericytes, astrocytes, and/or neurons) in different arrangements (A to F). Adapted from Wilhelm and Krizbai, 2014.

Co-culture of endothelial cells with glial cells/astrocytes

Glial cells ability to induce BBB properties is the main reason why they are broadly used nowadays in co-culture with endothelial cells (Wilhelm *et al.*, 2011), mostly for drug delivery studies (Zhang *et al.*, 2011). Usually, primary glial cells or the immortalized C6 cell line, which has been intensively used for the study of gliomas, are cultured (Abbott, 2013; Wilhelm *et al.*, 2011). On semi-permeable plate filters, astrocytes are usually seeded on the abluminal side and release factors which promote BBB characteristics such as: formation of more strict inter-endothelial tight junctions, increased expression of brain endothelial marker enzymes, transporters and efflux systems (Naik and Cucullo, 2012).

Studies indicate that co-culture of bovine endothelial cells and astrocytes promote an increase in TEER data and decrease in permeability values, comparing with endothelial cells monoculture (Zysk *et al.*, 2001). As with bovine cells, also similar results were obtained with rat or mouse endothelial cells and astrocytes. To achieve good TEER values, direct contact between endothelial cells and astrocytes is necessary (Wilhelm *et al.*, 2011). The robustness of a BBB model was also achieved through the incorporation of astrocytes-derived acellular extracellular matrix, which was derived from the lyses and decellularization of rat astrocytes (Zhang *et al.*, 2011).

Co-culture of endothelial cells with pericytes

At the *in vivo* BBB, endothelial cells and pericytes have a close contact, so this co-culture mixture could be very reliable. It is still unknown which type of pericytes plays a decisive role, but it has been established that there is an intrinsic relation between pericytes and the formation and maintenance of the cerebral microvasculature structure and functions (Ribeiro *et al.*, 2010). Corroborating this, *in vitro* studies already shown an increase of TEER due to the addition of pericytes (Hayashi *et al.*, 2004; Santaguida *et al.*, 2006), indicate that direct contact between these cells leads to the tightest barrier formed (Hayashi *et al.*, 2004). Furthermore, pericytes have been also shown to induce Mrp 6 expression (Berezowski *et al.*, 2004) in endothelial cells.

Co-culture of endothelial cells with neurons

More recently, it has been proved that neurons induce the production of BBB related enzymes in cultured cerebral endothelial cells (Tontsch and Bauer, 1991). The co-culture of rat brain endothelial cells with cortical neurons has shown that a direct contact between them is not necessary for the induction of occludin (one of the TJ proteins) expression (Cestelli *et al.*, 2001).

Triple co-culture

A combination of three different cells is also possible but not so usual due to the complexity of such model. Still, most common triple co-cultures associate pericytes or astrocytes on the bottom side of Transwell® inserts plus endothelial cells seeding on the upper side (Wilhelm *et al.*, 2011). The presence of both pericytes and astrocytes is frequently described as advantageous since brain endothelial cells express higher levels of TJ proteins and greater tightness (Nakagawa *et al.*, 2009).

A multi-culture human cell system study with endothelial cells, astrocytes, and pericytes in a three-dimensional (3D) configuration, based on Transwell® filters, has also been performed. Mono-, co-, and tri-cultivation were investigated to find the most effective model (Hatherell *et al.*, 2011). Authors conclude that co-cultivation of astrocytes with endothelial cells produced the most successful model, as determined by TEER values that were significantly higher than for the pericyte co-culture. Nevertheless, pericytes co-culture improved TJ formation, but did not improve the model to such an extent when grown in tri-cultivation with astrocytes (Hatherell *et al.*, 2011).

4.3. Blood-brain barrier apparatus

Various factors intrinsic to *in vivo* environment are crucial to maintain an optimally functioning BBB (Prabhakarpandian *et al.*, 2013). Several *in vitro* BBB apparatus have been developed and can be distinguished into two main groups: static and dynamic systems. The main difference is related to the fluid flow of dynamic systems that results in SS over the cells surface (Booth and Kim, 2012), which is an essential characteristic of the *in vivo* BBB.

4.3.1. Static models

The semi-permeable plate filters, with a side-by-side diffusion support, are the best and most well known bi-dimensional static model. This system consists of a microporous semi-permeable membrane that separates the luminal (vascular) and the abluminal (parenchymal side) compartments, and is submerged in feeding medium (Naik and Cucullo, 2012; Santaguida *et al.*, 2006). Such apparatus, characterized for its easiness to establish cultures and low cost (Cucullo *et al.*, 2008; Naik and Cucullo, 2012; Santaguida *et al.*, 2006), is indicated to study permeability of drugs across BBB. However, the semi-permeable

membranes cannot reproduce the physiological tangential force generated by the blood flow (SS) across the apical surfaces affecting the structure and function of endothelial cells (Cucullo *et al.*, 2011; Naik and Cucullo, 2012; Prabhakarpandian *et al.*, 2013). Shear stress promotes the differentiation process and maintenance of BBB phenotype; without it the cells lose their BBB properties (Cucullo *et al.*, 2008; Naik and Cucullo, 2012). In addition, lacking antimitotic influences by laminin and flow, cell cycle rate tends to increase, causing an uncontrolled growth of endothelial cells in a multilayer manner (Naik and Cucullo, 2012; Santaguida *et al.*, 2006).

4.3.2. Dynamic *in vitro* (DIV) models

Although Transwell® apparatus (**Figure 1.4 A**) cannot mimic the intraluminal blood flow that is essential for the formation and differentiation of the BBB, dynamic models use physical stimuli to create SS. Replicating both functionally and anatomically the brain microvasculature, these models create quasi-physiological conditions (Ribeiro *et al.*, 2010; Santaguida *et al.*, 2006).

The first attempt to dynamically mimic BBB was performed by Bussolari and co-researchers through the use of a purpose-built cone and plate viscometer (Bussolari *et al.*, 1982). This apparatus allowed them to expose cells to a quasi/uniform laminar or pulsatile SS. However, due to the turbulence presented by the created flow, it did not faithfully reproduce the flow experienced *in vivo*. Nonetheless, this was the first step to produce dynamic BBB models. The realized importance of SS as a vital component of any *in vitro* model was increasing, so researchers decided to focus on the development of new generations of dynamic *in vitro* systems as the dynamic *in vitro* model of the BBB (DIV-BBB; **Figure 1.4 B**) (Naik and Cucullo, 2012; Ribeiro *et al.*, 2010).

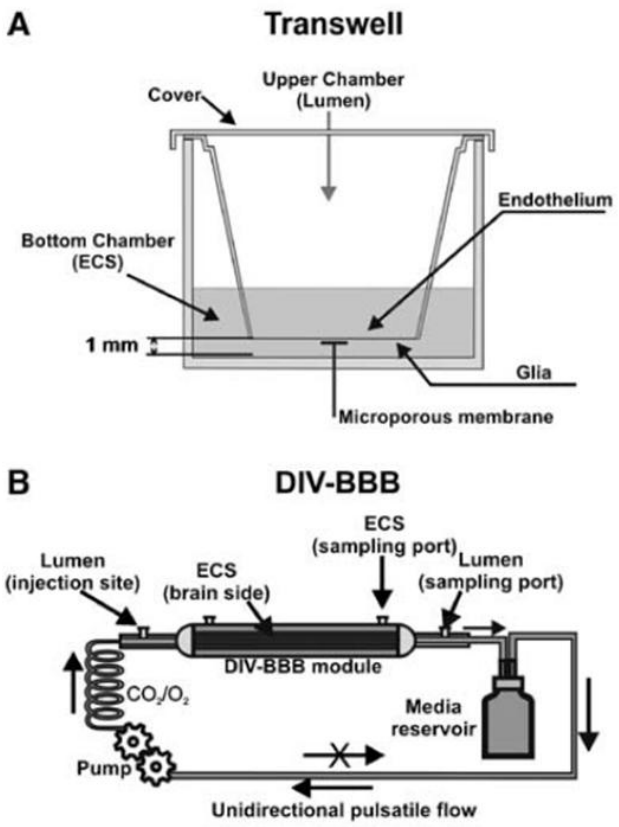

Figure 1.4. Schematic representation of the Transwell® and the DIV-BBB systems. (**A**) The static Transwell® system consists of cells grown on microporous membranes, and allows the study of bidirectional transport across the BBB. (**B**) A bundle of porous polypropylene hollow fibers is suspended in the DIV-BBB chamber. These fibers are in continuity with a medium source through a flow path consisting of gas-permeable silicon tubing. ECS stands for extracellular space. Adapted from Cucullo *et al.*, 2008.

This system allows the use of co-cultures and creates intraluminal flow through artificial capillary-like structural supports (hollow fibers) (Cucullo *et al.*, 2008; Naik and Cucullo, 2012). Endothelial cells are cultured in the lumen of hollow-fibers inside a sealed chamber and are exposed to flow while, for example, astrocytes are seeded in the extraluminal compartment to promote cellular stimuli. The intraluminal flow is generated by a pulsatile pump, which can be regulated (through the diameter of the hollow fibers and the viscosity of the medium) to produce SS levels and intraluminal pressure physiologically comparable to that observed in capillaries *in vivo* (Naik and Cucullo, 2012; Ribeiro *et al.*, 2010). DIV-BBB has several significant advantages, namely low permeability to intraluminal polar molecules, high TEER, expression of specialized transporters, ion channels, and efflux systems (Naik and Cucullo, 2012). Nonetheless, disadvantages are also present since this system is not intended to be used in drug permeability studies, requires more time and

technical skills to be established, and a high cell load is required to start the process (Naik and Cucullo, 2012). Moreover, its design does not allow for visualization of the intraluminal compartment to assess morphological and/or phenotypic changes of the vascular endothelium. Also, in contrast to conventional static BBB models, this apparatus is not designed for a high throughput pharmaceutical study (Naik and Cucullo, 2012).

Studies performed with DIV-BBB demonstrated that the co-culture of brain endothelial cells with astrocytes when under dynamic conditions developed a more stringent barrier as demonstrated by high TEER (15- to 20-fold higher values (Cucullo *et al.*, 2008)) and a selective permeability (Santaguida *et al.*, 2006).

After DIV-BBB, other models based on culturing cells using tri-dimensional extracellular matrix supports were created (Nagpal *et al.*, 2013; Ong *et al.*, 2010). These 3D systems enable close interactions between cells as well as the formation of quasi-physiological biochemical gradient exposure. Furthermore, these apparatus could also be used to study specific roles of various extracellular proteins in cell differentiation. Despite dynamic models clear advantages, their drawbacks are also assured, as more expensive and less convenient than static models (Montesano *et al.*, 1983; Naik and Cucullo, 2012).

4.3.3. Microfluidic models

Another example of dynamic models recently developed to mimic BBB is the microfluidic-BBB (MicroBBB) (Yeon *et al.*, 2012). This apparatus is a polymeric multi-layered device with a membrane in between which separates the top and bottom channel. This system not only allows cell culturing procedure, permeability tests and TEER measurements (Booth and Kim, 2012; Griep *et al.*, 2013), but also enables monitoring cell migration in a 3D environment (Naik and Cucullo, 2012). When compared to the models previously discussed, MicroBBB presents more advantages including rapid and low-cost fabrication; controlled and repeated environment with realistic microcirculatory dimensions; physiological fluid flow and SS; and a very thin culture membrane which decreases the distance between co-cultured cells (Booth and Kim, 2012; Griep *et al.*, 2013; Wilhelm *et al.*, 2011). However, the top-bottom architecture of this model limits simultaneous real-time visualization of both vascular and neuronal sides of BBB (Wilhelm *et al.*, 2011). Another key feature of this model is related to its ability to monitor changes in barrier function, which occur in response to various environmental stimuli namely diseases (Booth and Kim, 2012; Griep *et al.*, 2013; Prabhakarpandian *et al.*, 2013).

A microfluidic chip was studied by Griep and colleagues when using hCMEC/D3 cells and exposure to fluid SS. The BBB chip study showed that hCMEC/D3 cultures had comparable TEER values (36.9 ± 0.9 Ωcm^2) with the well-established Transwell® assay (28.2 ± 1.3 Ωcm^2). Furthermore, when cells were exposed to SS, barrier tightness increased up to 120 Ωcm^2 (Griep *et al.*, 2013). In another 3D microfluidic work, hCMEC/D3 cells were co-cultured with astrocytes. Authors have shown that application of SS facilitates TJ formation in the endothelial monolayer, with and without the presence of astrocyte in the surrounding matrix (Partyka *et al.*, 2017). Moreover, in several different MicroBBB studies, tighter endothelial membranes with a lower permeation of tested molecules, as well as an up regulation of TJ proteins and/or P-gp was demonstrated, compared to Transwell® BBB systems (Prabhakarpandian *et al.*, 2013; Wang *et al.*, 2016).

5. How to overcome the blood-brain barrier

Concerning reaching brain limitations, several administration strategies may be used, which can be divided into two categories: local delivery (such as intraparenchymal and intraventricular) (Alam *et al.*, 2010)) and systemic delivery (such as intravenous and intranasal). Generally, the local route constitutes an invasive approach, enabling drug delivery directly into the parenchymal space (intraparenchymal (De Boer and Gaillard, 2007)) or into the cerebral ventricle (intraventricular (Alam *et al.*, 2010)). While direct injection can be an effective modality for local delivery in some cases (e.g., in some tumors), it is not efficient for brain metastasis or neurodegenerative diseases, which require therapeutic agents to be widely spread in the brain. Moreover, BBB disruption could also be used to directly deliver substances to the brain (Pardridge, 2005), using certain chemicals or applying energy (ultrasonic waves or electromagnetic radiations (Cho *et al.*, 2016)), which exposes brain to infection and damage (Alam *et al.*, 2010). Simultaneously, the potential partial irreversibility of the disruption of BBB compromises its protective role to the CNS. These restrictions are the main reasons for lack of successful strategies that can allow localized and controlled delivery of drugs across the BBB to the desired site of injury (Bhaskar *et al.*, 2010). On the other hand, intravenous delivery is the most commonly used route to administrate large doses of drugs (Huynh *et al.*, 2006) since, although drug availability is affected by its exposure to peripheral organs and rapid clearance, it avoids first-pass metabolism and has the great potential to deliver drugs to almost all neurons in the brain (almost all neurons have their own brain capillary for oxygen and nutrient supply) (Alam *et al.*, 2010; Pardridge, 2003). The intranasal route is based on the principle that drugs exit nose sub-mucosa space into the

brain compartment. Advantages of this route came from nasal epithelium high permeability, avoidance of first-pass metabolism and self-administration. However, this administration damages the nasal mucosa and decreases the quantity of drug available (Alam *et al.*, 2010; Nagpal *et al.*, 2013). Thus, the existence of few safe and effective therapeutic options for many devastating and pervasive brain disorders encourages the raising of drug delivery systems of colloidal dimensions.

5.1. Common strategies

To overcome the BBB, without compromising its integrity, four main strategies have been applied, namely direct transporter inhibition, targeting signaling pathways that control transporter regulation (function and/or expression), targeting inflammatory and stress pathways in order to modify the transporter synthesis, and direct down-regulation of efflux transporters expression and/or transport activity (Agarwal *et al.*, 2011).

Of all the xenobiotic efflux pumps highly expressed in brain capillary endothelial cells, P-gp handles the largest fraction of commonly prescribed drugs and thus is an obvious target for manipulation. Some mechanisms by which P-gp activity in the BBB can be modulated are, regarding the strategies mentioned: (i) direct inhibition by specific competitors, (ii) functional modulation, and (iii) transcriptional modulation. All have proved potential to specifically reduce P-gp function and thus selectively increase brain permeability of its substrates.

The first approach is related to the modification of pump function by inhibitors and intracellular signals. Several relatively specific P-gp inhibitors have been developed and tested (Kemper *et al.*, 2003; Kemper *et al.*, 2004). This option depends on numerous issues, as the inhibitor affinity and reversibility, which could become serious problems (Bauer *et al.*, 2005). The first P-gp inhibitor was found by chance in 1981 by Tsuruo *et al.*, who showed that verapamil, a calcium channel blocker, inhibits P-gp-mediated drug efflux in resistant tumor cells. Then, a variety of inhibitors were developed that differ in potency, selectivity, and side effects (Avendano and Menendez, 2002; Pleban and Ecker, 2005). However, until now, only a few compounds have been tested for their potential to enhance drug delivery to the brain (Agarwal *et al.*, 2011). Due to their similarities, P-gp and BCRP have an overlap in substrate specificity. Concerning this, there are some evidences that demonstrate, for some compounds, inhibition of either BCRP or P-gp alone is not sufficient to increase delivery into

the brain (Agarwal *et al.*, 2011). Thus, it became also important to study the combined impact of these two efflux transporters on the delivery of drugs across the BBB.

The first proof-of-principle that P-gp inhibition can be used to treat brain cancer came from a study in nude mice with intracerebrally implanted human glioblastoma. In this study, Fellner *et al.* identified P-gp as the major factor in limiting the anti-cancer therapeutic paclitaxel from crossing the BBB and permeating into the CNS. Consistent with this, treating glioblastoma-bearing mice with paclitaxel had no effect on tumor size but pre-treating mice with the P-gp inhibitor valspodar increased paclitaxel brain levels and reduced tumor size by 90% (Fellner *et al.*, 2002).

Some studies already showed that absence of both P-gp and BCRP resulted in an effect that was significantly larger than the combined effects from the single transporter knockout mice. These findings suggest that inhibition of either P-gp or BCRP can be compensated by the respective other transporter, and that both transporters “cooperate” with each other in preventing chemotherapeutic drugs from entering the brain. Furthermore, for the majority of drugs, P-gp is the dominant transporter, rather than BCRP. Given the synergic effect of P-gp and BCRP at the BBB, developing compounds that are potent inhibitors of both transporters may prove beneficial. As so, elacridar is a dual P-gp/BCRP inhibitor that has undergone extensive preclinical and clinical evaluation (Agarwal *et al.*, 2011; Hyafil *et al.*, 1993) – a phase I study was performed where the lowest effective dose of elacridar to obtain maximum oral bioavailability of topotecan was determined, as well as the optimal schedule of co-administration of both drugs (Kuppens *et al.*, 2007).

The second approach, ideally, is the transiently and specific decrease of efflux to the blood through rapid regulation of transporter function. Two signaling pathways have been identified that could potentially be used to down-regulate P-gp transport activity at the BBB – one involves inflammatory mediators through protein kinase C beta I, the other one involves vascular endothelial growth factor signaling (Agarwal *et al.*, 2011). The last one results in a reversible loss of P-gp function without a decrease in export protein expression. Depression of P-gp activity by this factor is associated with phosphorylation of caveolin-1, a signal known to trigger caveolin-dependent endocytosis (Mahringer *et al.*, 2011). As well, various signaling pathways have been shown to down-regulate BCRP. As an example, it was demonstrated that estrogens play a role in BCRP regulation – estrone and 17β-estradiol reverse BCRP-mediated drug resistance (Agarwal *et al.*, 2011; Imai *et al.*, 2002).

The third idea regards the alteration of the transporter synthesis due to enhanced or inhibited transcription and translation. This topic is related with the possibility of use inflammatory and stress pathways to lower P-gp expression at the BBB. Several promoter

elements have been found so far, as pregnane X receptor ligands, but it is not clear to what extent P-gp expression can be down-regulated by removing them from the diet. In contrast to inflammation and inflammatory mediators (as interleukin-6, interleukin-1b, and tumor necrosis factor-α) which reduces transporter expression (Hartmann *et al.*, 2002; McRae *et al.*, 2003), cellular stress (e.g., exposure to heavy metals, reactive oxygen species, and some chemotherapeutics as well as heat stress) up-regulates expression of P-gp (Bauer *et al.*, 2005).

The forth strategy related to directly down-regulate efflux transporters expression and/or transport activity constitute a new and promising approach which takes advantage of siRNA and is here further discussed.

5.2. siRNA mechanism and targets

There is a potential therapeutic exploitation of gene regulation based on RNA interference. Its endogenous regulatory mechanisms rely on the sequence specific interaction between siRNA and mRNA. Therefore, these mechanisms can be activated *via* the delivery of siRNA to the cell interior, which is a short double stranded RNA that guides sequence specific mRNA degradation, and highly result in specific inhibition of gene expression through degradation of target mRNA (Dorsett and Tuschl, 2004).

RNA interference was first discovered in *Caenorhabditis elegans* when it was observed that injected double stranded RNA was far more potent at limiting gene expression than either sense or antisense strands alone (Fire *et al.*, 1998). The RNA interference mechanism of action starts by cleavage of the RNA two strands into short ~21 nucleotide RNA sequences by an endonuclease called Dicer (Zamore *et al.*, 2000). These short sequences, the siRNAs, are rapidly taken up into an enzyme complex, RNA induced silencing complex (RISC), that degrades the mRNA through guidance to a specific target mRNA resulting in specific gene silencing (Fuest *et al.*, 2009; Hammond *et al.*, 2000). At RISC (Nascimento *et al.*, 2014), one siRNA strand is taken into the effector complex, the catalytic subunit Argonaute2, and then serves as a template, guiding the hydrolysis of complementary or near complementary mRNA sequences (Fountaine *et al.*, 2005; Martinez and Tuschl, 2004).

Moreover, since it is very specific, siRNA technology is considered to be a useful approach to study the role of various proteins in neuronal physiology. Even better than the

old methods of generating knockout mice who lack the target protein (Morrison *et al.*, 1996) or generating conditional knockdown or knockin mice that only remove or express the protein following a specific treatment (Christophorou *et al.*, 2005; Perez-Martinez *et al.*, 2012). However, as all existing strategies, the use of siRNA could also have some drawbacks important to mention. Among them is poor cellular uptake and instability under physiological conditions, therefore successful siRNA therapy needs the development of drug delivery systems. Besides, the saturation of the endogenous RNA interference pathway, silencing of unwanted genes known as off-target effects and the activation of innate immunity may also arise from siRNA approach (Sioud, 2015; Xu and Wang, 2015).

Regarding siRNA mechanism, it becomes clear how this molecule can be used as a unique strategy to directly down-regulate efflux transporters expression and increase the chances to overcome BBB and reach brain treatments. On a small study, siRNA was used to target P-gp in mouse brain capillary endothelial cells. siRNA was administrated intravenously (once/day during 4 days) and it resulted in a significant reduction of the P-gp-labeled area in the hippocampal hilus and parietal cortex. P-gp expression proved to be down-regulated in these brain regions by 31 and 16%, respectively (**Figure 1.5**). This was the first preliminary evidence that a down-regulation of P-gp can be achieved in brain capillary endothelial cells by administration of siRNA *in vivo*. Furthermore, since just 2 day-treatment was not able to down-regulate BBB P-gp in a significant manner, authors conclude that this down regulation could only be achieved with a prolonged treatment (Fuest *et al.*, 2009).

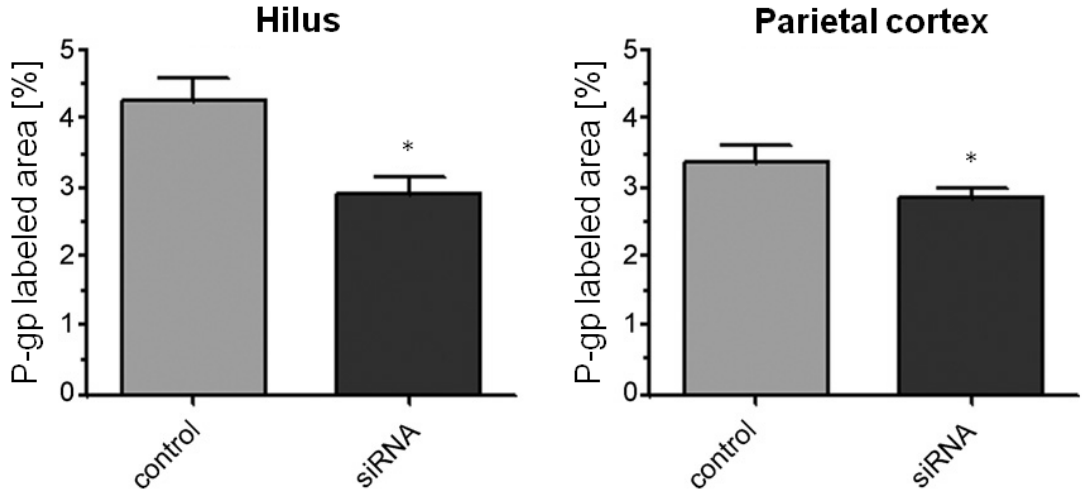

Figure 1.5. P-gp-labeled area of the hilus and the parietal cortex of control mice and mice treated with siRNA targeting Mdr1 for four consecutive days. * $p < 0.05$. Adapted from Fuest *et al.*, 2009.

Besides the most known and studied P-gp, other brain-related proteins have been siRNA targets. Hori and colleagues specifically silence the rat ABC transporter BCRP in brain capillary endothelial cells by transfection of siRNA. They were able to reduce BCRP mRNA between 55 to 79%, as well as protein levels. Additionally, BCRP-mediated mitoxantrone efflux transport was suppressed by the introduction of siRNA into cells. Authors also verified that used siRNA did not affect the mRNA levels of other ABC transporters, suggesting that it can selectively silence BCRP at the BBB (Hori *et al.*, 2005). Different studies also suggest the siRNA efficiency with other targets as the non-ABC transporter Oat3 (Hino *et al.*, 2006), and the TJ protein claudin-5 (Campbell *et al.*, 2008).

siRNA has already proven to be a promising strategy for the treatment of Huntington's disease, a progressive neurodegenerative disease caused by an expansion of a trinucleotide repeat in the Huntingtin gene, as it can specifically decrease the expression of the toxic mutant Huntingtin (HTT) protein. In order to locally and transiently disrupt the BBB to improve siRNA efficiency, focused ultrasound combined with intravascular delivery of microbubble contrast agent was used in the brain of adult rats. This technique is based on the application of concentrated acoustic energy to the target location and simultaneously systemic administration of a microbubble contrast agent. Then circulating microbubbles begin to oscillate, which leads to mechanical changes in the blood vessel wall and a transient increase in the permeability of the BBB (Hynynen *et al.*, 2001). Following this, siRNA against HTT gene treatment leads to a significant 32% reduction of HTT protein expression (which is similar to decreases observed in other studies (Rodriguez-Lebron *et al.*, 2005)) in a dose dependent manner (Burgess *et al.*, 2012).

5.3. siRNA delivery

Delivery is considered a hurdle for the development of siRNA-based therapeutics (Aagaard and Rossi, 2007). Therefore, several strategies had been proposed, including delivery of the siRNA precursor, short hairpin RNA, which is introduced in cells encoded on viral vectors. Although highly efficient and with a low rate of degradation and turnover, compared to siRNA short hairpin RNA has some disadvantages as safety concerns (some viral vectors are related to putative insertional mutagenesis), limited loading viral vectors capacity, and high production costs (Grimm *et al.*, 2006). Therefore, non-viral vectors arise as promising alternatives able to deliver siRNA and other nucleic acids into cells, potentially resulting in their functional expression (Gao *et al.*, 2011).

Chemical stabilization and conjugation with functional molecules can be used to improve the stability and permeability of siRNA (Lorenz *et al.*, 2004; Muratovska and Eccles, 2004; Turner *et al.*, 2007). However, the lack of cellular specificity could be an issue. In the case of P-gp, which is not only localized in brain capillary endothelial cells, but also in many other tissues including the gut (Watkins, 1997), its non-selective expression modulation by siRNA will enhance exposure of sensitive tissues to harmful xenobiotics (Fuest *et al.*, 2009; Loscher and Potschka, 2005). Regarding these topics, among the different approaches explored in recent years to overcome this limitation are nanoparticle-based systems, ranging from polymer particles to liposomes and inorganic systems as gold nanoparticles. In addition, different examples and types of nanoparticles were studied, proving their role on ease drug transport across the BBB (Murthy, 2007).

Nanoparticles have long been noticed to pass through the BBB, which is related to their advantageous properties as small size, customizable surface, improved drug solubility, targeted drug delivery and multifunctionality. These provide a substantial advantage for drug and gene delivery systems across the BBB, which is the first step for effective treatments of many CNS disorders (Bhaskar *et al.*, 2010). Regarding toxicity, polymeric and liposomal nanoparticles are probably the least problematic since typically they are made from or covered with natural or highly biocompatible components (Murthy, 2007).

To improve siRNA safe delivery to the CNS, the proper design of nanosystems needs to be considered to enhance BBB crossing, endosomal escape and siRNA efficiency (O'Mahony *et al.*, 2013; Perez-Martinez *et al.*, 2012). As an example, chitosan nanoparticles were assessed as a siRNA delivery system to silence P-gp in an *in vitro* BBB model. Transfection of rat brain endothelial cells with siRNA loaded in chitosan nanoparticles mediated effective knockdown of P-gp, since P-gp mRNA levels reduced to approximately 20% compared to the untreated cells. As well, a subsequent decrease in P-gp substrate efflux was detected, resulting in increased cellular delivery and efficacy of the model drug doxorubicin (Malmo *et al.*, 2013).

Another strategy used to silence HTT gene were modified amphiphilic β-cyclodextrins (CDs), based on naturally occurring oligosaccharide molecules, as siRNA neuronal carriers (Godinho *et al.*, 2013). CDs form particles with a diameter between 100 and 350 nm, which were stable up to 6h in artificial cerebrospinal fluid. 24h post transfection, these complexes were able to reduce the expression of the HTT gene by 51% in rat striatal cells and 78% in human Huntington's disease primary fibroblasts. Additionally, HTT protein levels were found to be reduced by 35% 72h post transfection in the rat model. In order to investigate knockdown efficiency *in vivo*, mice were treated with HTT naked siRNA, CD-HTT-siRNA (CD

loaded with HTT targeted siRNA), or CD-NS-siRNA (CD loaded with non-silencing siRNA). CD-HTT-siRNA was able to significantly reduce the expression of the HTT gene *in vivo* since, 4h post injection, HTT gene expression was reduced by 85%, which was maintained up to seven days (**Figure 1.6**). Both naked siRNA and NS siRNA did not have any effect on HTT gene expression levels (Godinho *et al.*, 2013). Authors concluded that the potential application of these β-CDs as siRNA carriers for CNS delivery is not restricted to Huntington's disease, but applicable to other neurodegenerative diseases (Godinho *et al.*, 2013).

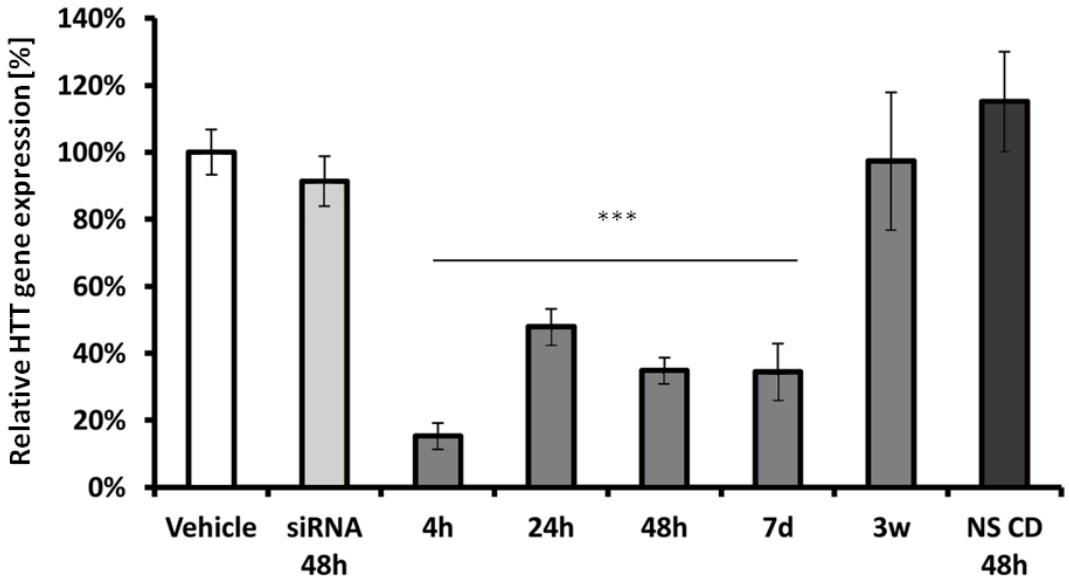

Figure 1.6. HTT gene expression in the mouse brain mediated through CD-HTT-siRNA. Mice were injected with vehicle (white), HTT naked siRNA (light grey), CD-HTT-siRNA (grey), and CD-NS-siRNA (dark grey) nanoparticles. RNA was extracted at different time points and HTT mRNA relative expression was assessed. $p < 0.001$, compared to vehicle treated animals (Godinho *et al.*, 2013).

In order to achieve stable and non toxic lipoplexes able to carry siRNA, Khatri and colleagues evaluated them as a transport system for siRNA targeted to RRM1 (enzyme responsible for development of resistance to gemcitabine in cancer cells). A cationic lipoplex composed by a mixture of different lipids was tested. Cell uptake studies and gene expression assays have confirmed intracellular availability of siRNA. Lipoplexes showed higher cellular uptake (5- to 6-fold) than that obtained with naked siRNA. Consequently, siRNA-loaded lipoplexes obtained 27% RRM1 gene expression while naked siRNA had 84%, on tested cancerous cells (Khatri *et al.*, 2014).

The combination of two systems could be advantageous, like Peddada and co-workers tested. A complex consisting of an anionic co-polymer and a cationic liposome was theirs idea to carry an antisense oligonucleotide against the apoptosis inhibitor Bcl-2. The siRNA complexes improved the gene silencing effect in human ovarian cancer cells, reducing its expression to 40% of the untreated control. *In vivo* studies showed that, after intraperitoneal injection in mice, a greater amount of siRNA is delivered to ovarian tumor xenografts using this delivery system, compared to the siRNA-loaded liposome complex. These results highlight the importance of the hydrophilic-lipophilic balance of the transport system in achieving stability and cellular uptake (Peddada *et al.*, 2014).

Other proteins were evaluated as siRNA targets, such as: green fluorescent protein (GFP) (Kumar *et al.*, 2007), Rho-associated kinase (ROCK) (Liu *et al.*, 2013), phosphatase and tensin homolog (PTEN) protein highly expressed in pyramidal neurons (Rungta *et al.*, 2013), glutamate ionotropic from aspartate receptor (GRIN1) (Rungta *et al.*, 2013), interleukin-10 (IL10) (Pradhan *et al.*, 2014), depicted on **Table 1.1**.

5.4. siRNA/drug co-delivery

In order to create an even more efficient system, the combination of siRNA and drugs in the same formulation could be really advantageous, since it would have distinct ways to act. Several works have already been performed taking the advantage of this possible synergic effect. Polymeric functionalized micelles with a nose-to-brain delivery system are an example where authors investigated the combined therapeutic effects on a rat model of malignant glioma. siRNA against Raf-1 (which plays a role in cell proliferation and apoptosis) and camptothecin anticarcinogenic drug were loaded in the same system, that was then functionalized with a trans-activator protein (TAT) to brain delivery (Kanazawa *et al.*, 2014). siRNA- and siRNA/drug-loaded functionalized systems have promoted cell death in rat glioma cells after high cellular uptake. The mean survival period of rats treated with naked siRNA solution (18.4 days) was not significantly different from that of untreated rats (16.6 days). However, the mean survival period of rats treated with siRNA-loaded functionalized nanoparticles was 20.4 days, for siRNA control/drug-loaded functionalized nanoparticles 20.6 days, and for both siRNA and drug-loaded functionalized nanoparticles was 28.4 days. This last case was significantly greater than any other option (**Figure 1.7**). The highest therapeutic effect was promoted by the additive effects of drug and siRNA co-delivery (Kanazawa *et al.*, 2014).

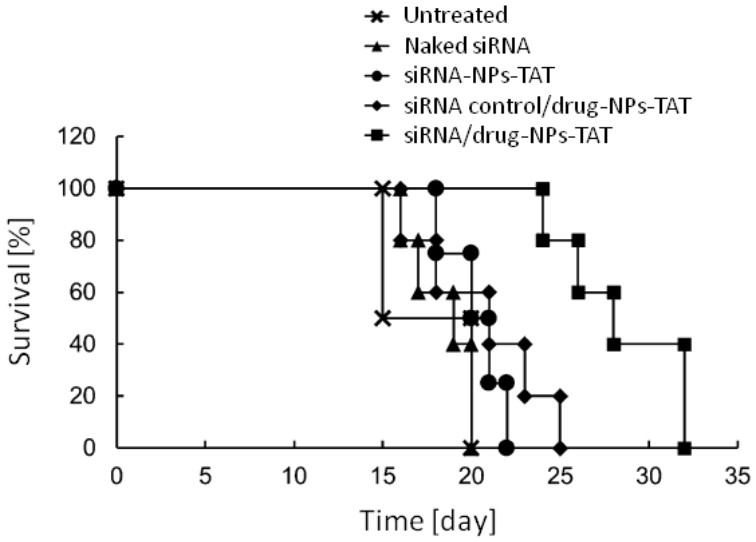

Figure 1.7. Effect of intranasal administration of Raf-1-siRNA complexed with camptothecin-loaded micelles on the survival of intracranial glioma-bearing rats. Adapted from Kanazawa *et al.*, 2014.

6. Brain Targeting

Nanoparticles have several different flexible properties that can be modified according to their aim, which make them advantageous carriers to transport drugs/genes through the organism and also, due to their ability to be functionalized, to target specific environments, tissues or organs. In order to have an efficient delivery upon administration, nanoparticles surface can be coated with polyethylene glycol (PEG), surfactants or target molecules (Wohlfart *et al.*, 2012), among other options. Nanoparticles structure and features will define the drug/gene release kinetics and characteristics. Furthermore, the internalization of nanoparticles in different cells depends on their physicochemical properties, such as size and surface charge.

Functionalization of nanocarriers is one of the most important steps and challenges in formulating nanocarriers for drug/gene delivery. Effective and highly specific conjugation strategies are used to attach biomolecules to nanoparticles surface (Bhaskar *et al.*, 2010); and there are numerous ways to functionalize nanocarriers according to its final goal. Targeting mechanisms could be either passive (as the enhanced permeability and retention effect) or active (a non-invasive way to transport drugs to pre-determined target

cells using site-specific ligands (Bhaskar *et al.*, 2010)).The main advantage of active targeting is the increase of the amount of drug/gene in the targeted tissue, thereby increasing the pharmacological response and reducing systemic side effects (De Boer and Gaillard, 2007). There are several ways (**Figure 1.8**) further described that can be followed, individually or in combination, to develop a BBB targeted effective system.

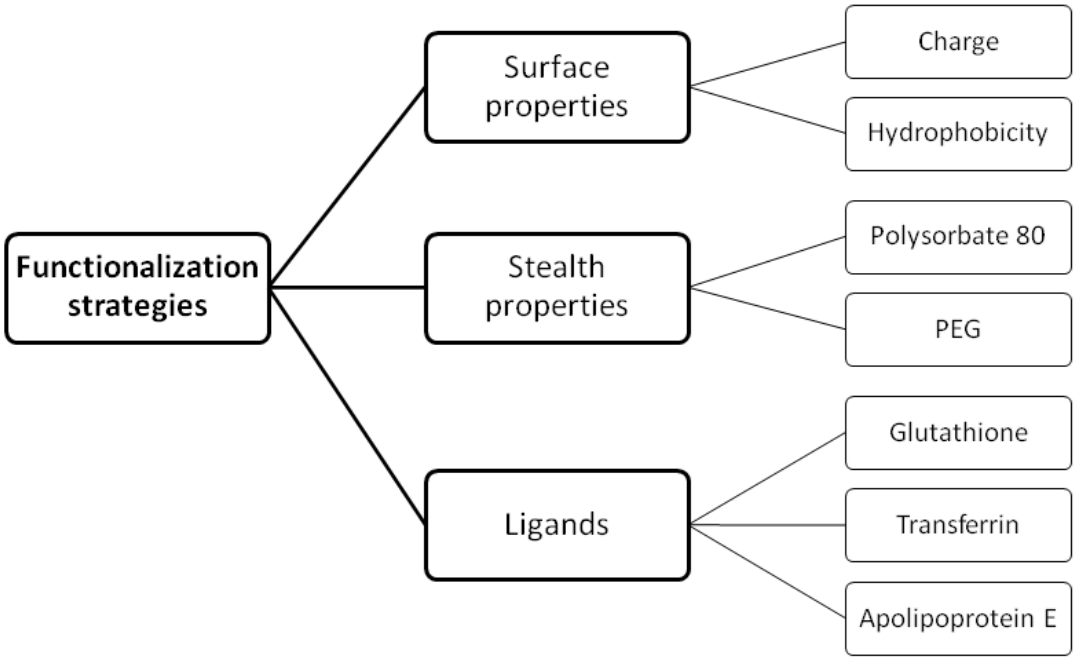

Figure 1.8. Possible strategies used to functionalize nanoparticles, directing them to the brain.

6.1. Surface properties

Nanoparticles surface properties are the key factor for a successful brain delivery. Not only surface charge but also hydrophobicity influence the adsorption of blood proteins into the systems surface, influencing nanoparticles clearance, cellular uptake, and transcytosis rate (Gessner *et al.*, 2002). The surface charge need to be assessed according to the permeability through the BBB and consequent brain distribution profiles, as well as to their toxicity and BBB-related integrity. Part of the research community agrees that neutral and slightly negative particles have no effect on BBB integrity, while high concentrations of anionic or cationic systems disrupt it (Lockman *et al.*, 2004). Despite their immediate toxic effect at the BBB, cationic nanoparticles may promote their transport across this barrier due

to the adsorption to BBB cells, which are negatively charged, through electrostatic interactions (Alam *et al.*, 2010).

6.2. Stealth properties

Usually, unmodified nanoparticles are rapidly adsorbed, mainly by opsonins, and eliminated from the organism by the macrophages of the reticuloendothelial system (Wohlfart *et al.*, 2012). Therefore, coating nanoparticles surface with proper hydrophilic and non-ionic surfactants (Araujo and Kreuter, 1999), such as polysorbate 80, or the attachment of biocompatible coatings as PEG (Brigger *et al.*, 2002) prolong nanoparticles blood circulation. Consequently, the body distribution can be modified significantly, which in some cases might improve brain delivery (Bhaskar *et al.*, 2010).

In the nanotechnology field, surfactants act especially as stabilizers and/or coating agents. Generally, nanoparticles coated with proper surfactants show decreased hepatic uptake, increased blood levels, and some revealed increased drug levels in the brain (Wilson *et al.*, 2008). Thus, it is commonly accepted that right coating could have an impact on the delivery to the BBB. Among the surfactants already investigated as coatings, the most promising is the polysorbate 80, which proved to be effective as a brain delivery enhancer in different types of systems, such as those based on poly(lactic-co-glycolic acid) (PLGA) nanoparticles (Tahara *et al.*, 2011) and lipid nanoparticles (Azhari *et al.*, 2016; Goppert and Muller, 2005). The incorporation of PEG on the nanoparticles surface is a widespread technique for delivery systems, namely the intravenously administered ones. PEG is not recognized as a foreign material by macrophages in blood, and can therefore increase the half-life of carriers (Murthy, 2007; Perez-Martinez *et al.*, 2012), enhancing the ability to cross the BBB by promoting their exposition to receptors (Schlachetzki *et al.*, 2004).

6.3. Ligands

Another strategy applied to enhance nanoparticles ability to cross the BBB is based on transporter-mediated delivery. Conjugation of nanoparticles to ligands that recognize receptors expressed at the BBB is done to take advantage of native physiological BBB nutrient transport systems (Gabathuler, 2010). Peptides and small molecules may use

specific transporters expressed on endothelial cells to promote nanoparticles uptake. Thus, only drugs/systems that closely mimic the endogenous carrier substrates would be transported into the brain (Allen *et al.*, 2003; Chen and Liu, 2012; Gabathuler, 2010). In this way, biomolecules as peptides, proteins and antibodies have been extensively used as ligands (targeting molecules) to selectively direct drugs/genes. These molecules act by recognizing and binding to target receptors or antigens. This approach is predominantly used in circumstances that these receptors/antigens are over expressed or selectively expressed by particular cells or tissue components. The most important concepts and the basis of binding targeting molecules to nanoparticles are: the ligand should selectively bind to the cell surface receptors on the targeted cells; the receptor should only be expressed on the target cells, or the expression should be higher at the target cells than in the non-target cells; and the modified nanoparticle should be stable enough in the systemic circulation to reach target cells in an effective concentration. In addition, targeting ligands can be conjugated on the surface of nanocarriers either by covalent or non-covalent linkage (Juillerat-Jeanneret, 2008).

One of the most prominent candidates to use at nanoparticles surface are cell-penetrating peptides (CPP), such as TAT, that facilitate intracellular delivery (Bhaskar *et al.*, 2010). CPPs are generally peptides of less than 30 amino acids (Lindgren and Langel, 2011). They have an enormous potential for diagnostic and therapeutic applications due to their low cytotoxicity and the tremendous variety of cargo that can be loaded (Lindgren and Langel, 2011). Recently, Liu and co-workers made a polymer core-shell system with TAT molecules anchored on its surface to antibiotic delivery. The results shown that the nanoparticles with TAT improved their cellular uptake by endothelial cells (Liu *et al.*, 2008). In order to deliver siRNA for use in neurodegenerative diseases, Malhotra and co-workers synthesized PEG coated chitosan, with further conjugation of PEG tip with a TAT. Nanoparticles were tested to deliver a functional siRNA against the Ataxin-1 gene in an *in vitro* established model of a neurodegenerative disease – spino cerebellar ataxia. This disorder is characterized by an over expression of this ataxin protein, and a loss of cells from the cerebellum and spinal cord affecting motor coordination, posture and balance. The results indicated a successful suppression of the ataxin protein 48h post transfection, as siRNA loaded on these systems was able to down-regulate more its target than bare siRNA (Malhotra *et al.*, 2013).

Glutathione (GSH) is a peptide that is being used to brain-targeting. It is an endogenous tripeptide that possesses antioxidant properties and plays a central role in the detoxification of intracellular metabolites. GSH receptor is abundantly expressed at the BBB and thus is able to mediate safe targeting and enhanced delivery of drugs to the brain (Georgieva *et al.*, 2014). Gaillard and colleagues showed an improved drug brain delivery by

using GSH PEGylated (GSH-PEG) liposomes. They studied these liposomes in healthy rats and observed that drug plasma circulation and brain uptake were significantly increased after encapsulating in GSH-PEG liposomes. Similarly, in vivo results with an autoimmune encephalomyelitis model rat showed that, while free drug had no effect, when loaded in GSH-PEG liposomes significantly reduced the disease clinical signs. In addition, the targeting by itself led to a significant more effective treatment compared non-targeted PEGylated liposomes (Gaillard *et al.*, 2012).

Besides previously reported peptides, proteins are also utilized as targeting agents. However, proteins have some clear disadvantages since they are more difficult to modify to generate derivatives. Moreover, due to the presence of the tertiary structure in proteins, they often undergo physical degradation, which may interfere with the molecular recognition (Majumdar and Siahaan, 2012).

Transferrin receptor (TfR) has been widely studied and has shown to be a promising molecular probe for targeted drug delivery. Transferrin receptors are known to be expressed in the luminal membrane of the capillary endothelium of the BBB, among other body regions. Drug targeting to the TfR, which mediates cellular uptake of iron, can be achieved by using the endogenous ligand transferrin itself, or by using antibodies/peptides directed against the TfR (Gabathuler, 2010; Moos and Morgan, 2000). Pardridge and co-researchers worked with OX-26, an antibody against the TfR. Their data have shown that drug targeting and delivery to the brain is promoted by this additional system component (De Boer and Gaillard, 2007; Pardridge *et al.*, 1991).

Another biomolecule used to functionalize nanoparticles is the apolipoprotein E (ApoE) that is involved in the transport of lipids into the brain by the low density lipoprotein (LDL) receptors, which is essential to maintain cholesterol homeostasis (Vance and Hayashi, 2010). Besides ApoE binding to various receptors on the BBB, it also binds to receptors in other CNS regions (De Boer and Gaillard, 2007). Therefore, nanoparticles could be modified with ApoE in order to improve their uptake mechanism and brain translocation (Michaelis *et al.*, 2006), which are regulated by LDL receptors (Gabathuler, 2010).

Magnetic nanoparticles are also used to transport siRNA to brain. Veiseh and colleagues studied a cancer-cell specific magnetic nanosystem for siRNA delivery and simultaneous non-invasive monitoring through magnetic resonance imaging (Veiseh *et al.*, 2010). Their nanosystem was composed by a superparamagnetic iron oxide nanoparticle core coated with PEG-grafted chitosan and polyethylenimine. It was loaded with siRNA (against GFP) and functionalized with a tumor-targeting peptide (chlorotoxin, CTX). Rat glioma cells were treated with targeted and non-targeted nanovectors, and nanoparticles-

siRNA-CTX were internalized 2-fold more than non-targeted systems, which highlights that functionalized systems readily binds to glioma cells through the affinity of CTX to its receptor. Moreover, the knockdown transgene expression of GFP in GFP+ cells were evaluated and found to be enhanced when cells were treated with targeted nanoparticles (62% reduction in GFP expression). These results suggest how receptor-mediated cellular internalization affects an enhanced knockdown (Veiseh *et al.*, 2010).

Some examples of previous works developed through the production of functional systems that act as siRNA carriers have been here described and are summarized on **Table 1.1**.

Nanoparticles are important not only due to their ability to be functionalized and improve the delivery to target cells/tissues, but also, and most significantly, thanks to their multifunctional properties. These systems can work as both diagnostic and therapeutic platforms. *In vivo* imaging of nanomaterials is an exciting recent field that can provide real-time tracking of those nanocarriers, monitoring drug delivery. With multifunctional systems, the field of brain imaging is being improved, since it became possible to monitor events at the molecular and cellular levels, as well as to track the development of neurological diseases and cancerous formations (Bhaskar *et al.*, 2010).

Table 1.1. Examples of enhanced siRNA delivery *via* nanosystems.

Nanosystem	**Target**	**Main results**	**References**
Peptide RVG	FITC GFP	siRNA delivered specifically to neuronal cells	(Kumar *et al.*, 2007)
Chitosan nanoparticles	P-gp	P-gp mRNA levels 20% reduced compared to the untreated cells	(Malmo *et al.*, 2013)
Amphiphilic cyclodextrins	HTT	HTT expression reduced by 85%, 4h post injection	(Godinho *et al.*, 2013)
Nanoparticles complexes PEG-PEI	ROCK-II	Expression of ROCK-II mRNA inhibited by 20%	(Liu *et al.*, 2013)
TAT-PEGylated chitosan nanoparticles	Ataxin-1	Target protein suppressed, 48h post transfection	(Malhotra *et al.*, 2013)
Lipid nanoparticles	PTEN GRIN1	Expression reduced by 72% and 51%, compared with non-injected control	(Rungta *et al.*, 2013)
Pathogen-mimicking microparticles	IL10	Significantly enhanced DCs Th1/Th2 cytokine ratio	(Pradhan *et al.*, 2014)
Copolymer and liposome combination	Bcl-2	Gene expression reduced to 40% of the untreated control	(Peddada *et al.*, 2014)
Cationic lipoplex	RRM1	Increased cellular uptake (6× higher than with naked siRNA); reduced gene expression (27%; 84% with naked siRNA)	(Khatri *et al.*, 2014)
CTX-magnetic nanoparticles	GFP	GFP expression reduced by 62% for nanoparticles-siRNA-CTX, compared to 35% for nanoparticles-siRNA	(Veiseh *et al.*, 2010)

Abbreviations: **Bcl-2**, apoptosis inhibitor; **CTX**, chlorotoxin; **DCs**, dendritic cells; **FITC**, fluorescein isothiocyanate; **GFP**, green fluorescent protein; **GRIN1**, glutamate ionotropic from aspartate receptor; **HTT**, Huntingtin protein; **IL10**, interleukin-10; **PEG**, polyethylene glycol; **PEI**, polyethyleneimine; **PTEN**, phosphatase and tensin homolog; **ROCK**, Rho-associated kinase; **RRM1**, ribonucleoside-diphosphate reductase large subunit; **RVG**, rabies virus glycoprotein; **TAT**, trans-activator protein; **Th1**, T helper 1 cells; **Th2**, T helper 2 cells

7. Concluding highlights

As neurological disorders numbers arise, the need for effective treatments increases. CNS distinctive environment and BBB defensive functions enhance the reaching-brain complexity. Therefore, the development of a feasible and truthful *in vitro* BBB model where blood-to-brain permeability could be assessed is fundamental for a successful study of drug-BBB interaction. Concurrently, siRNA, as a key to several approaches that silence specific genes associated to BBB protective role, turned out to be a promising and hopeful way to surpass BBB. To transport and target siRNA to attain its final goal, nanotechnology systems are used. By targeting these systems surface to the brain, their capacity to reach the target cells increase, which improves their efficacy. As well, off-target and harmful systemic side effects decrease.

8. References

Aagaard, L. and Rossi, J.J. 2007. RNAi therapeutics: principles, prospects and challenges. Adv Drug Deliv Rev. 59: 75-86.

Abbott, N.J. 2013. Blood–brain barrier structure and function and the challenges for CNS drug delivery. J Inherit Metab Dis. 36 (3): 437-449.

Abbott, N.J., Patabendige, A.A., Dolman, D.E., Yusof, S.R. and Begley, D.J. 2010. Structure and function of the blood-brain barrier. Neurobiol Dis. 37 (1): 13-25.

Abbott, N.J., Ronnback, L. and Hansson, E. 2006. Astrocyte-endothelial interactions at the blood-brain barrier. Nat Rev Neurosci. 7 (1): 41-53.

Agarwal, S., Hartz, A.M.S., Elmquist, W.F. and Bauer, B. 2011. Breast cancer resistance protein and P-glycoprotein in brain cancer: two gatekeepers team up. Curr Pharm Design. 17: 2793-2802.

Akanuma, S., Hosoya, K., Ito, S., Tachikawa, M., Terasaki, T. and Ohtsuki, S. 2010. Involvement of multidrug resistance-associated protein 4 in efflux transport of prostaglandin E(2) across mouse blood-brain barrier and its inhibition by intravenous administration of cephalosporins. J Pharmacol Exp Ther. 333 (3): 912-919.

Alam, M.I., Beg, S., Samad, A., Baboota, S., Kohli, K., Ali, J., Ahuja, A. and Akbar, M. 2010. Strategy for effective brain drug delivery. Eur J Pharm Sci. 40 (5): 385-403.

Allen, D.D., Lockman, P.R., Roder, K.E., Dwoskin, L.P. and Crooks, P.A. 2003. Active transport of high-affinity choline and nicotine analogs into the central nervous system

by the blood-brain barrier choline transporter. J Pharmacol Exp Ther. 304 (3): 1268-1274.

Araujo, L.L., R. and Kreuter, J. 1999. Influence of the surfactant concentration on the body distribution of nanoparticles. J Drug Target. 6 (5): 373-385.

Armulik, A., Genové, G., Mäe, M., Nisancioglu, M.H., Wallgard, E., Niaudet, C., He, L., Norlin, J., Lindblom, P. and Strittmatter, K. 2010. Pericytes regulate the blood-brain barrier. Nature. 468 (7323): 557-561.

Avendano, C. and Menendez, J.C. 2002. Inhibitors of multidrug resistance to antitumor agents (MDR). Curr Med Chem. 9 (2): 159-193.

Azhari, H., Strauss, M., Hook, S., Boyd, B.J. and Rizwan, S.B. 2016. Stabilising cubosomes with Tween 80 as a step towards targeting lipid nanocarriers to the blood-brain barrier. Eur J Pharm Biopharm. 104: 148-155.

Ballabh, P., Braun, A. and Nedergaard, M. 2004. The blood-brain barrier: an overview: structure, regulation, and clinical implications. Neurobiol Dis. 16 (1): 1-13.

Bauer, B., Hartz, A.M.S., Fricker, G. and Miller, D.S. 2005. Modulation of P-glycoprotein transport function at the blood-brain barrier. Exp Biol Med. 230 (2): 118-127.

Berezowski, V., Landry, C., Dehouck, M.P., Cecchelli, R. and Fenart, L. 2004. Contribution of glial cells and pericytes to the mRNA profiles of P-glycoprotein and multidrug resistance-associated proteins in an in vitro model of the blood-brain barrier. Brain Res. 1018 (1): 1-9.

Bhaskar, S., Tian, F., Stoeger, T., Kreyling, W., de la Fuente, J.M., Grazu, V., Borm, P., Estrada, G., Ntziachristos, V. and Razansky, D. 2010. Multifunctional nanocarriers for diagnostics, drug delivery and targeted treatment across blood-brain barrier: perspectives on tracking and neuroimaging. Part Fibre Toxicol. 7 (3): 1-25.

Booth, R. and Kim, H. 2012. Characterization of a microfluidic in vitro model of the blood-brain barrier (muBBB). Lab Chip. 12 (10): 1784-1792.

Brigger, I., Morizet, J., Aubert, G., Chacun, H., Terrier-Lacombe, M.J., Couvreur, P. and Vassal, G. 2002. Poly(ethylene glycol)-coated hexadecylcyanoacrylate nanospheres display a combined effect for brain tumor targeting. J Pharmacol Exp Ther. 303 (3): 928-936.

Buckley, S.T., Fischer, S.M., Fricker, G. and Brandl, M. 2012. In vitro models to evaluate the permeability of poorly soluble drug entities: challenges and perspectives. Eur J Pharm Sci. 45 (3): 235-250.

Burgess, A., Huang, Y., Querbes, W., Sah, D.W. and Hynynen, K. 2012. Focused ultrasound for targeted delivery of siRNA and efficient knockdown of Htt expression. J Control Release. 163 (2): 125-129.

Bussolari, S.R., Dewey, C.F. and Gimbrone, M.A. 1982. Apparatus for subjecting living cells to fluid shear stress. Rev Sci Instrum. 53 (12): 1851-1854.

Campbell, M., Kiang, A.S., Kenna, P.F., Kerskens, C., Blau, C., O'Dwyer, L., Tivnan, A., Kelly, J.A., Brankin, B., Farrar, G.J. and Humphries, P. 2008. RNAi-mediated reversible opening of the blood-brain barrier. J Gene Med. 10 (8): 930-947.

Cardoso, F.L., Brites, D. and Brito, M.A. 2010. Looking at the blood–brain barrier: molecular anatomy and possible investigation approaches. Brain Res Rev. 64 (2): 328-363.

Cestelli, A., Catania, C., D'Agostino, S., Liegro, I.D., Licata, L., Schiera, G., Pitarresi, G.L., Savettieri, G., Caro, V.D., Giandalia, G. and Giannola, L.I. 2001. Functional feature of a novel model of blood brain barrier: studies on permeation of test compounds. J Control Release. 76: 139-147.

Chen, Y. and Liu, L. 2012. Modern methods for delivery of drugs across the blood–brain barrier. Adv Drug Deliver Rev. 64 (7): 640-665.

Cho, H., Lee, H.Y., Han, M., Choi, J.R., Ahn, S., Lee, T., Chang, Y. and Park, J. 2016. Localized down-regulation of P-glycoprotein by focused ultrasound and microbubbles induced blood-brain barrier disruption in rat brain. Sci Rep. 6: 31201.

Choi, Y.K. and Kim, K.-W. 2008a. Blood-neural barrier: its diversity and coordinated cell-to-cell communication. Genesis. 10: 11.

Choi, Y.K. and Kim, K.W. 2008b. Blood-neural barrier: its diversity and coordinated cell-to-cell communication. BMB Rep. 41 (5): 345-352.

Christophorou, M.A., Martin-Zanca, D., Soucek, L., Lawlor, E.R., Brown-Swigart, L., Verschuren, E.W. and Evan, G.I. 2005. Temporal dissection of p53 function in vitro and in vivo. Nat Genet. 37: 718-726.

Cucullo, L., Couraud, P.O., Weksler, B., Romero, I.A., Hossain, M., Rapp, E. and Janigro, D. 2008. Immortalized human brain endothelial cells and flow-based vascular modeling: a marriage of convenience for rational neurovascular studies. J Cereb Blood Flow Metab. 28 (2): 312-328.

Cucullo, L., Hossain, M., Puvenna, V., Marchi, N. and Janigro, D. 2011. The role of shear stress in blood-brain barrier endothelial physiology. BMC Neurosci. 12 (40): 1-15.

De Boer, A.G. and Gaillard, P.J. 2007. Drug targeting to the brain. Annu Rev Pharmacol Toxicol. 47: 323-355.

Demeuse, P., Fragner, P., Leroy-Noury, C., Mercier, C., Payen, L., Fardel, O., Couraud, P.O. and Roux, F. 2004. Puromycin selectively increases mdr1a expression in immortalized rat brain endothelial cell lines. J Neurochem. 88: 23-31.

Dorsett, Y. and Tuschl, T. 2004. siRNAs: applications in functional genomics and potential as therapeutics. Nat Rev Drug Discov. 3: 318-329.

Engesland, A., Skar, M., Hansen, T., Skalko-Basnet, N. and Flaten, G.E. 2013. New applications of phospholipid vesicle-based permeation assay: permeatiom model mimicking skin barrier. J Pharm Sci. 102 (5): 1588-1600.

Farm, H. on Brain Tumour Research, Inc. Available Web Page: http://www.braintumourresearch.org/statistics (last accessed October 17, 2014).

Fellner, S., Bauer, B., Miller, D.S., Schaffrik, M., Fankhänel, M., Spruß, T., Bernhardt, G., Graeff, C., Färber, L., Gschaidmeier, H., Buschauer, A. and Fricker, G. 2002. Transport of paclitaxel (Taxol) across the blood-brain barrier in vitro and in vivo. J Clin Invest. 110 (9): 1309-1318.

Fire, A., Xu, S., Montgomery, M.K., Kostas, S.A., Driver, S.E. and Mello, C.C. 1998. Potent and specific genetic interference by double-stranded RNA in Caenorhabditis elegans. Nature. 391: 806-811.

Fisher, M. 2009. Pericyte signaling in the neurovascular unit. Stroke. 40: S13-S15.

Fisher, M., Abramov, M., Van Aerschot, A., Xu, D., Juliano, R.L. and Herdewijn, P. 2007. Inhibition of MDR1 expression with altritol-modified siRNAs. Nucleic Acids Res. 35 (4): 1064-1074.

Flaten, G.E., Dhanikula, A.B., Luthman, K. and Brandl, M. 2006. Drug permeability across a phospholipid vesicle based barrier: a novel approach for studying passive diffusion. Eur J Pharm Sci. 27 (1): 80-90.

Flaten, G.E., Luthman, K., Vasskog, T. and Brandl, M. 2008. Drug permeability across a phospholipid vesicle-based barrier 4. The effect of tensides, co-solvents and pH changes on barrier integrity and on drug permeability. Eur J Pharm Sci. 34 (2-3): 173-180.

Fountaine, T.M., Wood, M.J.A. and Wade-Martins, R. 2005. Delivering RNA interference to the mammalian brain. Curr Gene Ther. 5: 399-410.

Fuest, C., Bankstahl, M., Winter, P., Helm, M., Pekcec, A. and Potschka, H. 2009. In vivo down-regulation of mouse brain capillary P-glycoprotein: a preliminary investigation. Neurosci Lett. 464 (1): 47-51.

Gabathuler, R. 2010. Approaches to transport therapeutic drugs across the blood-brain barrier to treat brain diseases. Neurobiol Dis. 37 (1): 48-57.

Gaillard, P.J., Appeldoorn, C.C., Rip, J., Dorland, R., van der Pol, S.M., Kooij, G., de Vries, H.E. and Reijerkerk, A. 2012. Enhanced brain delivery of liposomal methylprednisolone improved therapeutic efficacy in a model of neuroinflammation. J Control Release. 164 (3): 364-369.

Gao, Y., Liu, X.L. and Li, X.R. 2011. Research progress on siRNA delivery with nonviral carriers. Int J Nanomedicine. 6: 1017-1025.

Georgieva, J.V., Hoekstra, D. and Zuhorn, I.S. 2014. Smuggling drugs into the brain: an overview of ligands targeting transcytosis for drug delivery across the blood-brain barrier. Pharm. 6 (4): 557-583.

Gessner, A., Lieske, A., Paulke, B.R. and Muller, R.H. 2002. Influence of surface charge density on protein adsorption on polymeric nanoparticles: analysis by two-dimensional electrophoresis. Eur J Pharm Biopharm. 54 (2): 165-170.

Gilmore, J.L., Yi, X., Quan, L. and Kabanov, A.V. 2008. Novel nanomaterials for clinical neuroscience. J Neuroimmune Pharmacol. 3 (2): 83-94.

Godinho, B.M., Ogier, J.R., Darcy, R., O'Driscoll, C.M. and Cryan, J.F. 2013. Self-assembling modified beta-cyclodextrin nanoparticles as neuronal siRNA delivery vectors: focus on Huntington's disease. Mol Pharm. 10 (2): 640-649.

Goppert, T.M. and Muller, R.H. 2005. Polysorbate-stabilized solid lipid nanoparticles as colloidal carriers for intravenous targeting of drugs to the brain: comparison of plasma protein adsorption patterns. J Drug Target. 13 (3): 179-187.

Griep, L.M., Wolbers, F., de Wagenaar, B., ter Braak, P.M., Weksler, B.B., Romero, I.A., Couraud, P.O., Vermes, I., van der Meer, A.D. and van den Berg, A. 2013. BBB on chip: microfluidic platform to mechanically and biochemically modulate blood-brain barrier function. Biomed Microdevices. 15 (1): 145-150.

Grimm, D., Streetz, K.L., Jopling, C.L., Storm, T.A., Pandey, K., Davis, C.R., Marion, P., Salazar, F. and Kay, M.A. 2006. Fatality in mice due to oversaturation of cellular microRNA/short hairpin RNA pathways. Nature. 441 (7092): 537-541.

Hammond, S.M., Bernstein, E., Beach, D. and Hannon, G.J. 2000. An RNA-directed nuclease mediates post-transcriptional gene silencing in Drosophila cells. Nature. 404: 293-296.

Hartmann, G., Cheung, A.K. and Piquette-Miller, M. 2002. Inflammatory cytokines, but not bile acids, regulate expression of murine hepatic anion transporters in endotoxemia. J Pharmacol Exp Ther. 303: 273-281.

Hatherell, K., Couraud, P.O., Romero, I.A., Weksler, B. and Pilkington, G.J. 2011. Development of a three-dimensional, all-human in vitro model of the blood-brain barrier using mono-, co-, and tri-cultivation Transwell models. J Neurosci Methods. 199 (2): 223-229.

Hawkins, B.T. and Davis, T.P. 2005. The blood-brain barrier/neurovascular unit in health and disease. Pharmacol Rev. 57 (2): 173-185.

Hayashi, K., Nakao, S., Nakaoke, R., Nakagawa, S., Kitagawa, N. and Niwa, M. 2004. Effects of hypoxia on endothelial/pericytic co-culture model of the blood-brain barrier. Regul Pept. 123 (1-3): 77-83.

Hermann, D.M. and Patak, P. 2011. Bringing drugs into the injured brain and keeping them there. Curr Pharm Design. 17: 2748-2749.

Hino, T., Yokota, T., Ito, S., Nishina, K., Kang, Y.S., Mori, S., Hori, S., Kanda, T., Terasaki, T. and Mizusawa, H. 2006. In vivo delivery of small interfering RNA targeting brain capillary endothelial cells. Biochem Bioph Res Co. 340 (1): 263-267.

Hori, S., Ohtsuki, S., Ichinowatari, M., Yokota, T., Kanda, T. and Terasaki, T. 2005. Selective gene silencing of rat ATP-binding cassette G2 transporter in an in vitro blood-brain barrier model by short interfering RNA. J Neurochem. 93 (1): 63-71.

Huynh, G.H., Deen, D.F. and Szoka Jr, F.C. 2006. Barriers to carrier mediated drug and gene delivery to brain tumors. J Control Release. 110 (2): 236-259.

Hyafil, F., Vergely, C., Du Vignaud, P. and Grand-Perret, T. 1993. In vitro and in vivo reversal of multidrug resistance by GF120918, an acridonecarboxamide derivative. Cancer Res. 53 (19): 4595-4602.

Hynynen, K., McDannold, N., Vykhodtseva, N. and Jolesz, F.A. 2001. Noninvasive MR imaging-guided focal opening of the blood–brain barrier in rabbits. Radiology. 220: 640-646.

Imai, Y., Tsukahara, S., Ishikawa, E., Tsuruo, T. and Sugimoto, Y. 2002. Estrone and 17beta-estradiol reverse breast cancer resistance protein-mediated multidrug resistance. Jpn J Cancer Res. 93 (3): 231-235.

Juillerat-Jeanneret, L. 2008. The targeted delivery of cancer drugs across the blood–brain barrier: chemical modifications of drugs or drug-nanoparticles? Drug Discov Today. 13 (23-24): 1099-1106.

Kanazawa, T., Morisaki, K., Suzuki, S. and Takashima, Y. 2014. Prolongation of life in rats with malignant glioma by intranasal siRNA/drug codelivery to the brain with cell-penetrating peptide-modified micelles. Mol Pharm. 11 (5): 1471-1478.

Kemper, E.M., van Zandbergen, A.E., Cleypool, C., Mos, H.A., Boogerd, W., Beijnen, J.H. and van Tellingen, O. 2003. Increased penetration of paclitaxel into the brain by inhibition of P-glycoprotein. Clin Cancer Res. 9: 2849-2855.

Kemper, E.M., Verheij, M., Boogerd, W., Beijnen, J.H. and van Tellingen, O. 2004. Improved penetration of docetaxel into the brain by co-administration of inhibitors of P-glycoprotein. Eur J Cancer. 40: 1269-1274.

Khatri, N., Baradia, D., Vhora, I., Rathi, M. and Misra, A. 2014. Development and characterization of siRNA lipoplexes: effect of different lipids, in vitro evaluation in cancerous cell lines and in vivo toxicity study. AAPS PharmSciTech. 15 (6): 1630-1643.

Kumar, P., Wu, H., McBride, J.L., Jung, K.E., Kim, M.H., Davidson, B.L., Lee, S.K., Shankar, P. and Manjunath, N. 2007. Transvascular delivery of small interfering RNA to the central nervous system. Nature. 448 (7149): 39-43.

Kuppens, I.E., Witteveen, E.O., Jewell, R.C., Radema, S.A., Paul, E.M., Mangum, S.G., Beijnen, J.H., Voest, E.E. and Schellens, J.H. 2007. A phase I, randomized, open-label, parallel-cohort, dose-finding study of elacridar (GF120918) and oral topotecan in cancer patients. Clin Cancer Res. 13 (11): 3276-3285.

Li, G., Simon, M.J., Cancel, L.M., Shi, Z.D., Ji, X., Tarbell, J.M., Morrison, B., 3rd and Fu, B.M. 2010. Permeability of endothelial and astrocyte cocultures: in vitro blood-brain barrier models for drug delivery studies. Ann Biomed Eng. 38 (8): 2499-2511.

Lin, F., Marchetti, S., Pluim, D., Iusuf, D., Mazzanti, R., Schellens, J.H., Beijnen, J.H. and van Tellingen, O. 2013. Abcc4 together with abcb1 and abcg2 form a robust cooperative drug efflux system that restricts the brain entry of camptothecin analogues. Clin Cancer Res. 19 (8): 2084-2095.

Lindgren, M. and Langel, U. 2011. Classes and prediction of cell-penetrating peptides. Methods Mol Biol. 683: 3-19.

Liu, L., Guo, K., Lu, J., Venkatraman, S.S., Luo, D., Ng, K.C., Ling, E.A., Moochhala, S. and Yang, Y.Y. 2008. Biologically active core/shell nanoparticles self-assembled from cholesterol-terminated PEG–TAT for drug delivery across the blood–brain barrier. Biomaterials. 29 (10): 1509-1517.

Liu, Q., Hou, J., Chen, X., Liu, G., Zhang, D., Sun, H. and Zhang, J. 2014. P-Glycoprotein mediated efflux limits the transport of the novel anti-Parkinson's disease candidate drug FLZ across the physiological and PD pathological in vitro BBB models. PLoS One. 9 (7): 1-9.

Liu, Y., Liu, Z., Wang, Y., Liang, Y.R., Wen, X., Hu, J., Yang, X., Liu, J., Xiao, S. and Cheng, D. 2013. Investigation of the performance of PEG-PEI/ROCK-II-siRNA complexes for Alzheimer's disease in vitro. Brain Res. 1490: 43-51.

Lockman, P.R., Koziara, J.M., Mumper, R.J. and Allen, D.D. 2004. Nanoparticle surface charges alter blood-brain barrier integrity and permeability. J Drug Target. 12 (9-10): 635-641.

Lorenz, C., Hadwiger, P., John, M., Vornlocher, H.P. and Unverzagt, C. 2004. Steroid and lipid conjugates of siRNAs to enhance cellular uptake and gene silencing in liver cells. Bioorg Med Chem Lett. 14: 4975-4977.

Loscher, W. and Potschka, H. 2005. Role of drug efflux transporters in the brain for drug disposition and treatment of brain diseases. Prog Neurobiol. 76: 22-76.

Mahringer, A., Ott, M., Reimold, I., Reichel, V. and Fricker, G. 2011. The ABC of the blood-brain barrier - regulation of drug efflux pumps. Curr Pharm Design. 17: 2762-2770.

Majumdar, S. and Siahaan, T.J. 2012. Peptide-mediated targeted drug delivery. Med Res Rev. 32 (3): 637-658.

Malhotra, M., Tomaro-Duchesneau, C. and Prakash, S. 2013. Synthesis of TAT peptide-tagged PEGylated chitosan nanoparticles for siRNA delivery targeting neurodegenerative diseases. Biomaterials. 34 (4): 1270-1280.

Malmo, J., Sandvig, A., Varum, K.M. and Strand, S.P. 2013. Nanoparticle mediated P-glycoprotein silencing for improved drug delivery across the blood-brain barrier: a siRNA-chitosan approach. PLoS One. 8 (1): 1-8.

Martinez, J. and Tuschl, T. 2004. RISC is a 5' phosphomonoester-producing RNA endonuclease. Genes Dev. 18: 975-980.

McRae, M.P., Brouwer, K.L. and Kashuba, A.D. 2003. Cytokine regulation of P-glycoprotein. Drug Metab Rev. 35: 19-33.

Michaelis, K., Hoffmann, M.M., Dreis, S., Herbert, E., Alyautdin, R.N., Michaelis, M., Kreuter, J. and Langer, K. 2006. Covalent linkage of apolipoprotein e to albumin nanoparticles strongly enhances drug transport into the brain. J Pharmacol Exp Ther. 317 (3): 1246-1253.

Montesano, R., Orci, L. and Vassalli, P. 1983. In vitro rapid organization of endothelial cells into capillary-like networks is promoted by collagen matrices. J Cell Biol. 97: 1648-1652.

Moos, T. and Morgan, E.H. 2000. Transferrin and transferrin receptor function in brain barrier systems. Cell Mol Neurobiol. 20 (1): 77-95.

Morrison, R.S., Wenzel, H.J., Kinoshita, Y., Robbins, C.A., Done-hower, L.A. and Schwartzkroin, P.A. 1996. Loss of the p53 tumor suppressor gene protects neurons from kainate-induced cell death. J Neurosci. 16: 1337-1345.

Muratovska, A. and Eccles, M.R. 2004. Conjugate for efficient delivery of short interfering RNA (siRNA) into mammalian cells. Febs Lett. 558: 63-68.

Murthy, S.K. 2007. Nanoparticles in modern medicine: State of the art and future challenges. Int J Nanomedicine. 2 (2): 129-141.

Nagpal, K., Singh, S.K. and Mishra, D.N. 2013. Drug targeting to brain: a systematic approach to study the factors, parameters and approaches for prediction of permeability of drugs across BBB. Expert Opin Drug Deliv. 10 (7): 927-955.

Naik, P. and Cucullo, L. 2012. In vitro blood-brain barrier models: current and perspective technologies. J Pharm Sci. 101 (4): 1337-1354.

Nakagawa, S., Deli, M.A., Kawaguchi, H., Shimizudani, T., Shimono, T., Kittel, A., Tanaka, K. and Niwa, M. 2009. A new blood-brain barrier model using primary rat brain endothelial cells, pericytes and astrocytes. Neurochem Int. 54 (3-4): 253-263.

Nascimento, A.V., Bousbaa, H., Ferreira, D. and Sarmento, B. 2014. Non-small cell lung carcinoma: an overview on targeted therapy. Curr Drug Targets. 15 (8): 1-16.

O'Mahony, A.M., Godinho, B.M., Cryan, J.F. and O'Driscoll, C.M. 2013. Non-viral nanosystems for gene and small interfering RNA delivery to the central nervous system: formulating the solution. J Pharm Sci. 102 (10): 3469-3484.

Ong, S.M., Zhao, Z., Arooz, T., Zhao, D., Zhang, S., Du, T., Wasser, M., van Noort, D. and Yu, H. 2010. Engineering a scaffold-free 3D tumor model for in vitro drug penetration studies. Biomaterials. 31 (6): 1180-1190.

Pardridge, W.M. 2003. Blood-brain barrier drug targeting: the future of brain drug development. Mol Interv. 3 (2): 90-105.

Pardridge, W.M. 2005. The blood-brain barrier: bottleneck in brain drug development. NeuroRx. 2 (1): 3-14.

Pardridge, W.M., Buciak, J.L. and Friden, P.M. 1991. Selective transport of an anti-transferrin receptor antibody through the blood-brain barrier in vivo. J Pharmacol Exp Ther. 259 (1): 66-70.

Partyka, P.P., Godsey, G.A., Galie, J.R., Kosciuk, M.C., Acharya, N.K., Nagele, R.G. and Galie, P.A. 2017. Mechanical stress regulates transport in a compliant 3D model of the blood-brain barrier. Biomaterials. 115: 30-39.

Paturi, D.K., Kwatra, D., Ananthula, H.K., Pal, D. and Mitra, A.K. 2010. Identification and functional characterization of breast cancer resistance protein in human bronchial epithelial cells (Calu-3). Int J Pharm. 384 (1-2): 32-38.

Peddada, L.Y., Garbuzenko, O.B., Devore, D.I., Minko, T. and Roth, C.M. 2014. Delivery of antisense oligonucleotides using poly(alkylene oxide)-poly(propylacrylic acid) graft copolymers in conjunction with cationic liposomes. J Control Release. 194C: 103-112.

Perez-Martinez, F.C., Carrion, B. and Cena, V. 2012. The use of nanoparticles for gene therapy in the nervous system. J Alzheimers Dis. 31 (4): 697-710.

Pleban, K. and Ecker, G.F. 2005. Inhibitors of p-glycoprotein--lead identification and optimisation. Mini Rev Med Chem. 5 (2): 153-163.

Prabhakarpandian, B., Shen, M.C., Nichols, J.B., Mills, I.R., Sidoryk-Wegrzynowicz, M., Aschner, M. and Pant, K. 2013. SyM-BBB: a microfluidic blood brain barrier model. Lab Chip. 13 (6): 1093-1101.

Pradhan, P., Qin, H., Leleux, J.A., Gwak, D., Sakamaki, I., Kwak, L.W. and Roy, K. 2014. The effect of combined IL10 siRNA and CpG ODN as pathogen-mimicking microparticles on Th1/Th2 cytokine balance in dendritic cells and protective immunity against B cell lymphoma. Biomaterials. 35 (21): 5491-5504.

Research And Markets 2007. Drug delivery technology - revolutionizing CNS therapies. (PharmaVision).

Ribeiro, M.M.B., Castanho, M.A.R.B. and Serrano, I. 2010. In vitro blood-brain barrier models-latest advances and therapeutic applications in a chronological perspective. Mini-Rev Med Chem. 10 (3): 263-271.

Robillard, K.R., Chan, G.N., Zhang, G., la Porte, C., Cameron, W. and Bendayan, R. 2014. Role of P-glycoprotein in the distribution of the HIV protease inhibitor atazanavir in the brain and male genital tract. Antimicrob Agents Chemother. 58 (3): 1713-1722.

Rodriguez-Lebron, E., Denovan-Wright, E.M., Nash, K., Lewin, A.S. and Mandel, R.J. 2005. Intrastriatal rAAV-mediated delivery of anti-huntingtin shRNAs induces partial reversal of disease progression in R6/1 Huntington's disease transgenic mice. Mol Ther. 12: 618-633.

Rungta, R.L., Choi, H.B., Lin, P.J., Ko, R.W., Ashby, D., Nair, J., Manoharan, M., Cullis, P.R. and Macvicar, B.A. 2013. Lipid nanoparticle delivery of siRNA to silence neuronal gene expression in the brain. Mol Ther Nucleic Acids. 2: 1-12.

Sanchez-Covarrubias, L., Slosky, L.M., Thompson, B.J., Zhang, Y., Laracuente, M.L., DeMarco, K.M., Ronaldson, P.T. and Davis, T.P. 2014. P-glycoprotein modulates morphine uptake into the CNS: a role for the non-steroidal anti-inflammatory drug diclofenac. PLoS One. 9 (2): 1-11.

Santaguida, S., Janigro, D., Hossain, M., Oby, E., Rapp, E. and Cucullo, L. 2006. Side by side comparison between dynamic versus static models of blood? brain barrier in vitro: a permeability study. Brain Res. 1109 (1): 1-13.

Sauna, Z.E., Nandigama, K. and Ambudkar, S.V. 2004. Multidrug resistance protein 4 (ABCC4)-mediated ATP hydrolysis: effect of transport substrates and characterization of the post-hydrolysis transition state. J Biol Chem. 279 (47): 48855-48864.

Schinkel, A.H., Wagenaar, E. and Mol, C.A.v.D., L. 1996. P-glycoprotein in the blood-brain barrier of mice influences the brain penetration and pharmacological activity of many drugs. J Clin Invest. 97 (11): 2517-2524.

Schlachetzki, F., Zhang, Y., Boado, R.J. and Pardridge, W.M. 2004. Gene therapy of the brain: the trans-vascular approach. Neurology. 62 (8): 1275-1281.

Shi, D., Sun, L., Mi, G., Sheikh, L., Bhattacharya, S., Nayar, S. and Webster, T.J. 2014. Controlling ferrofluid permeability across the blood-brain barrier model. Nanotechnology. 25 (7): 1-5.

Sioud, M. 2015. Overcoming the challenges of siRNA activation of innate immunity: design better therapeutic siRNAs. Method Mol Biol. 1218: 301-319.

Tahara, K., Miyazaki, Y., Kawashima, Y., Kreuter, J. and Yamamoto, H. 2011. Brain targeting with surface-modified poly(D,L-lactic-co-glycolic acid) nanoparticles delivered via carotid artery administration. Eur J Pharm Biopharm. 77 (1): 84-88.

Tontsch, U. and Bauer, H.C. 1991. Glial cells and neurons induce blood-brain barrier related enzymes in cultured cerebral endothelial cells. Brain Res. 539: 247-253.

Turner, J.J., Jones, S., Fabani, M.M., Ivanova, G., Arzumanov, A.A. and Gait, M.J. 2007. RNA targeting with peptide conjugates of oligonucleotides, siRNA and PNA. Blood Cells Mol Dis. 38: 1-7.

United Nations. 2007. World Population Prospects, The 2006 Revision: Population Division, Department of Economic and Social Affairs. New York, NY, USA.

Vance, J.E. and Hayashi, H. 2010. Formation and function of apolipoprotein E-containing lipoproteins in the nervous system. Biochim Biophys Acta. 1801 (8): 806-818.

Veiseh, O., Kievit, F.M., Fang, C., Mu, N., Jana, S., Leung, M.C., Mok, H., Ellenbogen, R.G., Park, J.O. and Zhang, M. 2010. Chlorotoxin bound magnetic nanovector tailored for cancer cell targeting, imaging, and siRNA delivery. Biomaterials. 31 (31): 8032-8042.

Vilas-Boas, V., Silva, R., Guedes-de-Pinho, P., Carvalho, F., Bastos, M.L. and Remiao, F. 2014. RBE4 cells are highly resistant to paraquat-induced cytotoxicity: studies on uptake and efflux mechanisms. J Appl Toxicol. 34 (9): 1023-1030.

Wang, J.D., Khafagy el, S., Khanafer, K., Takayama, S. and ElSayed, M.E. 2016. Organization of endothelial cells, pericytes, and astrocytes into a 3D microfluidic in vitro model of the blood-brain barrier. Mol Pharm. 13 (3): 895-906.

Watkins, P.B. 1997. The barrier function of CYP3A4 and P-glycoprotein in the small bowel. Adv Drug Deliv Rev. 27: 161-170.

Weiss, N., Miller, F., Cazaubon, S. and Couraud, P.O. 2009. The blood-brain barrier in brain homeostasis and neurological diseases. BBA-Biomembranes. 1788 (4): 842-857.

Wilhelm, I., Fazakas, C. and Krizbai, I.A. 2011. In vitro models of the blood-brain barrier. Acta Neurobiol Exp. 71: 113-128.

Wilhelm, I. and Krizbai, I.A. 2014. In vitro models of the blood-brain barrier for the study of drug delivery to the brain. Mol Pharm. 11 (7): 1949-1963.

Wilson, B., Samanta, M.K., Santhi, K., Kumar, K.P., Paramakrishnan, N. and Suresh, B. 2008. Targeted delivery of tacrine into the brain with polysorbate 80-coated poly(n-butylcyanoacrylate) nanoparticles. Eur J Pharm Biopharm. 70 (1): 75-84.

Wohlfart, S., Gelperina, S. and Kreuter, J. 2012. Transport of drugs across the blood–brain barrier by nanoparticles. J Control Release. 161 (2): 264-273.

Wohnsland, F. and Faller, B. 2001. High-throughput permeability pH profile and high-throughput alkane/water log P with artificial membranes. J Med Chem. 44: 923-930.

Xu, C.F. and Wang, J. 2015. Delivery systems for siRNA drug development in cancer therapy. Asian J Pharm Sci. 10 (1): 1-12.

Yeon, J.H., Na, D., Choi, K., Ryu, S.W., Choi, C. and Park, J.K. 2012. Reliable permeability assay system in a microfluidic device mimicking cerebral vasculatures. Biomed Microdevices. 14 (6): 1141-1148.

Zamore, P.D., Tuschl, T., Sharp, P.A. and Bartel, D.P. 2000. RNAi: double-stranded RNA directs the ATP-dependent cleavage of mRNA at 21 to 23 nucleotide intervals. Cell. 101: 25-33.

Zhang, Z., McGoron, A.J., Crumpler, E.T. and Li, C.Z. 2011. Co-culture based blood-brain barrier in vitro model, a tissue engineering approach using immortalized cell lines for drug transport study. Appl Biochem Biotechnol. 163 (2): 278-295.

Zysk, G., Schneider-Wald, B.K., Hwang, J.H., Bejo, L., Kim, K.S., Mitchell, T.J., Hakenbeck, R. and Heinz, H.P. 2001. Pneumolysin is the main inducer of cytotoxicity to brain microvascular endothelial cells caused by Streptococcus pneumoniae. Infect Immun. 69 (2): 845-852.

CHAPTER II

Overview and Aims

1. Overview

Nowadays, ageing population is widespread across the world and constitutes a potential factor for raising the incidence of brain disorders in modern society. It is most advanced in the highly developed countries, but also growing faster in less developed regions. Increasing life expectancy and declining fertility rates are the greatest causes for such epidemiologic data. Consequently, a number of brain-related disabilities as stroke, dementia, memory impairments and changes in levels of neurotransmitters and hormones are having an increasing importance in order to keep quality of life levels high.

Therefore, the CNS, where all central actions are coordinated and neuromodulators are produced, and the BBB, as the brain protective membrane, are the main subjects to study and to try to overcome, so the likeliness of a successful treatment could be improved.

siRNA, due to its strong specificity on temporarily silencing a particular gene, became a great biomolecular way to down-regulate efflux transporters such P-gp presented at the BBB. These transporters act as efflux systems pumping drugs from brain back to blood, decreasing the efficiency of most therapies. Adding nanotechnology to the line, siRNA-loaded nanoparticles protect the oligonucleotide from harsh conditions as enzymatic degradation, which results in a biodegradable system with siRNA increased bioavailability. As well, through surface modification, these systems could act as “Trojan horses”, improving siRNA accumulation in the desired site of action, simultaneously decreasing harmful side-effects.

In the present thesis, two main institutions had collaborated: the Institute for Research and Innovation in Health (i3S) at the University of Porto (Portugal) and the Department of Physics, Chemistry and Pharmacy from the University of Southern Denmark (Denmark). At i3S, the group has a broad experience in the development of drug/gene delivery systems based on lipids and polymers, additionally to an expertise in receptor-targeted nanoparticles surface modification. The main interests of the group are to overcome the physiological barriers, as the BBB, and develop systems to efficiently and in a target way deliver drugs/genes, decreasing the effects in the surrounding tissues. The group from the University of Southern Denmark is known for the development of non-cellular based membrane models that mimic *in vivo* protective membranes. Liposomes are used to resemble cellular membranes through a fast method, which was demonstrated to be effective, with outputs similar to the ones obtained *via in vitro* based models. Their research interest areas are also drug solubility and dissolution, drug delivery systems namely liposomes, and drug release. In

close partnership and through a great team work, these two main groups with minor interventions from the Faculty of Sciences from the University of Porto (Portugal), had combined their expertise to enable the fulfillment of the work reported in this thesis, dedicated to the development of a targeted siRNA delivery biomaterial to modulate the drug efflux at the BBB.

2. Aims

The present thesis aims to expose the current knowledge regarding CNS and its affecting disorders. In this scope, BBB and its over-protective function were essential topics here discussed. Since the main aim of this thesis project was to develop a safe and targeted nanoparticulate-based system able to modulate the drug efflux at the BBB, siRNA against P-gp was introduced in the approach (**Figure 2.1**). Therefore, besides physicochemical characterization, the permeability through BBB models (non-cellular and cellular-based) of developed formulations and their safety were evaluated. Finally, the ultimate objective was to use the targeted system as a BBB permeation enhancer for P-gp substrates.

The specific objectives of this thesis were:

i) To investigate the feasibility of a BBB non-cellular based model supported by phospholipid vesicles that mimic cellular membranes, its structure and how a model drug interacts with and permeates through it; and further test the influence of lipid and polymeric nanoparticles on the permeability of siRNA through the developed model (Chapter III).

ii) To improve the siRNA delivery systems previously developed by functionalization of their surface with a BBB targeting peptide, and additional investigation of the influence of distinct biomaterial compositions and peptide binding approaches on their efficiency and safety as carrier systems, and interaction with human brain endothelial cells (Chapter IV).

iii) To assess the most promising BBB targeted nanoparticles on the siRNA permeation across a human brain cell-based monolayer, as well as further evaluation of their effect on P-gp expression and consequent drug efflux modulation through the permeability of a model P-gp substrate (Chapter V).

iv) To integrate precedent chapters by developing an overall discussion leading to the main conclusions of the work and its future perspectives (Chapter VI).

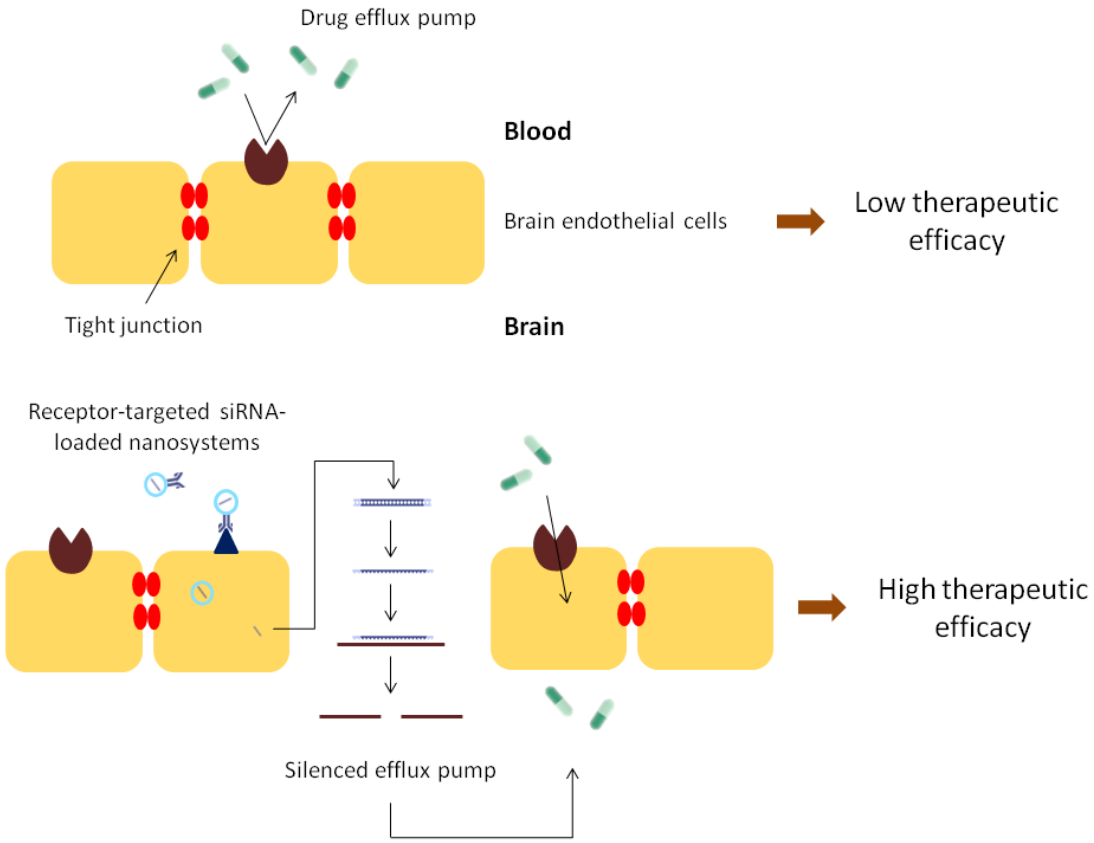

Figure 2.1. Schematic representation of the normal BBB behavior (top) and the ultimate aim of this thesis project (bottom).

CHAPTER III

A new approach for a blood-brain barrier model based on phospholipid vesicles: membrane development and siRNA-loaded nanoparticles permeability

This chapter was based on the following published paper:

- **Gomes, M.J.**, Dreier, J., Brewer, J., Martins, S., Brandl, M. and Sarmento, B. 2016. A new approach for a blood-brain barrier model based on phospholipid vesicles: membrane development and siRNA-loaded nanoparticles permeability. J Membrane Sci. 503: 8-15.

1. Abstract

Worldwide incidence of central nervous system (CNS) disorders is rising along with the age of population, making it an increasingly relevant subject. Protecting the CNS is the blood-brain barrier (BBB) which, consequently, hampers the success of current therapies by blocking drugs access to brain. Thus, developing innovative CNS treatments and improving the ability to cross BBB is urgent. Therefore, a BBB model where permeability experiments could be performed in a simple and fast way is crucially necessary to obtain high throughput screening tools. This is where phospholipid vesicle-based permeability assay (PVPA) method opportunity arises. Through this technique, a non-cellular based BBB model able to assess passive transcellular-like permeability was developed based on phospholipid vesicles that mimic cellular membranes. This model could be also used as a tool for *in vivo* permeability prediction. Simultaneously, use of small interfering RNA (siRNA) to specifically silence efflux proteins present at BBB surface could be a useful advantage to circumvent BBB blockage. To improve siRNA delivery to brain and increase its ability to permeate BBB, lipid and polymeric nanoparticles were tested and their effect was observed by measuring siRNA permeability through the BBB-PVPA model. The permeability of siRNA significantly increased from 3.7×10^{-6} cm s^{-1} (free siRNA) to 5.5×10^{-6} cm s^{-1} and 6.9×10^{-6} cm s^{-1} after encapsulation into polymeric and lipid nanoparticles, respectively.

KEYWORDS: Blood-brain barrier, artificial membrane, phospholipid, permeability, nanoparticles

2. Introduction

Nowadays, along with aging population, central nervous system (CNS) disorders are arising as an important theme due to their worldwide increasing incidence, frequently severe. Current therapies are not successful to treat these diseases (Bhaskar *et al.*, 2010), mainly because drugs cannot reach the brain due to blood-brain barrier (BBB) protective morphology (Gilmore *et al.*, 2008). BBB is a layer of endothelial cells very tightly bound to each other (tight junctions, TJ) that block the transport of drugs from blood to brain (Bhaskar *et al.*, 2010). Besides TJ, efflux systems, such as P-glycoprotein (P-gp), are also characteristic of brain endothelial cells and limit drug uptake (Agarwal *et al.*, 2011). Therefore, since the prevalence of brain diseases is raising, to find CNS treatments is needed, thus, improving the ability to cross BBB is urgent. Consequently, BBB studies are required, as well as the need for a BBB model where experiments could be performed.

Phospholipid vesicle-based permeability assay (PVPA) is a simple *in vitro* model with passive transcellular-like permeability used as a tool for *in vivo* permeability prediction (Flaten *et al.*, 2006b). The vesicle-based model is a tight barrier of liposomes, representing a much simpler and easier method to mimic the BBB compared to cell based approaches. This tool is made of a layer of phospholipid vesicles well compacted in a membrane filter, as developed by us (Flaten *et al.*, 2009; Flaten *et al.*, 2006a; Flaten *et al.*, 2006b; Flaten *et al.*, 2008). PVPA has similarities with cell-based systems since on a monoculture BBB model brain endothelial cells are seeded above the Transwell® membrane (Wilhelm and Krizbai, 2014). As well, on the BBB-PVPA model, liposomes that mimic brain endothelial cellular membranes are placed on the top of a Transwell® system-like (insert plus membrane filter). Small and large liposomes form a bilayer of phospholipid vesicles well compressed to create a membrane capable to mimic BBB tightness (TJ between BBB cells). All extracellular factors and cell-to-cell communications do not exist on the phospholipid-based model. Moreover, efflux systems present at this biological barrier are not mimicked on PVPA model. Therefore, since BBB-PVPA model lacks morphological features and the availability of active transport proteins, only passive transcellular-like diffusion is addressed. On the other hand, this disadvantage could become a plus as it could arise a way to differentiate between active and passive transport (Flaten *et al.*, 2006b), by comparison of PVPA and cell-based models. Despite non-cellular models limitations, PVPA membranes could be an alternative and/or complement to cellular models since they are easier to develop, less time consuming, can be simply adaptable to what is desired, and thus they could be an easy way to do a first fast screening before moving to cell-based models.

Our working hypothesis was that the PVPA barrier earlier introduced as an intestine model (Flaten *et al.*, 2009; Flaten *et al.*, 2006a; Flaten *et al.*, 2006b; Flaten *et al.*, 2008) should be adapted in order to better mimic passive transcellular-like diffusion at the BBB. For that, we prepare a model with a biomimetic bilayer lipid composition to achieve a tighter barrier, indicated by higher transendothelial electric resistance (TEER) values than the ones observed with the PVPA barrier so far (~600 Ωcm^2 (Fischer *et al.*, 2011)), and appropriate permeability of well-known compounds (e.g. verapamil, theophylline and calcein) by comparison with values reported for other BBB models.

The well-known parallel artificial membrane permeation assay (PAMPA) composition has been already modified positively for the prediction of BBB penetration (BBB-PAMPA (Di *et al.*, 2009)). This model uses a multi-well plate for the donor chambers and membrane/receptor compartments are placed on top. The membrane used on PAMPA is a lipid-infused artificial membrane located between donor and receptor compartments. However, previous studies (Flaten *et al.*, 2006b) revealed that the PAMPA model was less strong, reliable and robust than the PVPA model, as probably the liposome layer of the PVPA model resembles better the membrane of cells. Consequently it is expected that the BBB-PVPA will be a more reliable and robust model to predict brain permeation than the BBB-PAMPA. Beyond non-cellular based models, membranes made of cells are common as BBB models. Human brain endothelial cells (hCMEC/D3 cell line) are regularly used for static BBB cell based models, either in monoculture (Weksler *et al.*, 2013) as well as in co-culture (Hatherell *et al.*, 2011).

On the other hand, as efflux transporters are the main system that denies the access of drugs to CNS, one possible strategy to improve the efficacy of CNS drugs could be the modulation of these transporter proteins responsible for their passage across the BBB (Mahringer *et al.*, 2011). Here is where siRNA arises as a useful tool to specifically silence these efflux proteins, as for example the siRNA against P-gp used in this study (Gomes *et al.*, 2015). Briefly, siRNA guide chain, once at the cytoplasm of brain endothelial cells, has the ability to find its complementary mRNA chain and degrade it (Fuest *et al.*, 2009; Nascimento *et al.*, 2014). In this case, P-gp mRNA is the target thus the product of mRNA translation will decrease, resulting in P-gp down-regulation.

The main aims of this study were the development of a BBB non-cellular based model supported by phospholipid vesicles that mimic cellular membranes, and test the permeability of siRNA through the optimized *in vitro* BBB model. Furthermore, to improve its delivery and increase its ability to permeate BBB, siRNA-loaded nanosystems (solid lipid nanoparticles (SLN) and polymeric PLGA nanoparticles) were evaluated. Nanoparticles (NPs) have

advantageous features – small size, customizable surface, improved solubility, targeted drug delivery – that provide them the promising capacity to reach and cross the BBB, which could also improve the same capacity for what they incorporate (Bhaskar *et al.*, 2010). Lastly, the created barrier and its overall structure were observed, as well as how calcein as a model drug interacts/permeates through it.

3. Materials and Methods

3.1. Materials

Phosphatidylcholine from soybean (S100) and egg phosphatidylethanolamine (EPE) were purchased from Lipoid, phosphatidylserine from Corden Pharma, and cholesterol from Sigma. Other reagents were purchased from Sigma: all drugs – calcein, verapamil and theophylline, and PVA (mol wt 30000-70000, 87-90% hydrolyzed). From VWR, chloroform, methanol and ethyl acetate were purchased. Nitrocellulose filter 650 nm (DAWP 14250), 24-well plates (Millicell® 24), and filters 800 nm and 400 nm (Isopore membrane filters, 0.8 µm ATTP02500 and 0.4 µm HTTP02500) were purchased from Millipore. siRNA-FITC against P-gp was purchased from Santa Cruz Biotechnology, Witepsol E-85 from Gattefossé, PLGA 5004A from Corbion Purac, and Lissamine™ Rhodamine B 1,2-Dihexadecanoyl-sn-Glycero-3-Phosphoethanolamine Triethylammonium Salt (rhodamine DHPE) from Invitrogen.

3.2. Methods

3.2.1. Preparation of barriers

Since PVPA model may easily be modified with respect to lipid composition in order to better resemble the BBB (Engesland *et al.*, 2013), BBB-PVPA with different lipid compositions were produced in order to find the most suitable composition in terms of TEER and appropriate permeability of verapamil, theophylline and calcein. It is essential to mimic the lipid composition of brain capillaries, and not the overall lipid composition of the brain. Therefore, the average percentages (mol/mol) for each lipid present on the composition of brain endothelial cell lines were previously determined (Kramer *et al.*, 2002a; Kramer *et al.*,

2002b) and are here described: phosphatidylcholine (PC; 22.3%); cholesterol (CHO; 21.8%); phosphatidylethanolamine (PE; 14.2%); phosphatidylserine (PS; 10.5%); cholesterol ester (9.3%); sphingomyelin (6.7%); fatty acids (6.6%); phosphatidylinositol (4.2%); triglycerides (3.5%); cardiolipin (0.9%). According to these values, the lipids that exist in larger quantities were chosen, and different lipid mixtures were made (maintaining their proportionality) to develop distinct PVPA-barriers, assess their behavior, and select the one that better mimics BBB. Therefore, PC+PE, PC+CHO, PC+PE+PS and PC+PE+PS+CHO were studied, as well as just PC, which is the major BBB component, also acting as control and a primitive BBB model.

The BBB-PVPA was prepared according to the procedure earlier described and stored for up to 2 weeks at -80º C in accordance with previous stability studies (Flaten *et al.*, 2009; Flaten *et al.*, 2006a; Flaten *et al.*, 2006b; Flaten *et al.*, 2008; Flaten *et al.*, 2007). In brief, liposomes were prepared by film extrusion method. To make 2 x 24-well plates, a total lipid mass of 2.16 g was weighted to a round bottom flask where 7.2 mL of chloroform/methanol (2:1) was added. To produce the different lipid mixtures tested, lipids where weighted proportionally. After lipids dissolution, film formation was promoted by rotavapor (55°C, 150 rpm, with N_2 circulation). Then, liposome dispersion (6% w/v) was prepared by adding to the lipid film 10% ethanol in PBS and shaking the mixture until everything is dispersed. The 24-well plates were prepared by welding a nitrocellulose filter to the well plate by heat press HP60-250-ESM for 32 seconds. To prepare the barriers, liposome dispersions were extruded through filters with pore size 800 nm (large liposomes) and 800 + 400 nm (small liposomes), and were then deposited on a filter support through centrifugation. The liposomes were added in consecutive steps, first the smaller liposomes and then the larger ones. First, 182 µL of small liposomes were added to each insert of a 24-well plate with a membrane filter on the bottom, then first centrifugation was done at 600 × g, 25°C, 4 min. After the addition of the same amount of small liposomes, second centrifugation was done at 600 × g, 25°C, 10 min. The excess of liposomes still on the insert was discarded by dabbing them on a tissue and, with the lid on, plates were placed in an oven (Binder, Buch & Holm) at 50°C for 45 min. After they reached room temperature, large liposomes (182 µL) were added to each insert and the third centrifugation was done at 600 × g, 25°C, 30 min. Plates were covered with tissue paper and turned upside down, and the forth centrifugation was performed at 20 × g, 25°C, 5 min. Finally, barrier plates were stored at -80°C for at least 1h.

Labeled barriers were produced following the same protocol as the non-labeled ones, but with 0.2 mol% of labeled phospholipid (rhodamine DHPE, that stays within the lipid

matrix), which was weighted and mixed at the beginning with the lipids, maintaining the total weight (Flaten *et al.*, 2006a).

3.2.2. Nanoparticle production and characterization

Nanoparticles (lipid and polymeric) were prepared through a modified solvent emulsification evaporation method, based on the water-in-oil-in-water (w/o/w) double emulsion technique (Fonte *et al.*, 2014; Soares *et al.*, 2013). Twenty milligrams of polymer (PLGA) or lipid (Witepsol E-85) were dissolved in ethyl acetate (500 µL). Then, 100 µL of siRNA-FITC solution in RNAse free water (13.55 ng μL^{-1}) was added to the organic solution and homogenized for 90 s using a Vibra-Cell™ ultrasonic processor. The primary emulsion (w/o) formed was then added into 2 mL of the surfactant solution, 2% of PVA in deionized water, and homogenized again for 60 s. The second emulsion formed (w/o/w) was finally added to 6 mL of the same surfactant solution and was left under magnetic stirring at 300 rpm for at least 3 h for ethyl acetate evaporation.

After production, the nanoparticles were characterized regarding their average particle size, polydispersity index (PdI) and average zeta potential by electrophorethic light scattering using a Malvern Zetasizer Nano ZS instrument (Malvern Instruments Ltd). For these measurements, samples were diluted in MilliQ-water. To determine the association efficiency (AE) of the developed nanosystems, the amount of siRNA-FITC associated to the nanoparticles was calculated by fluorescence (ex. 494 nm, em. 517 nm). This calculation was made by the difference between the total amount of siRNA used to prepare the systems, and the amount that remained in the aqueous phase after nanoparticles isolation by centrifugation (50,000 × g, 4°C for 20 min (PLGA NPs) or 14h (SLN)), according to the following equation (Sarmento *et al.*, 2006):

$$\text{AE}\ [\%] = \frac{\text{Initial mass of siRNA} - \text{Mass of siRNA in supernatant}}{\text{Total mass of siRNA}} \times 100$$

Surface morphology (shape and size) of nanoparticles was evaluated by scanning electron microscopy (SEM). Nanoparticles were resuspended and purified three times with distilled water by ultracentrifugation in a Beckman Avanti J-26 XP ultracentrifuge (Beckman Coulter) at 20,000 × g for 15 min at 4°C, to remove the dissolved surfactant. Then, samples

were mounted onto metal stubs and vacuum-coated with a layer of gold/palladium before observation in the SEM microscope, using a FEI Quanta 400 FEG SEM, and analyzed with INCA Electronic Data System (EDS). EDS used in conjunction with the SEM apparatus is INCA Energy 350 (Oxford Instruments).

3.2.3. Permeation assay

To finish the preparation of barriers, a freeze-thaw cycle was used to promote fusion of liposomes and hence produce a tight barrier. Therefore, plates were thawed in the oven at 65°C (40 min without lid, then 20 min with lid), and after reached room temperature they were ready for the permeation experiment. All permeation experiments were performed until reach steady state, at sink conditions. Wells (receptor chamber) were filled with 800 µL of PBS pH 7.4 (mimicking brain) and the inserts (donor chamber) with 400 µL of PBS pH 7.4 (mimicking blood). Inserts were moved to the wells for an incubation period of 30 min. Then, resistance (TEER) was measured (Millicell® ERS, Millipore). For drug permeation assays, buffer was removed from the donor compartments and replaced for a drug solution with a known concentration (calcein 10 mM / verapamil 10 mM / theophylline 10 mM). Inserts were moved to new wells filled with 800 µL PBS pH 7.4, and light contact was avoided from now on. Further, inserts were moved to new wells according to these time points: 1h, 1h30, 2h, 2h30, 3h, 3h30, 4h, 4h30 and 5h. The resistance was measured again immediately after these 5h. Samples (200 µL) were taken from all wells (at each time point) to a titer plate (Microplate Costar 96) where the drug that crossed the membrane over time was quantified. The concentration of drug in solution was quantified using UV/Vis spectrophotometer for absorbance of verapamil (284 nm) and theophylline (271 nm), and for fluorescence of calcein (ex. 485 nm, em. 520 nm).

The apparent permeability (Papp) of each drug in solution was calculated by the following equation:

$$\mathrm{Papp}\ [\mathrm{cm\ s^{-1}}] = \frac{\mathrm{dm}}{\mathrm{dt}} \times \frac{1}{c_0 \times \mathrm{A}}$$

where dm/dt is the permeated mass over time, c_0 the initial concentration at the donor chamber, and A the surface area of the membrane (0.6 cm^2) (Kanzer *et al.*, 2010).

The protocol followed for the permeation of free-siRNA or siRNA-loaded NPs was similar. However, donor compartments were filled with 400 µL RNAse free water (blank for free siRNA-FITC), or free siRNA-FITC (167 ng mL^{-1}), or empty-NPs (blank for the respective siRNA-loaded NPs), or siRNA-FITC-loaded NPs. Moreover, time points were different: 1h, 2h, 3h, 4h and 5h; and when 200 µL were taken from the receptor compartment to a titer plate, the same volume of fresh buffer was added. siRNA-FITC that crossed the barrier over time was quantified through fluorescence with a plate reader. Papp was calculated for free-siRNA, siRNA-SLN and siRNA-PLGA using the same equation described before.

3.2.4. Confocal studies

After the preparation of the barriers and their freezing at -80°C, plates were thawed in the oven at 65°C (40 min without lid, then 20 min with lid), and after reach room temperature they were ready for the confocal experiment. Inserts of labeled barriers were filled with 400 µL PBS or 400 µL calcein 10mM. The wells were filled with 800 µL PBS pH 7.4 or 800 µL calcein 10mM, respectively. After an incubation period of 3h, donor compartments were discarded and the insert membrane was seen at the confocal microscope.

The images were recorded on a Zeiss confocal LSM 510 with an femtosecond Ti:Sa laser used as excitation source (Broadband Mai Tai XF W25 with a 10 W Millennia pump laser, Spectra Physics). Fluorophores were excited at 810 nm (multi photon excitation), emission was recorded with a bandpass filter 500-530 nm (for calcein, green) and a bandpass filter 565-615 nm (for Lissamine rhodamine B, red).

3.2.5. Statistical analysis

For the data analysis one-way analysis of variance (ANOVA) was performed to compare multiple groups. Differences between groups were compared with a post hoc test (Tukey's honestly significant difference). Results are reported as mean ± standard deviation from a minimum of three independent experiments. Differences were considered significant at * $p < 0.05$, ** $p < 0.01$, or *** $p < 0.001$. All statistical analyses were performed with the software PASW Statistics 20 (IBM Corporation).

4. Results and Discussion

4.1. Permeability and TEER of barriers made from different lipid mixtures

In order to mimic the BBB lipid composition, its most common lipids and phospholipids were chosen to prepare different barriers according to the PVPA method: PC+PE, PC+CHO, PC+PE+PS, PC+PE+PS+CHO. A schematic illustration of the PVPA barrier structure is depicted on **Figure 3.1**, where an insert and a well are represented as a Transwell® system-like, along with small and large liposomes deposited on the membrane filter. To assess these different barriers in terms of usefulness as a BBB model, TEER values were monitored (**Figure 3.2**). Also, the permeability of three drugs (calcein, theophylline and verapamil), which have distinct intrinsic properties and permeability behaviors, was determined (**Figure 3.3**).

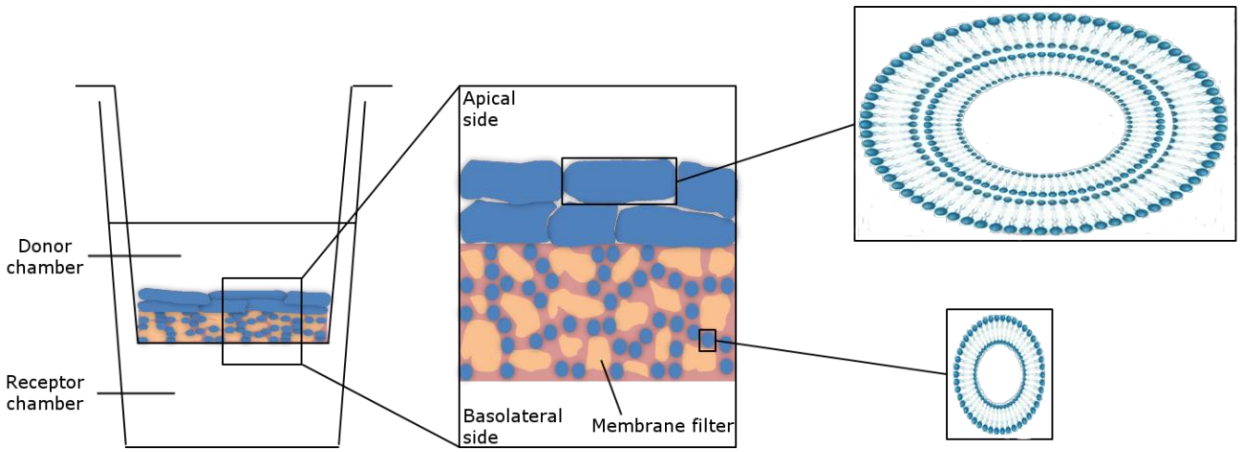

Figure 3.1. Schematic illustration of phospholipid vesicle-based barrier structure on a Transwell® system-like.

Our working hypothesis was based on the premise: the more similar the lipid mixture is to brain endothelial cells lipid composition, theoretically the closer its barrier tightness will be to the one shown by BBB. TEER is generally regarded as a good indicator of barrier tightness (Bates *et al.*, 2015). TEER was measured, for each type of membrane, before and after permeability experiments (5h; **Figure 3.2**).

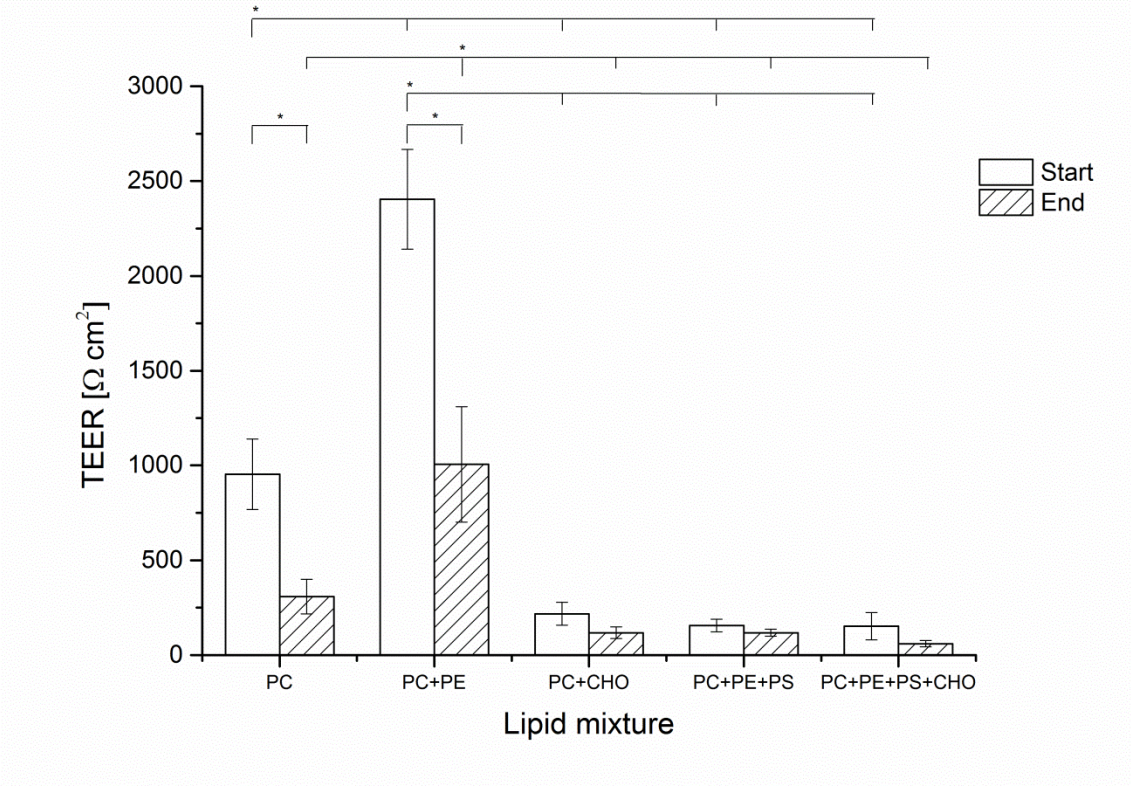

Figure 3.2. Transendothelial electrical resistance (TEER) of all studied barriers which were made of distinct phospholipid mixtures. TEER was measured on the beginning and at the end of permeability studies. PC: phosphatidylcholine; PE: phosphatidylethanolamine, PS: phosphatidylserine, CHO: cholesterol.

Most PVPA-barriers made of lipid mixtures resulted in lower TEER-values than the pure PC-barrier. The exception was the mixture of PC and PE, which resulted in significantly higher TEER-values indicating enhanced barrier tightness as compared to the pure PC-barrier. This observation may be explained by different effects. First, cholesterol is known to make phospholipid bilayers stiffer and less flexible (Dols-Perez *et al.*, 2014; Khajeh and Modarress, 2014). Higher stiffness of the vesicles may negatively affect their packing density during barrier preparation. On the other hand, PS is known to induce a strong net charge to the vesicles (Mitkova *et al.*, 2014), which also may negatively affect their packing density during barrier preparation, due to charge-charge-interactions. Lastly, mixtures with higher number of lipids result in different type of liposomes (different size and charge), which would be more unstable, and not able to pack so well with each other. This could cause disruption of the interactions between different liposomes, promoting less tight membranes and lower

TEER. Thus, PC+CHO, PC+PE+PS and PC+PE+PS+CHO present a loss of barrier tightness, which is not in accordance with one of the main BBB features.

Moreover, the differences observed between TEER values before and after the permeability assay could be related to that experiment, since the permeation of tested drugs may open some spaces within the barrier, decreasing its TEER.

For the permeability assays, three different model drugs were selected. Calcein (622.55 g mol^{-1}; a Biopharmaceutics Classification System class III compound), a hydrophilic charged marker commonly used as an indicator of trans-bilayer permeability (Patel *et al.*, 2009), was used since it is well studied on this field and therefore is easy to correlate (Fischer *et al.*, 2011; Flaten *et al.*, 2008; Kanzer *et al.*, 2010). Theophylline (180.164 g mol^{-1}; a BCS class I drug which Log P (octanol/water) is -0.02 (Hansch *et al.*, 1995)), and verapamil (454.602 g mol^{-1}; a BCS class I drug which Log P (octanol/water) is 3.8 (Yoshida *et al.*, 2010)) were chosen as standard drugs since, despite their hydrophilic character, present different values of coefficient O/W, being verapamil more hydrophobic than theophylline. Therefore, these drugs have different expected behavior on crossing a phospholipid membrane (Di *et al.*, 2003). Theophylline is a drug used in therapies for respiratory diseases since it acts both as a competitive non-selective phosphodiesterase inhibitor (Essayan, 2001) and as a non-selective adenosine receptor antagonist, explaining many of its cardiac effects. Verapamil acts by blocking voltage-dependent calcium channels and is used in the treatment of hypertension, angina pectoris, cardiac arrhythmia, and most recently, cluster headaches (Bleier *et al.*, 2015).

Permeability for these molecules was determined for all lipid mixtures-based membranes developed (**Figure 3.3**), simultaneously with the evaluation of TEER values. We further tested our working hypothesis that a barrier composed of a mixture of lipids (mainly PC+PE, based on TEER results), which better resembles the BBB lipid composition than just PC, would be more proper for the prediction of drugs permeability through the BBB than a pure PC barrier. Permeability results corroborate resistance data for PC+CHO, PC+PE+PS and PC+PE+PS+CHO, since such high permeability obtained for these mixtures are related to less tightness and compact barrier observed by TEER. Likewise, corroborating this hypothesis, calcein (which is the largest molecule tested and indicates lipid vesicle leakage) permeability increased on these multiple lipids mixtures. Thus, these mixtures were discarded to continue our studies as BBB models candidates. We could not see any significant difference between PC+PE and PC alone. However, for the same lipid mixture, verapamil crosses in a deeper extend than theophylline, which was expected due to the

improved interaction between a hydrophobic membrane and the most hydrophobic used drug rather than other more hydrophilic.

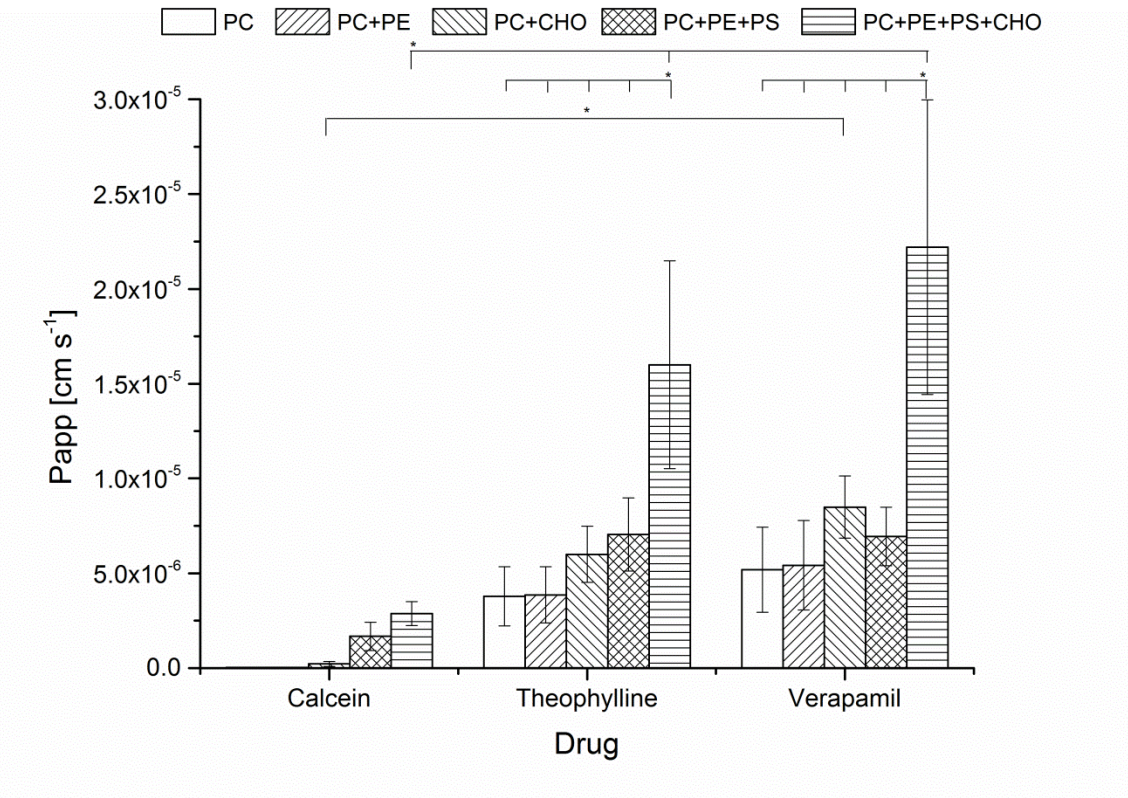

Figure 3.3. Permeability of calcein, theophylline and verapamil through different barriers made of distinct phospholipid mixtures. PC: phosphatidylcholine; PE: phosphatidylethanolamine, PS: phosphatidylserine, CHO: cholesterol.

Literature values for the permeability of verapamil and theophylline through other BBB models (as *in vitro* cell-based or PAMPA) were determined and set to be from 3.23 ± 0.54 × 10^{-5} cm s^{-1} to 3.35 ± 0.45 × 10^{-5} cm s^{-1} on a used BBB cellular model (MDCKII-MDR1 monolayer) and 3.43 ± 0.71 × 10^{-5} cm s^{-1} on PAMPA (Carrara *et al.*, 2007), for verapamil. For theophylline, values of 8.8 ± 2.0 × 10^{-6} cm s^{-1} on brain endothelial cells monoculture (bEnd.3 cell line) (Dhanikula *et al.*, 2009) were described. These values are within the obtained PVPA-data range (5.2 × 10^{-6} – 2.2 × 10^{-5} cm s^{-1} for verapamil and 3.8 × 10^{-6} – 1.6 × 10^{-5} cm s^{-1} for theophylline), having the same order of magnitude. Moreover, permeability for verapamil is higher than for theophylline, as cell-based or PAMPA models also demonstrated before. The innovation provided by PVPA method is, therefore, highlighted by these results, since it

enables the development of membrane models in a faster and easier fashion than conventional existing models, while retaining similar permeability values.

At flow conditions, on BBB models such as Dynamic *in vitro* (DIV) systems (system that mimics blood flow by creating intraluminal flow through artificial capillary-like structural supports (hollow fibers) (Naik and Cucullo, 2012)), steady state is achieved after 2 weeks, when TEER reaches 1200 Ωcm^2 (Cucullo *et al.*, 2008). On the other hand, static systems as Transwell® models just require 1 week to steady state but TEER could only reach 60-80 Ωcm^2 (15- to 20- fold lower values) (Cucullo *et al.*, 2008). With PVPA method, the highest TEER values are obtained in the same day of production, an advantage considering fast high throughput analysis. Furthermore, the lipid mixture PC+PE reaches even higher TEER than on flow conditions (keeping this value high enough after permeability experiments), in much less time.

In order to select the model that better mimics BBB, permeability and resistance values were evaluated and compared to other reported BBB models. Although permeability values were very similar between PC and PC+PE, TEER values for the mixture PC+PE were significantly higher than for PC. These higher TEER values are more often obtained with dynamic systems, which mimic better the BBB, rather than static models. Therefore, since this is an intended characteristic to achieve a better BBB model, this mixture was selected as the best one, still continuing to do all further experiments with PC barrier also. Besides its higher TEER, PC+PE is already more complex than just PC, and has the two main phospholipids present in the BBB.

4.2. Selected BBB model structure

As long as the liposomes are stable, which could be addressed through the proven barrier stability and integrity (with TEER results), we believe that the liposomes stay as vesicles organized on/above the filter material, mainly through adsorption of their bilayers to each other. Still, to track their structure, the two types of barriers composed of PC+PE and PC only were then labeled and visualized by confocal microscopy (**Figure 3.4 A**). Further, calcein was added to the apical side of these membranes to assess its permeability pathways (**Figure 3.4 B**).

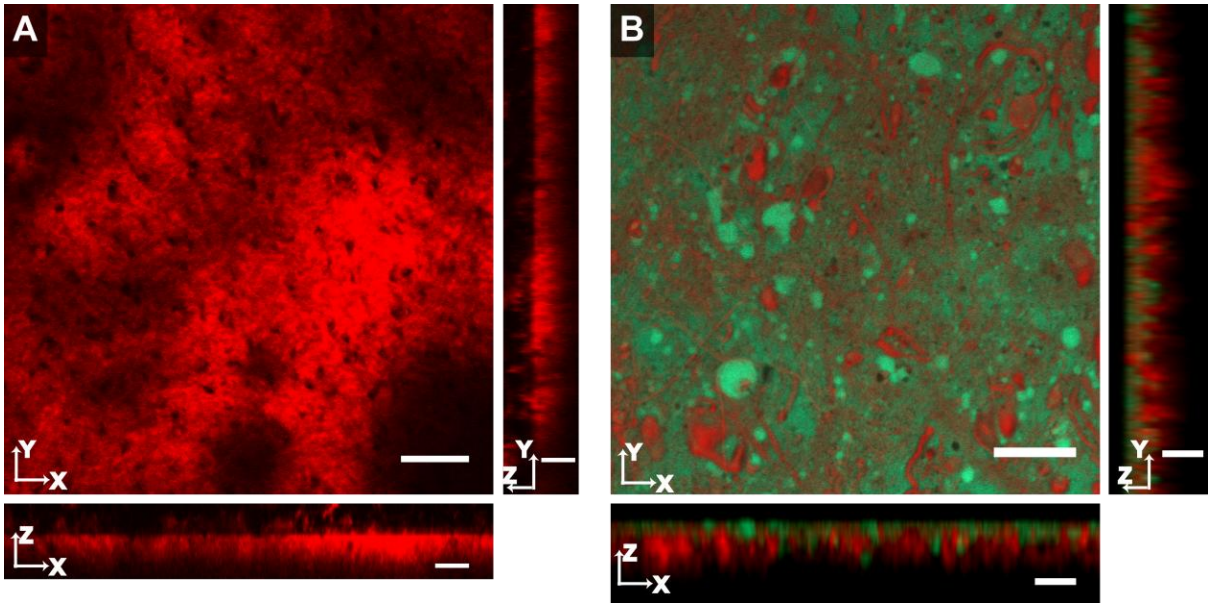

Figure 3.4. (**A**) BBB model (PC+PE) labeled with Lissamine rhodamine B. (**B**) BBB barrier (PC) labeled with Lissamine rhodamine B assessing calcein permeability. Large scale bar is 20 μm; small scale bar is 10 μm.

Figure 3.4 A shows the labeled barrier, it was possible to observe the BBB structure through the filaments created by the membrane filter and the barrier developed above it. For the calcein permeation assessed in the labeled BBB barrier (**Figure 3.4 B**), a much larger amount was found on the apical side of the barrier surface, and only a small amount crossing the barrier, which was expected due to its very low permeability values (**Figure 3.3**), in accordance to previous studies (Flaten *et al.*, 2006a). Similar location of calcein was observed for PC+PE model (data not shown).

The interaction between BBB model and calcein, as the largest hydrophilic molecule here used able to indicate lipid vesicle leakage, highlighted the integrity and stability (for at least three hours) of the created barrier.

4.3. Nanoparticles characterization

After the development and selection of a BBB model, it was used to test the permeability of siRNA and siRNA-loaded NPs. Two types of nanoparticles were produced,

namely lipid (SLN) and polymeric (PLGA), as systems to transport siRNA to the BBB. The mean size and zeta potential properties of developed nanoparticles are depicted on **Table 3.1**. To promote BBB crossing, a size below 200 nm is desired in order to avoid rapidly uptake by reticuloendothelial system (Chen *et al.*, 2004). Therefore blood circulation time is increased, as well as the contact time with the BBB (Chen *et al.*, 2004; Kaur *et al.*, 2008). This requisite was accomplished, with monodisperse and slightly negative populations. Moreover, the siRNA association efficiency of siRNA-loaded nanoparticles was also measured and calculated. Association efficiency between 53 and 56% was obtained, which constitutes a promising result since siRNA is very hydrophilic. Data related to nanoparticles characterization revealed similarities among produced nanoparticles, both SLN and PLGA, loaded and unloaded.

Table 3.1. Physicochemical characteristics of SLN and PLGA nanoparticles, both empty and siRNA-loaded.

NP system	Mean size [nm]	PdI	Zeta Potential [mV]	Association Efficiency [%]
SLN	139.3 ± 1.3	0.127 ± 0.023	-10.1 ± 0.5	-
siRNA-loaded SLN	137.3 ± 3.2	0.129 ± 0.024	-10.0 ± 1.0	53.1 ± 1.1
PLGA	142.9 ± 1.0	0.093 ± 0.018	-8.2 ± 0.1	-
siRNA-loaded PLGA	144.0 ± 1.4	0.121 ± 0.024	-10.1 ± 0.7	56.5 ± 1.8

PdI, polydispersity index

SEM analysis was also performed to obtain more information about the particle size and morphology. All evaluated nanoparticles exhibited a spherical shape (**Figure 3.5**) and a smooth surface, regardless of their composition. Nanoparticles sizes observed by SEM were shown to be similar to those obtained by Zetasizer measurements. However, it has been reported that solvent removal that occurs during SEM sample preparation may cause changes that can influence particle shape and size (Das and Chaudhury, 2011).

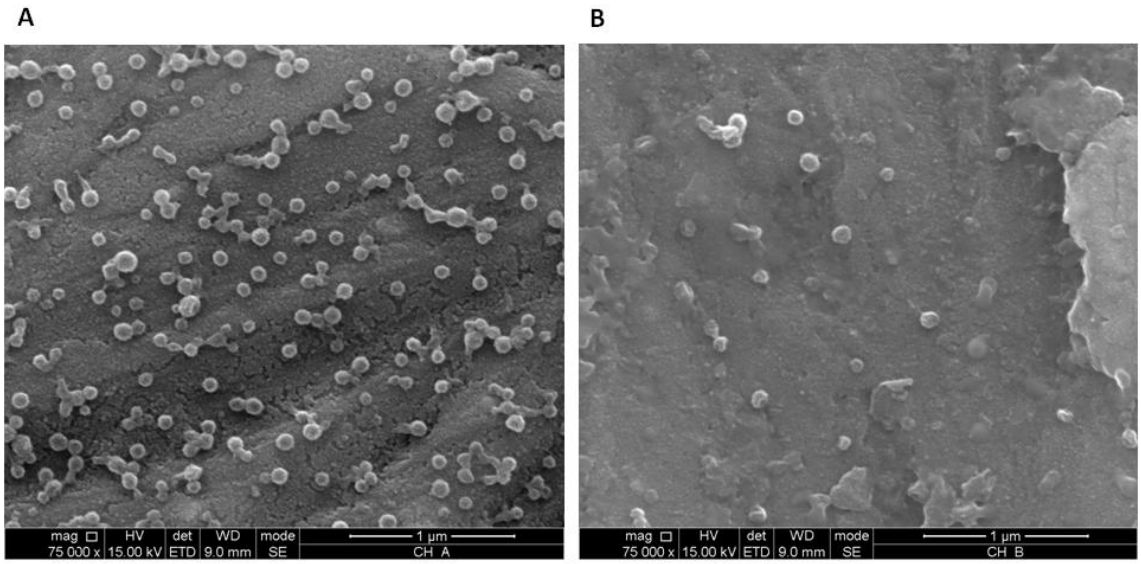

Figure 3.5. SEM images of (**A**) PLGA nanoparticles, and (**B**) siRNA-loaded PLGA nanoparticles. The scale bar shown below the images corresponds to 1 µm.

4.4. siRNA permeability

To evaluate the permeability of siRNA and the influence of nanoparticles, free-siRNA, siRNA-loaded SLN and siRNA-loaded PLGA nanoparticles were added to the apical side of both PC barrier and BBB selected model (PC+PE). The permeability values are depicted on **Figure 3.6**.

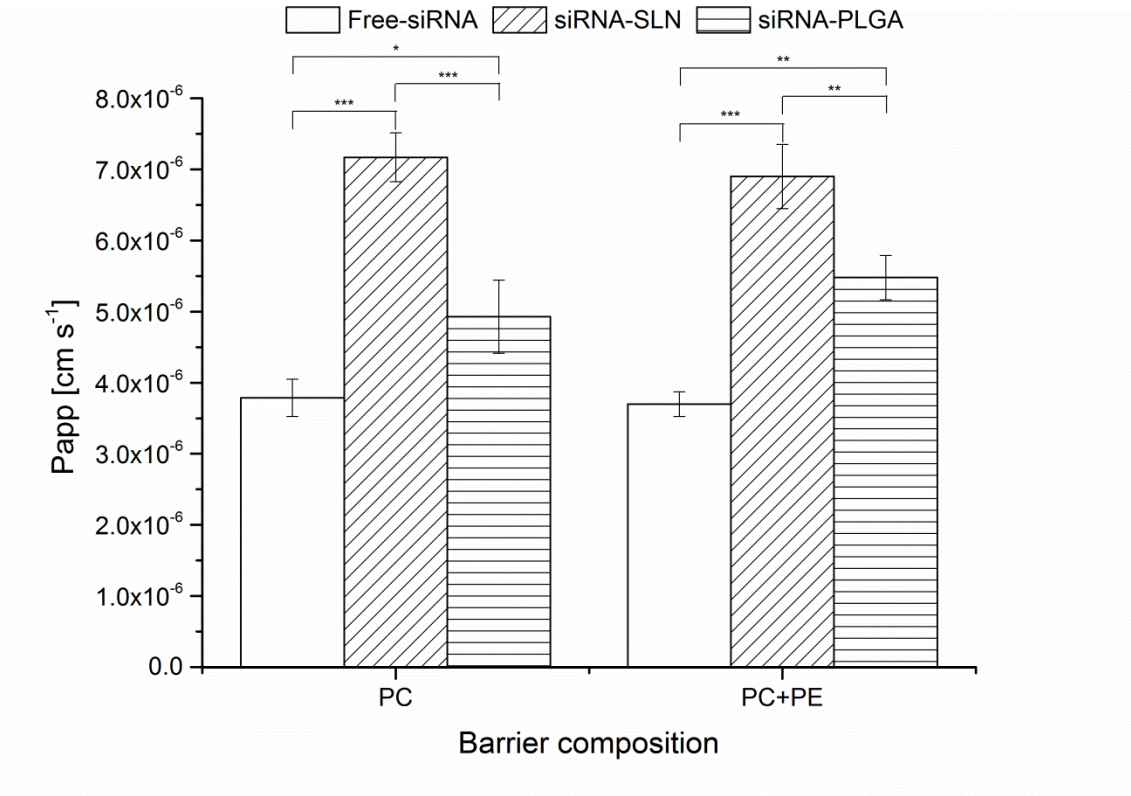

Figure 3.6. Permeability of free-siRNA and siRNA-loaded NPs (both SLN and PLGA) through the selected BBB model (PC+PE) and the control barrier (PC). PC: phosphatidylcholine; PE: phosphatidylethanolamine.

Permeability had the lowest value for free-siRNA, however, as a hydrophilic compound, it still had some permeation through the BBB model, which could be explained by its very small size. Both types of nanoparticles significantly increased siRNA transport across the barrier, since nanoparticles themselves permeate the lipid barrier, releasing then the siRNA. SLN were more efficient than PLGA nanoparticles, due to their hydrophobic lipid composition, which presented higher affinity to lipid membranes made of liposomes. However, no differences between results obtained for PC or PC+PE were observed.

The percentages of siRNA that crossed the membrane were similar for PC and PC+PE, close to 10% of free-siRNA, 14% of siRNA-PLGA, and 19% of siRNA-SLN. Concerning these values, it is clear the improvement of siRNA penetration through a BBB model membrane, from 10% to 19%, highlighting the influence of nanoparticles as a carrier and a siRNA permeability promoter. Other previous studies also emphasize the importance of siRNA carriers, stressing the significance of choosing the adequate carrier, as Khatri and colleagues who observed that siRNA loaded cationic lipoplexes increased siRNA cellular uptake (in two different lung cancer cell lines) by five to six fold compared to naked siRNA

(Khatri *et al.*, 2014). In another study, chitosan nanoparticles improved siRNA uptake in RBE4 cells (commonly used as a BBB model), which was monitored by fluorescence (Malmo *et al.*, 2013). Moreover, Godinho and co-workers evaluated cellular uptake of a fluorescently labeled siRNA loaded in amphiphilic-cyclodextrins nanoparticles through a rat neuronal *in vitro* model. After 48 h post transfection, up to 38% of cells were found to be positive for fluorescent siRNA complexes. In contrast, no significant uptake was observed in cells treated with naked siRNA (Godinho *et al.*, 2013). Therefore, as these cell-based studies also highlight, nanocarriers are crucial to potentiate siRNA efficiency since they promote its uptake thus increasing its permeability across cellular membranes.

Permeability through these barriers can be related and caused by charge (siRNA, nanoparticles and barrier are negative) and hydrophobicity (siRNA is hydrophilic; nanoparticles and barrier are hydrophobic). Opposite charges attract each other, as well as similar hydrophobicity surfaces. Interactions between different charges and hydrophobic surfaces influence the affinity increase/decrease and therefore may control the permeability. In this study, all the present elements are negative, so there is no great advantage from that, and therefore effects of charge on penetration are negligible. As the BBB-PVPA barrier, human BBB also carries a negative charge due to its glycosaminoglycan composition (Li and Fu, 2011). So, regarding charge consequences, created barrier mimics BBB at this level, which also validates a direct comparison between these membranes. Moreover, since PVPA membranes study passive transcellular-like permeability, produced nanoparticles (both SLN and PLGA) may cross this artificial BBB through the liposomes (transcellular-like pathway). Nanoparticles are believed to interact with liposomes from the barrier, being able to stay between them and thus go through them. Especially SLN, they may merge with the lipids in the barrier, which could then promote siRNA release. Furthermore, that could also affect the barrier tightness, another possible explanation for the decrease of resistance after the permeability experiment.

Therefore, nanoparticles were able to interact with BBB-PVPA liposomes, passively crossing the barrier through them, revealing capability to interact with BBB-like cellular membranes. As so, siRNA would have the possibility to act in these cells down-regulating the expression of P-gp. Consequently, any P-gp substrate drug that is desired to achieve the brain in a therapeutic concentration will benefit of this transient opportunity. Improving siRNA permeability by using nanoparticles could be the trigger to make all this process more likely to occur, ending with numerous drug reaching brain advantages.

5. Conclusions

The main innovative key in this work holds up to the phospholipid-vesicle based method to create membranes as a non-cellular based technique. This enables the development of membranes according to the desired lipid content. It has several advantages when compared to cell-based methods such as: easy to reproduce, less expensive, less time consuming, no contamination problems. Moreover, it is an excellent way for high throughput screening of permeability properties of potential drug/nanosystem candidates early in the development process, leading to a pre-selection of the best drug/nanosystem before continue to *in vitro* and *in vivo* studies. Our non-cellular based BBB model could be used as another model to compare results and can easily be improved/adapted (as shown in this study) by using other lipids or adjusting the production protocol. Also, it could be simply modified to mimic other type of barriers. Since it has no active transport, it evaluates only passive transport which could then be compared with passive and active transports that occur in other models *in vitro*/*in vivo* in order to verify the influence of both types of transport. One of the main objectives of barriers developed through this method is to enable results extrapolation and prediction.

The first goal of this work was to develop a non-cellular based BBB model. Although permeability studies with both drugs and siRNA do not indicate a difference between barriers made of PC and PC+PE, TEER values are clearly different and may influence the barrier behavior in other conditions, namely the permeability to other drugs. Thus, the mixture PC+PE was selected as the one that better mimics BBB.

As obtained permeability data suggest, similar values could be achieved by using BBB-PVPA method and cell-based models. Consequently, phospholipid-based method could lead to avoid cell based experiences with early drugs/nanosystems which could not be good enough yet. This underlines that PVPA, as a simple system, could be an easy way to do a first fast screening before moving to cell-based models. Therefore, it could be a faster and less expensive option.

Regarding siRNA permeability through the selected BBB model and the influence of nanosystems, nanoparticles were found to act as an efficient carrier since they significantly improve siRNA permeability through the BBB model. This indicates the importance of using siRNA delivery nanosystems. Moreover, these nanoparticles were shown to be promising enough to be further tested on a cell-based model.

6. References

Agarwal, S., Hartz, A.M.S., Elmquist, W.F. and Bauer, B. 2011. Breast cancer resistance protein and P-glycoprotein in brain cancer: two gatekeepers team up. Curr Pharm Design. 17: 2793-2802.

Bates, C.A., Fu, S., Ysselstein, D., Rochet, J.C. and Zheng, W. 2015. Expression and transport of a-synuclein at the blood-cerebrospinal fluid barrier and effects of manganese exposure. Admet & Dmpk. 3 (1): 15-33.

Bhaskar, S., Tian, F., Stoeger, T., Kreyling, W., de la Fuente, J.M., Grazu, V., Borm, P., Estrada, G., Ntziachristos, V. and Razansky, D. 2010. Multifunctional nanocarriers for diagnostics, drug delivery and targeted treatment across blood-brain barrier: perspectives on tracking and neuroimaging. Part Fibre Toxicol. 7 (3): 1-25.

Bleier, B.S., Kocharyan, A., Singleton, A. and Han, X. 2015. Verapamil modulates interleukin-5 and interleukin-6 secretion in organotypic human sinonasal polyp explants. Int Forum Allergy Rhinol. 5 (1): 10-13.

Carrara, S., Reali, V., Misiano, P., Dondio, G. and Bigogno, C. 2007. Evaluation of in vitro brain penetration: optimized PAMPA and MDCKII-MDR1 assay comparison. Int J Pharm. 345 (1-2): 125-133.

Chen, Y., Dalwadi, G. and Benson, H.A. 2004. Drug delivery across the blood-brain barrier. Curr Drug Deliv. 1 (4): 361-376.

Cucullo, L., Couraud, P.O., Weksler, B., Romero, I.A., Hossain, M., Rapp, E. and Janigro, D. 2008. Immortalized human brain endothelial cells and flow-based vascular modeling: a marriage of convenience for rational neurovascular studies. J Cereb Blood Flow Metab. 28 (2): 312-328.

Das, S. and Chaudhury, A. 2011. Recent advances in lipid nanoparticle formulations with solid matrix for oral drug delivery. AAPS PharmSciTech. 12 (1): 62-76.

Dhanikula, R.S., Hammady, T. and Hildgen, P. 2009. On the mechanism and dynamics of uptake and permeation of polyether-copolyester dendrimers across an in vitro blood-brain barrier model. J Pharm Sci. 98 (10): 3748-3760.

Di, L., Kerns, E.H., Bezar, I.F., Petusky, S.L. and Huang, Y. 2009. Comparison of blood-brain barrier permeability assays: in situ brain perfusion, MDR1-MDCKII and PAMPA-BBB. J Pharm Sci. 98 (6): 1980-1991.

Di, L., Kerns, E.H., Fan, K., McConnell, O.J. and Carter, G.T. 2003. High throughput artificial membrane permeability assay for blood–brain barrier. Eur J Med Chem. 38 (3): 223-232.

Dols-Perez, A., Fumagalli, L. and Gomila, G. 2014. Structural and nanomechanical effects of cholesterol in binary and ternary spin-coated single lipid bilayers in dry conditions. Colloid Surface B. 116: 295-302.

Engesland, A., Skar, M., Hansen, T., Skalko-Basnet, N. and Flaten, G.E. 2013. New applications of phospholipid vesicle-based permeation assay: permeatiom model mimicking skin barrier. J Pharm Sci. 102 (5): 1588-1600.

Essayan, D.M. 2001. Cyclic nucleotide phosphodiesterases. J Allergy Clin Immunol. 108 (5): 671-680.

Fischer, S.M., Flaten, G.E., Hagesaether, E., Fricker, G. and Brandl, M. 2011. In-vitro permeability of poorly water soluble drugs in the phospholipid vesicle-based permeation assay: the influence of nonionic surfactants. J Pharm Pharmacol. 63 (8): 1022-1030.

Flaten, G., Awoyemi, O., Luthman, K., Brandl, M. and Massing, U. 2009. The phospholipid vesicle-based drug permeability assay: 5. development toward an automated procedure for high-throughput permeability screening. J Lab Autom. 14 (1): 12-21.

Flaten, G.E., Bunjes, H., Luthman, K. and Brandl, M. 2006a. Drug permeability across a phospholipid vesicle-based barrier 2. characterization of barrier structure, storage stability and stability towards pH changes. Eur J Pharm Sci. 28 (4): 336-343.

Flaten, G.E., Dhanikula, A.B., Luthman, K. and Brandl, M. 2006b. Drug permeability across a phospholipid vesicle based barrier: a novel approach for studying passive diffusion. Eur J Pharm Sci. 27 (1): 80-90.

Flaten, G.E., Luthman, K., Vasskog, T. and Brandl, M. 2008. Drug permeability across a phospholipid vesicle-based barrier 4. The effect of tensides, co-solvents and pH changes on barrier integrity and on drug permeability. Eur J Pharm Sci. 34 (2-3): 173-180.

Flaten, G.E., Skar, M., Luthman, K. and Brandl, M. 2007. Drug permeability across a phospholipid vesicle based barrier: 3. Characterization of drug-membrane interactions and the effect of agitation on the barrier integrity and on the permeability. Eur J Pharm Sci. 30 (3-4): 324-332.

Fonte, P., Soares, S., Sousa, F., Costa, A., Seabra, V., Reis, S. and Sarmento, B. 2014. Stability study perspective of the effect of freeze-drying using cryoprotectants on the structure of insulin loaded into PLGA nanoparticles. Biomacromolecules. 15 (10): 3753-3765.

Fuest, C., Bankstahl, M., Winter, P., Helm, M., Pekcec, A. and Potschka, H. 2009. In vivo down-regulation of mouse brain capillary P-glycoprotein: a preliminary investigation. Neurosci Lett. 464 (1): 47-51.

Gilmore, J.L., Yi, X., Quan, L. and Kabanov, A.V. 2008. Novel nanomaterials for clinical neuroscience. J Neuroimmune Pharmacol. 3 (2): 83-94.

Godinho, B.M., Ogier, J.R., Darcy, R., O'Driscoll, C.M. and Cryan, J.F. 2013. Self-assembling modified beta-cyclodextrin nanoparticles as neuronal siRNA delivery vectors: focus on Huntington's disease. Mol Pharm. 10 (2): 640-649.

Gomes, M.J., Martins, S. and Sarmento, B. 2015. siRNA as a tool to improve the treatment of brain diseases: mechanism, targets and delivery. Ageing Res Rev. 21: 43-54.

Hansch, C., Leo, A. and Hoekman, D.H. 1995. Exploring QSAR - hydrophobic, electronic, and steric constants. (Washington, DC: American Chemical Society).

Hatherell, K., Couraud, P.O., Romero, I.A., Weksler, B. and Pilkington, G.J. 2011. Development of a three-dimensional, all-human in vitro model of the blood-brain barrier using mono-, co-, and tri-cultivation Transwell models. J Neurosci Methods. 199 (2): 223-229.

Kanzer, J., Tho, I., Flaten, G.E., Magerlein, M., Holig, P., Fricker, G. and Brandl, M. 2010. In-vitro permeability screening of melt extrudate formulations containing poorly water-soluble drug compounds using the phospholipid vesicle-based barrier. J Pharm Pharmacol. 62 (11): 1591-1598.

Kaur, I.P., Bhandari, R., Bhandari, S. and Kakkar, V. 2008. Potential of solid lipid nanoparticles in brain targeting. J Control Release. 127 (2): 97-109.

Khajeh, A. and Modarress, H. 2014. The influence of cholesterol on interactions and dynamics of ibuprofen in a lipid bilayer. Biochim Biophys Acta. 1838 (10): 2431-2438.

Khatri, N., Baradia, D., Vhora, I., Rathi, M. and Misra, A. 2014. Development and characterization of siRNA lipoplexes: effect of different lipids, in vitro evaluation in cancerous cell lines and in vivo toxicity study. AAPS PharmSciTech. 15 (6): 1630-1643.

Kramer, S.D., Hurley, J.A., Abbott, N.J. and Begley, D.J. 2002a. Lipids in blood-brain barrier models in vitro I: thin-layer chromatography and high-performance liquid chromatography for the analysis of lipid classes and long-chain polyunsaturated fatty acids. In Vitro Cell Dev Biol - Animal. 38: 557-565.

Kramer, S.D., Schutz, Y.B., Wunderli-Allenspach, H., Abbott, N.J. and Begley, D.J. 2002b. Lipids in blood-brain barrier models in vitro II: influence of glial cells on lipid classes and lipid fatty acids. In Vitro Cell Dev Biol - Animal. 38: 566-571.

Li, G. and Fu, B.M. 2011. An electrodiffusion model for the blood-brain barrier permeability to charged molecules. J Biomech Eng. 133 (2): 1-12.

Mahringer, A., Ott, M., Reimold, I., Reichel, V. and Fricker, G. 2011. The ABC of the blood-brain barrier - regulation of drug efflux pumps. Curr Pharm Design. 17: 2762-2770.

Malmo, J., Sandvig, A., Varum, K.M. and Strand, S.P. 2013. Nanoparticle mediated P-glycoprotein silencing for improved drug delivery across the blood-brain barrier: a siRNA-chitosan approach. PLoS One. 8 (1): 1-8.

Mitkova, D., Marukovich, N., Ermakov, Y.A. and Vitkova, V. 2014. Bending rigidity of phosphatidylserine-containing lipid bilayers in acidic aqueous solutions. Colloid Surface A. 460: 71-78.

Naik, P. and Cucullo, L. 2012. In vitro blood-brain barrier models: current and perspective technologies. J Pharm Sci. 101 (4): 1337-1354.

Nascimento, A.V., Bousbaa, H., Ferreira, D. and Sarmento, B. 2014. Non-small cell lung carcinoma: an overview on targeted therapy. Curr Drug Targets. 15 (8): 1-16.

Patel, H., Tscheka, C. and Heerklotz, H. 2009. Characterizing vesicle leakage by fluorescence lifetime measurements. Soft Matter. 5 (15): 2849-2851.

Sarmento, B., Ribeiro, A., Veiga, F. and Ferreira, D. 2006. Development and characterization of new insulin containing polysaccharide nanoparticles. Colloid Surface B. 53 (2): 193-202.

Soares, S., Fonte, P., Costa, A., Andrade, J., Seabra, V., Ferreira, D., Reis, S. and Sarmento, B. 2013. Effect of freeze-drying, cryoprotectants and storage conditions on the stability of secondary structure of insulin-loaded solid lipid nanoparticles. Int J Pharm. 456 (2): 370-381.

Weksler, B., Romero, I.A. and Couraud, P.O. 2013. The hCMEC/D3 cell line as a model of the human blood brain barrier. Fluids Barriers CNS. 10 (16): 1-10.

Wilhelm, I. and Krizbai, I.A. 2014. In vitro models of the blood-brain barrier for the study of drug delivery to the brain. Mol Pharm. 11 (7): 1949-1963.

Yoshida, M.I., Gomes, E.C., Soares, C.D., Cunha, A.F. and Oliveira, M.A. 2010. Thermal analysis applied to verapamil hydrochloride characterization in pharmaceutical formulations. Molecules. 15 (4): 2439-2452.

CHAPTER IV

Tailoring lipid and polymeric nanoparticles as siRNA carriers towards the blood-brain barrier – from targeting to safe administration

This chapter was based on the following published paper:

- **Gomes, M.J.**, Fernandes, C., Martins, S., Borges, F. and Sarmento, B. 2016. Tailoring lipid and polymeric nanoparticles as siRNA carriers towards the blood-brain barrier - from targeting to safe administration. J Neuroimmune Pharmacol., in press doi: 10.1007/s11481-016-9685-6.

1. Abstract

Blood-brain barrier is a tightly packed layer of endothelial cells surrounding the brain that acts as the main obstacle for drugs enter the central nervous system (CNS), due to its unique features, as tight junctions and drug efflux systems. Therefore, since the incidence of CNS disorders is increasing worldwide, medical therapeutics need to be improved. Consequently, aiming to surpass blood-brain barrier and overcome CNS disabilities, silencing P-glycoprotein as a drug efflux transporter at brain endothelial cells through siRNA is considered a promising approach. For siRNA enzymatic protection and efficient delivery to its target, two different nanoparticles platforms, solid lipid (SLN) and poly(lactic-co-glycolic acid) (PLGA) nanoparticles were used in this study. Polymeric PLGA nanoparticles were around 115 nm in size and had 50% of siRNA association efficiency, while SLN presented 150 nm and association efficiency up to 52%. The siRNA release profile was assessed and verified as sustained, reaching around 60% after 24h. Nanoparticles surface was functionalized with a peptide-binding transferrin receptor, in a site-oriented manner. This surface modification was confirmed by NMR, and their targeting ability against human brain endothelial cells was successfully demonstrated by fluorescence microscopy and flow cytometry. The interaction of modified nanoparticles with brain endothelial cells increased 3-fold compared to non-modified lipid nanoparticles, and 4-fold compared to non-modified PLGA nanoparticles, respectively. These nanosystems, which were also demonstrated to be safe for human brain endothelial cells, without significant cytotoxicity, bring a new hopeful breath to the future of brain diseases therapies.

KEYWORDS: Blood-brain barrier; Functionalization; Nanoparticles; siRNA; TfR-peptide

2. Introduction

Currently, there is a huge and increasing incidence of central nervous system (CNS) disorders, which emphasizes such disorders as the major medical challenge of the 21st century, as indicated by the World Health Organization (ResearchAndMarkets, 2007). CNS disorders affect a large portion of population worldwide involving frequent and rare disorders, with unknown etiology or already identified causes, but the great majority is very disabling and not yet curable. From brain cancer to amyotrophic lateral sclerosis and diseases like Alzheimer's, Parkinson or Huntington's, there are numerous distinct disorders, characterized as unsolved clinical conditions, that lead to the same need, i.e., drug reaching brain in therapeutic concentrations, with few side effects and through a minimally invasive way (Gomes *et al.*, 2015). This therapeutic gap is related to the complex CNS environment and its protective barriers, being, therefore, identified as the main challenge for the development of an efficient brain therapy.

Blood-brain barrier (BBB) is one of the most relevant CNS barriers that restrict the passage of foreign substances into the brain by blocking drug/molecules transport. This biological membrane is mainly comprised by brain endothelial cells forming a cerebral microvascular endothelium, which presents molecular and receptor structures able to mediate the transport of substances in and out of the brain (Abbott *et al.*, 2010). Additionally, the BBB holds tight junctions between adjacent endothelial cells which make this barrier very tight, and exhibits a lack of fenestrations and low endogenous pinocytotic activity (Abbott *et al.*, 2010; Bhaskar *et al.*, 2010). As one of the central contributors for brain penetration limitations are drug efflux systems, present at the luminal membrane of BBB. These are transporters that cause the efflux of many compounds, including drugs, from brain back to blood (Bhaskar *et al.*, 2010). Among these systems is the P-glycoprotein (P-gp), which is a phosphorylated glycoprotein present in several tissues namely at the luminal plasma membrane of the capillary endothelium (Mahringer *et al.*, 2011). Due to their described roles, drug efflux systems are considered to be a very attractive target to inhibit, in order to improve drug passage across the BBB, thus increasing the efficacy of CNS therapies (Fisher *et al.*, 2007; Mahringer *et al.*, 2011).

In order to study how to circumvent obstacles that difficult brain entrance, a feasible BBB *in vitro* model is crucial. Immortalized cell lines, as hCMEC/D3 (human brain endothelial cells), are commonly used as a human BBB model (Weksler *et al.*, 2013). Surpass this compactly packed layer of endothelial cells, specifically drug efflux systems, will potentiate drug reaching brain ability. With this purpose, small interfering RNA (siRNA) arises as a

promising option for drug efflux systems temporary silence, since efflux systems known inhibitors have issues – as the inhibitor affinity and reversibility – that could become serious problems (Bauer *et al.*, 2005). By directly down-regulate efflux transporters expression and/or transport activity, siRNA could be the key for these brain "over protective" issues. Despite siRNA large potential, efficient methods for its delivery must be devised. Nanomedicine, as an expanding and promising field for innovative advances to the diagnosis and treatment of devastating and pervasive diseases (Gilmore *et al.*, 2008), could be a great ally for that approach. Nanoparticles, namely, have advantageous properties like small size, and potentiate targeted drug delivery, features that make them feasible to cross BBB (Gilmore *et al.*, 2008). Furthermore, polymeric and lipid-based nanoparticles, made from natural or highly biocompatible materials, are considered the least problematic regarding toxicity (Murthy, 2007). When used as siRNA carriers, nanoparticles protect oligonucleotides from enzymatic degradation and target them to desired cells through surface functionalization.

Using site-specific ligands it is possible to target particular cells/tissues and thus direct nanoparticles delivery (Gabathuler, 2010). Therefore, functionalizing nanoparticles surface with a peptide against transferrin receptor (TfR) would direct these systems to the BBB, since there is an over expression of transferrin receptors at this biological membrane, among other body regions (Gabathuler, 2010; Huang *et al.*, 2007; Moos and Morgan, 2000).

Gathering all this knowledge, this study proposes a nanosystem able to carry and control the release of siRNA against P-gp to the BBB, in order to further silence this protein receptor, temporarily transforming BBB in a more permeable membrane for P-gp substrates. The core aims of this study were the development and step-by-step improvement of lipid and polymeric nanoparticles loading siRNA, and functionalized with a TfR-peptide that enables the system to be more interactive with BBB cells. Different lipids and polymers were used to produce nanoparticles, and distinct functionalization processes were assessed to obtain better siRNA loaded and targeted carriers. The cytotoxicity of created particles was evaluated to ensure the safety of these nanoparticles promising future.

3. Materials and Methods

3.1. Materials

Poly(lactic-co-glycolic acid), PLGA 5004A, was purchased from Corbion – Purac, PLGA-PEG-NH_2 from PolySciTech, Witepsol E85 from Gattefossé and Stearylamine from Sigma-Aldrich. Ethyl acetate was purchased from VWR, siRNA-FITC against P-gp from Santa Cruz Biotechnology, TfR-peptide from AnaSpec, TfR-peptide-Cys from Eurogentec, and SM$(PEG)_{24}$ was from Thermo Scientific. Deuterated water was purchased from Sigma-Aldrich. EBM-2 medium from Lonza and Triton X-100 from Spi-Chem. Several materials were purchased from Sigma: Tween 80, EDC (1-ethyl-3-(3-dimethylaminopropyl)carbodiimide), NHS (N-hydroxysuccinimide), MES (2-(N-morpholino)ethanesulfonic acid), hydrocortisone, ascorbic acid, HEPES, bFGF (basic fibroblast growth factor), MTT, DMSO and PFA (paraformaldehyde). Others were purchased from Invitrogen: Rhodamine 123, CellMask™ Orange, primary antibody against TfR (OX26, PA5-24661), and secondary antibody (A-11070). From Gibco it was purchased FBS, penicillin-streotomycin, chemically defined lipid concentrate, HBSS, collagen I rat protein and trypsin-EDTA.

3.2. Methods

3.2.1. Nanoparticles production

Nanoparticles (polymeric and solid lipid nanoparticles, SLN) were prepared through a modified solvent emulsification evaporation method based on the water-in-oil-in-water (w/o/w) double emulsion technique (Fonte *et al.*, 2014; Soares *et al.*, 2013). Twenty milligrams of polymer (PLGA) or lipid (Witepsol E85) were dissolved in ethyl acetate (500 µL). Then, 100 µL of siRNA-FITC solution in RNAse free water (13.55 ng μL^{-1}) were added and the solution was homogenized for 90 s using a Vibra-Cell™ ultrasonic processor. The primary formed emulsion (w/o) was then added into 2 mL of the surfactant solution, 2% of Tween 80 in deionized water, and homogenized again for 60 s. The second formed emulsion (w/o/w) was finally added to 6 mL of the same surfactant solution, and was left under magnetic stirring at 300 rpm for at least 3h for ethyl acetate evaporation.

Additional polymer (PLGA-PEG-NH_2) and lipid (stearylamine) were added to polymeric and lipid systems, respectively, to allow further nanoparticle functionalization. Different ratios of PLGA:PLGA-PEG-NH_2 were used, namely 100:0, 97.5:2.5 and 95:5 (% w/w), as well as of Witepsol E85:stearylamine, with 100:0, 99:1 and 98:2 (% w/w).

After production, the nanoparticles were characterized regarding mean particle size, polydispersity index (PdI) and zeta potential by electrophorethic light scattering using a Malvern Zetasizer Nano ZS instrument (Malvern Instruments Ltd). For these measurements, samples were diluted in MilliQ-water. To determine the association efficiency (AE) of the developed nanosystems, the amount of siRNA-FITC associated to the nanoparticles was calculated by a fluorescence (ex. 494 nm, em. 517 nm) assay. AE was determined indirectly by the difference between the total amount of siRNA used to prepare the systems and the amount that remained in the aqueous phase after nanoparticles isolation by centrifugation (20,000 × g, 4°C for 20 min for polymeric nanoparticles or 50,000 × g, 4°C for 4 h for lipid nanoparticles), according to the following equation:

$$\text{AE}\ [\%] = \frac{\text{Initial mass of siRNA} - \text{Mass of siRNA in supernatant}}{\text{Total mass of siRNA}} \times 100$$

3.2.2. siRNA release profile

The *in vitro* release of siRNA-FITC from nanoparticles was evaluated using a dialysis bag diffusion technique. Previously washed nanoparticles (7 mL) were placed in cellulose dialysis bags with a 12-14 kDa MWCO and sealed at both ends. The dialysis bag was immersed in the receptor compartment containing PBS (70 mL, pH 7.4), which was kept stirring at 100 rpm over 24 hours. Aliquots of 200 μL were taken from the receptor compartment at pre-determined time points up to 24h, and the same volume of fresh buffer was added. The siRNA-FITC content of each sample was analyzed through fluorescence using a plate reader.

3.2.3. Nanoparticles functionalization and characterization

Two different approaches were followed to conjugate the peptide to nanoparticles surface and direct them to BBB: (1) the carbodiimide chemistry, to link an amine group to a carboxyl group (Araújo *et al.*, 2015; Wang *et al.*, 2015), using a 12 amino acid peptide (Thr-

His-Arg-Pro-Pro-Met-Trp-Ser-Pro-Val-Trp-Pro, named here as pept); or (2) the maleimide chemistry, to link an amine group to a sulfhydryl group (Esfandyari-Manesh *et al.*, 2015; Zimmermann *et al.*, 2010), using a 13 amino acid peptide (the same pept with an extra cysteine on the carboxyl termination; Thr-His-Arg-Pro-Pro-Met-Trp-Ser-Pro-Val-Trp-Pro-Cys, named here as pept-Cys).

Nanoparticles were functionalized according to their ending functional groups: PLGA (carboxyl group) with pept (amine group); PLGA:PLGA-PEG-NH_2(95:5) (amine group) with pept-Cys (sulfhydryl group); Witepsol E85:Stearylamine(99:1) (amine group) with pept (carboxyl group); Witepsol E85:Stearylamine(99:1) (amine group) with pept-Cys (sulfhydryl group).

For the amide formation, the EDC/NHS coupling chemistry method was used. The activation of the carboxyl groups of polymeric nanoparticles was attained by using 1 mg of nanoparticles dispersed in 1 mL of MES solution (10 mM, pH~5.5). Then, EDC (3.14 µL, 17 mM) and NHS (1.2 mg) were added to the dispersion and the pH was adjusted to 5.5. This mixture was stirred (300 rpm) for 30 min at room temperature. The pept (100 µL, 1 mg mL^{-1}) was added and pH adjusted to 7.5. Finally, the mixture was kept stirring (300 rpm) at room temperature for 3h30. For lipid nanoparticles carbodiimide conjugation, the carboxyl groups of peptide (pept) were activated by a similar procedure. In this last case, nanoparticles were only added to the mixture after the addition of the peptide, and pH was kept at 5.5. Both described processes were performed in the dark.

The maleimide conjugation chemistry was performed by dispersing 1 mg of amine terminated nanoparticles (polymeric particles with PLGA-PEG-NH_2 and lipid particles with stearylamine) on 1 mL of PB solution (0.1 M, pH~7). The cross linker $SM(PEG)_{24}$ was added (2 µL, 250 mM) and the mixture was stirred in the dark, at 300 rpm for 4h, at room temperature. Then, pept-Cys was added (50 µL, 6.2 mg mL^{-1}) and the mixture was stirred for another 4h.

Afterwards, nanoparticles were collected by centrifugation at 20,000 × g, 4°C for 20 min, for polymeric nanoparticles, or 50,000 × g, 4°C for 4h, for lipid nanoparticles, and then washed with MilliQ-water. Functionalized nanoparticles were then analyzed by Zetasizer.

3.2.4. Nanoparticles labeling

The same protocol to produce siRNA-loaded nanoparticles was used to obtain fluorescent nanoparticles encapsulating rhodamine 123 (0.5% w/w loading) instead of siRNA,

as already described (das Neves *et al.*, 2012). Nanoparticles were resuspended and purified three times with Milli-Q water by centrifugation to remove rhodamine 123 excess. Rhodamine 123-loaded nanoparticles were measured with Zetasizer, AE was determined, rhodamine 123 was detected through fluorescence (ex. 507 nm, em. 529 nm), and its release was studied. The release assay was performed with a dialysis membrane (cellulose dialysis bag with a 12-14 kDa MWCO). Rhodamine 123-loaded formulations were located inside the dialysis membrane, which was well closed at the top and bottom. Membrane was placed inside a flask with 70 mL of PBS solution (pH 7.4), with constant stirring at room temperature. Samples (200 µL) were taken at pre-determined time points up to 24h, and the same volume taken was added again (PBS). Samples were analyzed by fluorescence.

3.2.5. ^{1}H Nuclear Magnetic Resonance (^{1}H NMR)

Non-functionalized and functionalized nanoparticles, as well as respective peptides, were dissolved (1 mg) on deuterated water and placed on appropriate NMR tubes. Analysis were performed at room temperature on a Brüker AMX 300 spectrometer operating at 400.13 MHz, with chemical shifts expressed in δ (ppm) values relative to tetramethylsilane (TMS) as internal reference.

3.2.6. Cell culturing

Immortalized human Cerebral Microvascular Endothelial Cell Line (hCMEC/D3 cell line) was purchased from Cedarlane (Canada). The cells (passage 35-41) were grown in tissue culture flasks (Orange Scientific), in EBM-2 medium supplemented with FBS (5%, v/v), penicillin-streotomycin (1%, v/v), hydrocortisone (1.4 µM), ascorbic acid (5 µg mL^{-1}), chemically defined lipid concentrate (1/100, v/v), HEPES (10 mM) and bFGF (1 ng mL^{-1}). This last supplement was added extemporaneously in the culture medium. Cells were maintained in an incubator (CellCulture CO_2 incubator, ESCO) at 37°C with 5% CO_2 in water saturated atmosphere. Cells were subcultured every 3-4 days using trypsin-EDTA to detach them from the flasks. The culture medium was replaced every other day.

3.2.7. Nanoparticles safety – MTT assay

Cells were seeded in a 96-well plate (4×10^4 cells/mL) in a supplemented EBM-2 medium. After 24h of incubation, medium was removed and cells were washed twice with

200 µL PBS. Then, cells were incubated with different concentrations of nanoparticles (naked, siRNA-loaded, siRNA-loaded and functionalized) for 24h. Nanoparticles solution was discarded, cells were washed twice, and then were treated with 200 µL of MTT solution (0.5 mg mL^{-1}, in medium) per well, during 4h in the dark. Finally, MTT was removed and 200 µL of DMSO were added to dissolve MTT formazan crystals during a 10 min slight shake at room temperature. In the end, absorbance was measured at 590 and 630 nm. Metabolic activity (as described on the following equation) was expressed as a percentage compared to the cells incubated only with EBM-2 medium (negative control). Triton X-100 (1%, in medium) was used as the positive control, since the detergent action disrupts the cells.

$$\text{Metabolic activity [\%]} = \frac{\text{Experimental value} - \text{Positive control}}{\text{Negative control} - \text{Positive control}} \times 100$$

3.2.8. Cell-nanoparticle interaction

Transferrin receptor expression

To verify whether hCMEC/D3 cells express transferrin receptor, these cells were fixed with PFA 4% during 10 min. After washing, cells were incubated with a blocking solution (10% FBS in PBS, 30 min), and then seeded on a round bottom 96-well plate (0.1×10^6 cells/well). The primary antibody (OX26, against TfR) was added (1:50 or 1:200) and incubated during 1h. Cells were washed thrice (1,500 × g, 1 min) and then incubated with the secondary antibody (1:2,000) during 1h. After washing three times, cells were resuspended in blocking solution, filtered (70 µm) and placed in cytometer tubes.

The quantification of the secondary antibody associated to the cells was evaluated using flow cytometry (FACS Calibur, two laser excitation (488 nm/635 nm)), where the labeled antibody was detected through the 488 nm channel. The results were analyzed using the software FlowJo vX.0.7. The fold increase parameter was calculated as the fluorescence geometric mean of all samples normalized to the control, as described on the following equation:

$$\text{Fold increase} = \frac{\text{Fluorescence geometric mean of the sample}}{\text{Fluorescence geometric mean of the control}}$$

Fluorescence microscopy

Cells were seeded in glass cover slips (2.5×10^5 cells/mL, 400 µL) pre-coated with type I collagen, and were allowed to attach overnight. Glass cover slips (14 mm) were placed inside a 24-well plate, one cover slip per well. The cells were washed twice with pre-warmed 400 µL PBS pH 7.4, and then 200 µL of rhodamine 123-loaded nanoparticles (50 µg mL^{-1}, in 10 mM HBSS-HEPES) were added to each well and incubated for 15 min, 1h or 4h at 37°C. After incubation, the cells were washed twice with PBS. Afterwards, the plasma membrane was stained by adding 200 µL of CellMask™ Orange and incubated for 3 min at 37°C. The excess of staining solution was washed twice with pre-warmed fresh PBS (pH 7.4) and the cells were fixed using 4% PFA for 20 min.

The interaction between nanoparticles and human brain endothelial cells was assessed through an inverted fluorescence microscope (Axiovert 200M from Zeiss), where nanoparticles were detected through the green channel, while cells through the red one. The control was cells without nanoparticles.

Flow cytometry

Cells were seeded in a 24-well plate (5×10^5 cells/mL, 200 µL) and were allowed to attach overnight. The cells were washed twice with pre-warmed 200 µL PBS pH 7.4, and then 200 µL of rhodamine 123-loaded nanoparticles (50 µg mL^{-1}, in 10 mM HBSS-HEPES) were added to each well and incubated for 15 min, 1h or 4h at 37°C. After incubation, the cells were washed twice with PBS and detached with trypsin-EDTA. The cells were then washed with medium and PBS through centrifugation at 1,500 × g during 1 min, and fixed with PFA 4% in PBS during 10 min. PFA was removed through centrifugation and cells were washed again. Finally, cells were resuspended in PBS, filtered (70 µm) and placed in cytometer tubes.

The quantification of the nanoparticles associated to the cells was evaluated using flow cytometry (FACS Calibur, two laser excitation (488 nm/635 nm)), where nanoparticles were detected through the 488 nm channel. The results were analyzed using the software FlowJo vX.0.7. The fold increase parameter was calculated as the fluorescence geometric mean of all samples normalized to the control, as described previously.

3.2.9. Statistical analysis

For the data analysis one-way analysis of variance (ANOVA) was performed to compare multiple groups. Differences between groups were compared with a post hoc test (Tukey's honestly significant difference). Results are reported as mean ± standard deviation from a minimum of three independent experiments. Differences were considered significant at * $p < 0.05$, ** $p < 0.01$, or *** $p < 0.001$. All statistical analyses were performed with the software PASW Statistics 20 (IBM Corporation).

4. Results and Discussion

4.1. Nanoparticles production

The development of targeted nanoparticles has been proposed as a more convenient and efficient strategy for take advantage of therapeutic drugs. Different kind of ligands can be anchored to the surface of nanoparticles, providing a receptor-mediated interaction with target cells. In the present approach, to functionalize nanoparticles to BBB, a peptide with affinity to bind to TfR was selected. Functional groups at nanoparticles surface are, thus, required, so PLGA-PEG-NH_2 and stearylamine were added to bare nanoparticles to provide chemical bridges to ligands. On polymeric nanoparticles, regular PLGA carboxyl terminated was used in addition to the copolymer PLGA-PEG-NH_2 in different ratios (100:0, 97.5:2.5 and 95:5). For lipid nanoparticles, Witepsol E85 was used with stearylamine, a lipid with amine groups, in different ratios (100:0, 99:1 and 98:2). All nanoparticles were studied regarding mean size, PdI, zeta potential and siRNA association efficiency through Zetasizer and fluorescence methods (**Table 4.1**).

Table 4.1. Physicochemical characteristics of polymeric and lipid nanoparticles unloaded and loaded with siRNA.

NP system	siRNA Loading	Mean Size [nm]	PdI	Zeta Potential [mV]	Association Efficiency [%]
PLGA	No	114.1 ± 1.4	0.241 ± 0.012	-30.3 ± 2.5	-
	Yes	113.5 ± 1.7	0.233 ± 0.017	-31.9 ± 1.7	49.7 ± 0.6
PLGA:PLGA-PEG-NH_2 (97.5:2.5)	No	112.6 ± 2.7	0.226 ± 0.016	-32.3 ± 1.9	-
	Yes	113.0 ± 3.3	0.239 ± 0.014	-31.2 ± 1.1	48.9 ± 0.2
PLGA:PLGA-PEG-NH_2 (95:5)	No	117.6 ± 3.6	0.271 ±0.026	-30.5 ± 1.4	-
	Yes	118.1 ± 2.1	0.252 ± 0.014	-29.3 ± 0.5	50.3 ± 1.3
Witepsol E85	No	155.7 ± 5.7	0.451 ± 0.033	-21.2 ± 2.0	-
	Yes	152.8 ± 6.9	0.438 ± 0.024	-20.1 ± 2.9 *	18.2 ± 1.1 *
Witepsol E85: Stearylamine (99:1)	No	147.4 ± 7.6	0.425 ± 0.041	-7.6 ± 1.0	-
	Yes	144.1 ± 8.5	0.455 ± 0.037	-8.0 ± 0.4 *	30.8 ± 2.5 *
Witepsol E85: Stearylamine (98:2)	No	152.7 ± 6.9	0.471 ± 0.044	-2.5 ± 0.6	-
	Yes	150.1 ± 7.9	0.433 ± 0.039	-2.9 ± 0.7 *	51.5 ± 1.5 *

PdI, polydispersity index; * $p < 0.05$

Physicochemical characteristics of empty and siRNA-loaded nanoparticles were similar. Likewise, no differences were observed when the new polymer/lipid were added to the system matrices. Differences were only detected for surface charge of SLN, as amine groups from stearylamine originate an increase in charge, resulting in higher siRNA association efficiency. In previous studies, this charge-related stearylamine effect was also observed (Cui *et al.*, 2015). Non-phospholipid liposomes composed of stearylamine and cholesterol had higher positive surface charge and enhanced particle stability than traditional phospholipid liposomes (Cui *et al.*, 2015). In another previous work, SLN were used to promote saquinavir penetration through human brain endothelial cells; these systems were characterized as cationic due to stearylamine and dioctadecyldimethyl ammonium bromide used on nanoparticles preparation (Kuo and Chen, 2010). Additionally, stearylamine was

also used as a charge modifier for a SLN delivery system of clozapine (Venkateswarlu and Manjunath, 2004). Accordingly, siRNA AE also increased when stearylamine was included due to charge interactions between negative nucleotide and cationic lipid, which turned this association more stable and stronger. Stearylamine was already used to promote iloprost (which is a potent vasorelaxing agent negatively charged at physiological pH) encapsulation on liposomal nanoparticles. In fact, the use of this cationic lipid promoted iloprost encapsulation to at least more 50% (Jain *et al.*, 2014). Regarding polymeric nanoparticles, siRNA AE reached 50% for all formulations tested, which was already a good achievement regarding its hydrophilic character.

In order to have simple polymeric systems that already have carboxyl and amine terminal groups in their composition, nanoparticles of PLGA and PLGA:PLGA-PEG-NH_2(95:5) were chosen, respectively. Also, as mean particle size and AE results did not reveal any significant difference between the ratios 97.5:2.5 and 95:5, 95:5 was selected to guarantee that amine groups are present in significant amount.

For lipid systems, since Witepsol E85 by itself does not contain any functional groups of interest, nanoparticles with stearylamine were chosen to proceed. Between 99:1 and 98:2, 99:1 was selected since this quantity of the new lipid was already enough to increase zeta potential which means that amine groups are significantly present. Moreover, regarding toxicity issues already described for this cationic lipid, it would be advantageous to proceed with the lowest amount (Caldeira *et al.*, 2015).

4.2. siRNA release profile

The siRNA release profile from previously selected nanoparticles was assessed and is depicted in **Figure 4.1**. It was found that the release kinetics was very similar to all formulations. During the first hour, a burst release was observed, following a slower release until 5h, and afterwards, a controlled, linear release was achieved, reaching around 60% after 24h. These profiles are consistent with sustained drug delivery systems, meaning that produced nanoparticles yield a prolonged and slowly release of siRNA from their matrices, which would further promote the desired siRNA prolonged effect (Li *et al.*, 2014).

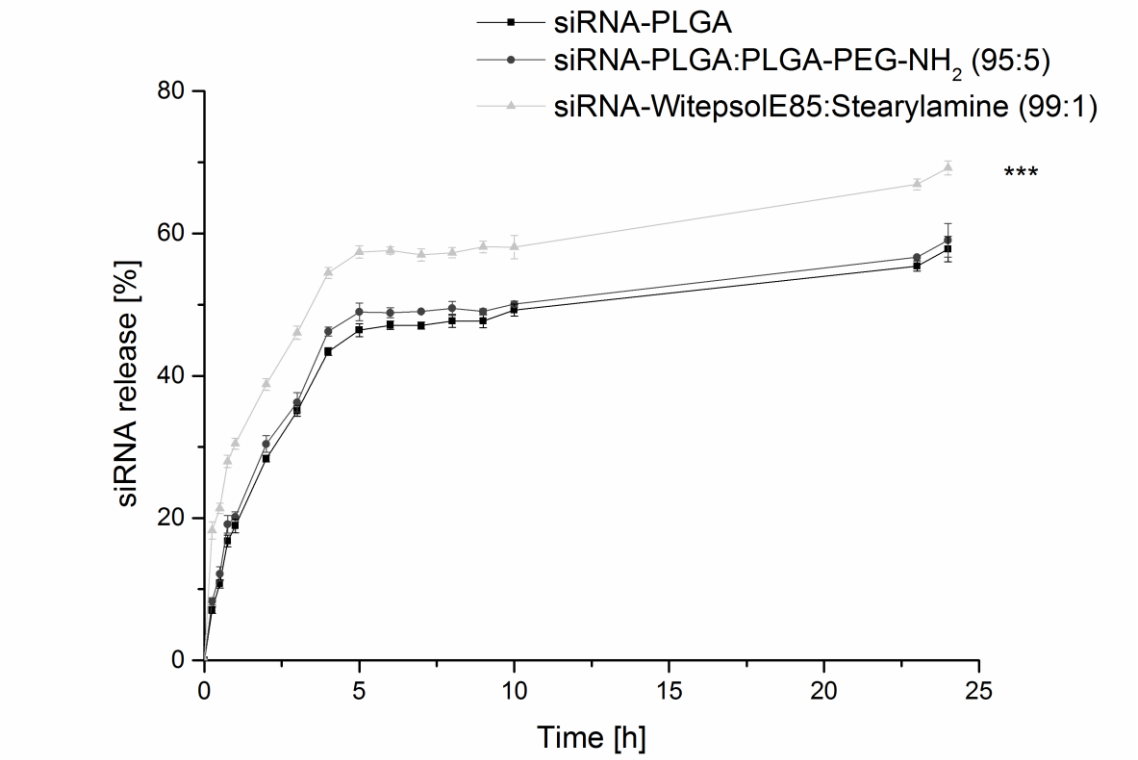

Figure 4.1. siRNA release profile from developed polymeric and lipid nanoparticles over 24h (PBS pH 7.4).

Generally, the release of the encapsulated molecule from nanoparticles depends on the physicochemical properties of the vehicle and the molecule employed (Kikwai *et al.*, 2005). Both polymeric and lipid nanoparticles are characterized as biodegradable systems, which could promote siRNA release from them. However, in an *in vitro* study as this, siRNA release may occur mainly due to its diffusion through the system, rather than to the degradation of nanoparticles matrices. siRNA hydrophilic character may have a great role on its diffusion from a hydrophobic nanoparticle to a hydrophilic environment (Cruz *et al.*, 2010; Qi *et al.*, 2012). The same explanation can be extrapolated for the fact that siRNA was released faster and sooner from lipid nanoparticles than from polymeric ones, as these systems are obviously extremely lipophilic.

4.3. Nanoparticles functionalization and characterization

In order to target BBB and, therefore, avoid unspecific delivery and potential side effects, nanoparticles were functionalized with a transferrin receptor-peptide. Two chemistry approaches were performed to try distinct methods to obtain a better functionalized nanosystem, with higher specificity. The way that the peptide binds to nanoparticles could influence crucial features for a future specific binding of the peptide to its target receptor, such as functional peptide availability and spatial distribution.

Carbodiimide chemistry is less specific than maleimide one, since there are several carboxyl and amine groups at the pept, therefore different possibilities for the binding process. On the other hand, for the maleimide reaction, there is only one sulfhydryl group on pept-Cys, thus only one way (the correct one) to link the peptide to the nanoparticle. The functionalization of nanoparticles was evaluated by Zetasizer (**Table 4.2**).

Table 4.2. Physicochemical characteristics of unloaded polymeric and lipid nanoparticles: non-functionalized and functionalized with pept/pept-Cys.

NP system	Mean Size [nm]	PdI	Zeta Potential [mV]
PLGA	114.1 ± 1.4 ***	0.241 ± 0.012	-30.3 ± 2.5
PLGA with pept	321.3 ± 25.1 ***	0.447 ± 0.108	-19.8 ± 8.5
PLGA:PLGA-PEG-NH_2 (95:5)	117.6 ± 3.6 ***	0.271 ± 0.026 ***	-30.5 ± 1.4 **
PLGA:PLGA-PEG-NH_2 (95:5) with pept-Cys	477.3 ± 29.5 ***	0.582 ± 0.027 ***	-39.5 ± 2.3 **
Witepsol E85:Stearylamine (99:1)	147.4 ± 7.6 ***	0.425 ± 0.041 *	-7.6 ± 1.0
Witepsol E85:Stearylamine (99:1) with pept	389.3 ± 18.8 ***	0.551 ± 0.046 *	-10.4 ± 2.1
Witepsol E85:Stearylamine (99:1)	147.4 ± 7.6 ***	0.425 ± 0.041 **	-7.6 ± 1.0 **
Witepsol E85:Stearylamine (99:1) with pept-Cys	505.6 ± 28.9 ***	0.620 ± 0.018 **	-15.3 ± 1.8 **

PdI, polydispersity index; * $p < 0.05$, ** $p < 0.01$, *** $p < 0.001$

Functionalization significantly increased the nanoparticles mean size, from 114.1 to 477.3 nm for polymeric nanoparticles, and 147.4 to 505.6 nm for lipid nanoparticles. Both lipid and polymeric nanoparticles with pept-Cys became larger than the ones with pept, which could be related to the different intermediate molecules size (the cross-linker used for the maleimide reaction has a PEG chain of 95.4 Å that leads to a higher particle hydrodynamic radius), as well as peptide size (pept-Cys has one more amino acid than pept). Similarly, PdI increased more for nanoparticles with this maleimide functionalization, and zeta potential became significantly more negative when pept-Cys was present. Moreover, the large size and PdI could have to do with some nanoparticles aggregation probably promoted by the amine groups (Bagwe *et al.*, 2006). Changes on zeta potential values could be a consequence of different chemistries and intermediate molecules/reagents used.

Previous studies already observed this nanoparticles size increase as a consequence of functionalization. As an example, Lamichhane and colleagues synthesized and characterized PLGA nanoparticles bearing glycosaminoglycans, namely hyaluronic acid. When PLGA nanoparticles were functionalized with hyaluronic acid, their mean size increased from ~150 to ~350 nm, depending on the ligand concentration (Lamichhane *et al.*, 2015). In another study, the same trend was monitored when PLGA nanoparticles mean size (~290 nm) increased after polymeric coating with PEG (~590 nm) or chitosan (~745 nm) onto their surface (Martin-Banderas *et al.*, 2015).

To confirm the attachment of peptide to nanoparticle surface, ^{1}H NMR was used for the detection of differences on spectra from non-functionalized and functionalized nanoparticles (**Figure 4.2**). Regarding ^{1}H NMR data for the polymeric nanoparticles (**Figure 4.2**, spectra **A** and **B**), it was possible to verify the presence of characteristic signals related to PLGA at δ1.5 and δ5.4 ppm, which can be attributed to the hydrogens present in -CH- and -CH_3, respectively (Hong *et al.*, 2014). In addition, an intense signal related to Tween 80 used for nanoparticles preparation was detected at δ3.7 ppm (Zhang *et al.*, 2015). The signal commonly attributed to PEG methylene group (Hong *et al.*, 2014), usually located around δ3.6 ppm, was not detected here probably due to PEG reduced concentration compared to free PLGA. Moreover, this PEG signal could also be masked behind the Tween 80 peak.

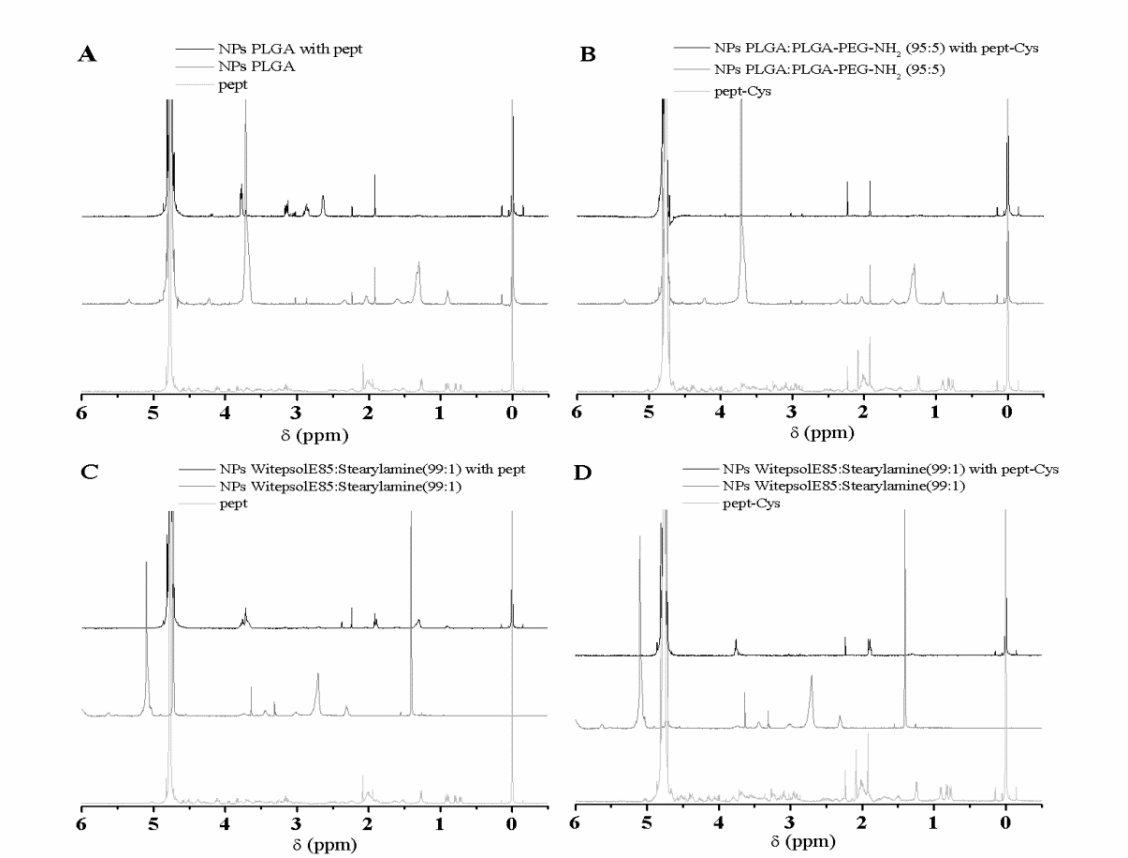

Figure 4.2. ^{1}H NMR spectra of polymeric nanoparticles functionalized with pept (**A**) and pept-Cys (**B**), and lipid nanoparticles functionalized with pept (**C**) and pept-Cys (**D**).

Interestingly, the spectra of functionalized nanoparticles, both with the pept and pept-Cys, were not an overlap of spectra from respective non-functionalized particles plus the peptide. In fact, after functionalization the spectra showed new signals between δ2 and δ4 ppm. These peaks could be related with the presence of MES and/or PB used during functionalization, which were probably adsorbed at particle surface (Bataineh *et al.*, 2012). Moreover, a close spectra observation allowed us to conclude that the intensity of the peaks related with PLGA, Tween 80 and PEG have decreased. From the attained data it can be hypothesized that the presence of MES or PB at nanoparticle surface can act like a shell and contribute to this decreasing effect. Even though the amount of peptide used on functionalized samples was very limited compared to the polymer and lipid, the peak at δ-0.1 ppm strongly suggest the presence of the pept and pept-Cys at the functionalized nanoparticles (Platzer *et al.*, 2014). Thus, NMR data suggested the presence of the two different peptides on the nanoparticles surface, indicating their successful functionalization.

^{1}H NMR has been commonly applied to characterize this kind of surface modification. Campbell and his research group functionalized polymeric nanoparticles with branched poly(ethylene-imine) and characterized this surface modification through ^{1}H NMR, which was performed for non-functionalized and functionalized particles. Conclusions about the effectiveness of the functionalization process were taken after the comparison of NMR chemical shifts between these spectra, as they observed new peaks on modified particles (Campbell *et al.*, 2015).

4.4. Nanoparticles labeling

Nanoparticles were labeled by rhodamine 123 entrapment in order to further detect them when performing cell studies (das Neves *et al.*, 2012). General nanoparticles features were analyzed by Zetasizer, AE was calculated (**Table 4.3**) and rhodamine 123 release profile was determined (**Figure 4.3**). Both SLN and PLGA nanoparticles loaded with rhodamine 123 presented similar features as the ones loaded with siRNA. After 24h, only ~2% of rhodamine 123 was released from both nanosystems, meaning that fluorescence observed on experiments where these nanoparticles were used corresponds to nanoparticles and not free fluorescent dye.

Table 4.3. Physicochemical characteristics of polymeric (PLGA) and lipid (SLN, Witepsol E85) nanoparticles loaded with rhodamine 123.

NP system	Mean Size [nm]	PdI	Zeta Potential [mV]	Association Efficiency [%]
Rhodamine 123-PLGA	113.9 ± 1.4	0.243 ± 0.012	-30.3 ± 0.7	54.3 ± 1.8
Rhodamine 123-SLN	152.2 ± 4.3	0.431 ± 0.032	-23.0 ± 2.5	71.1 ± 3.2

PdI, polydispersity index

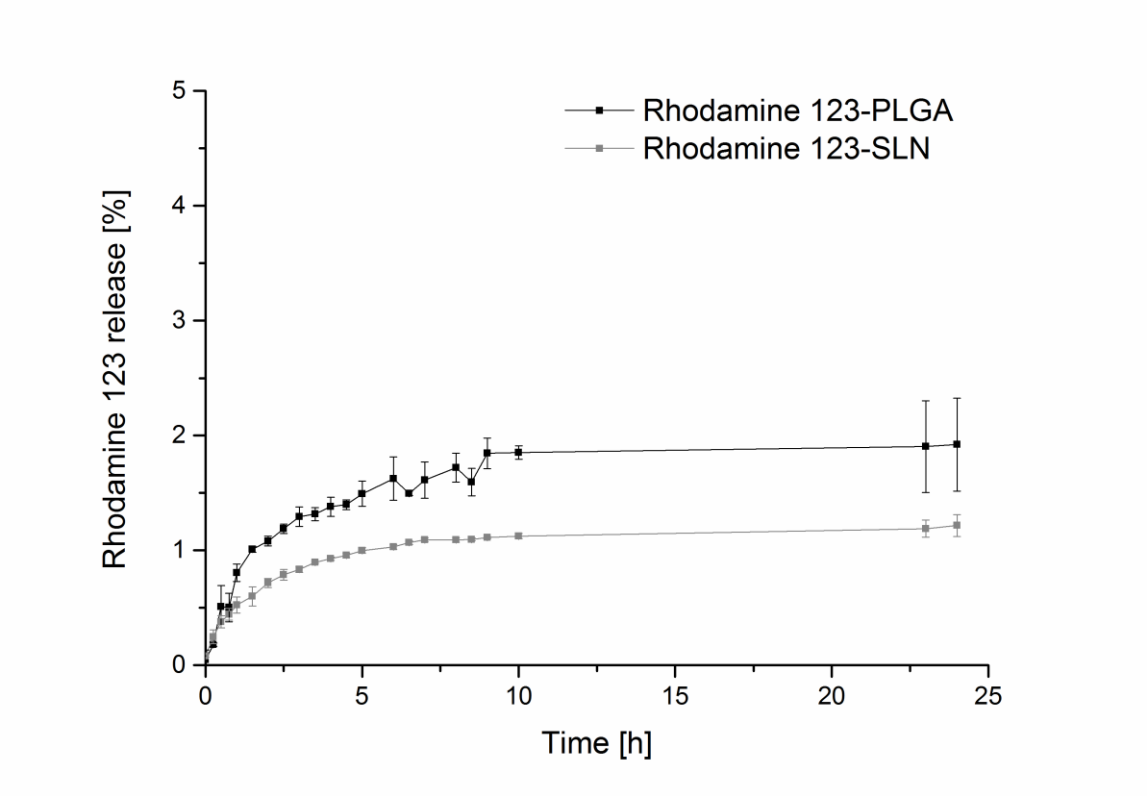

Figure 4.3. Rhodamine 123 release profile from polymeric (PLGA) and lipid (SLN) nanoparticles over 24h (PBS pH 7.4).

Moreover, the surface functionalization of nanoparticles is not expected to change rhodamine 123, as well as siRNA, release profile. Low amounts of short (12 or 13 amino acids) peptides were used to functionalize nanoparticles, which therefore are not believed to modify their nature and hydrophobicity character (Thamake *et al.*, 2011).

4.5. Nanoparticles safety

Nanoparticles *in vitro* cytotoxicity was assessed by cell viability determination through a 3-(4,5-dimethylthiazol-2-yl)-2,5-diphenyltetrazolium bromide (MTT) assay in human brain endothelial cells (hCMEC/D3). A range of nanoparticle concentrations was tested on these cells, and then metabolic activity was determined. Metabolic activity of brain endothelial cells was found to be always above 80% when in contact with all nanoparticles at all evaluated concentrations, except for the two highest concentrations of SLN, which nevertheless led to a cellular metabolic activity never lower than 60% (**Figure 4.4** and **Figure 4.5**). Moreover, the

highest concentration (1000 μg mL^{-1}) of all polymeric carriers (**Figure 4.4**) was significantly different than the others, since it induced a significant decrease on cellular metabolic activity, suggesting that as a maximum concentration limit for the safe use of these nanoparticles. Therefore, it is possible to state that these studied systems are safe to be used with hCMEC/D3 cell line, which is commonly utilized as a BBB model (Weksler *et al.*, 2013), particularly the polymeric-based ones at all tested concentrations and lipid-based ones for concentrations not higher than 10 μg mL^{-1}. Unloaded and non-functionalized nanoparticles had cytotoxic profiles similar to siRNA-loaded and siRNA-loaded peptide-functionalized nanoparticles, indicating that both siRNA-loading and functionalization with pept or pept-Cys do not influence systems safety.

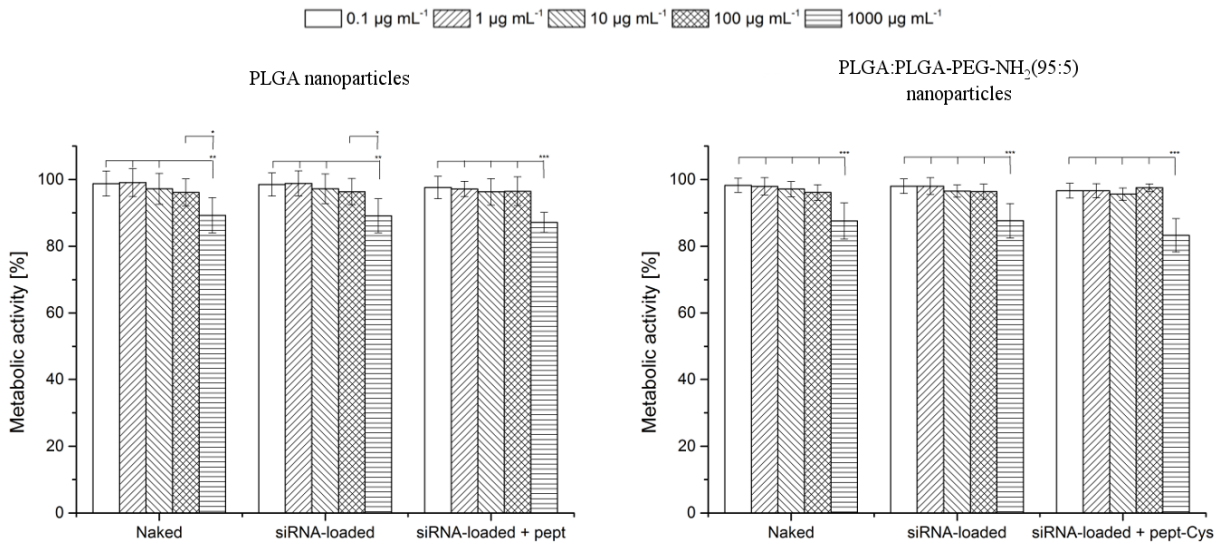

Figure 4.4. Metabolic activity of brain endothelial cells (hCMEC/D3) when incubated with different concentrations of PLGA and PLGA:PLGA-PEG-NH_2(95:5) nanoparticles during 24h. Nanoparticles concentrations were calculated based on polymer(s) concentrations. Naked nanoparticles were unloaded and non-functionalized; siRNA-loaded were loaded and non-functionalized; siRNA-loaded + peptide were loaded and functionalized with pept or pept-Cys.

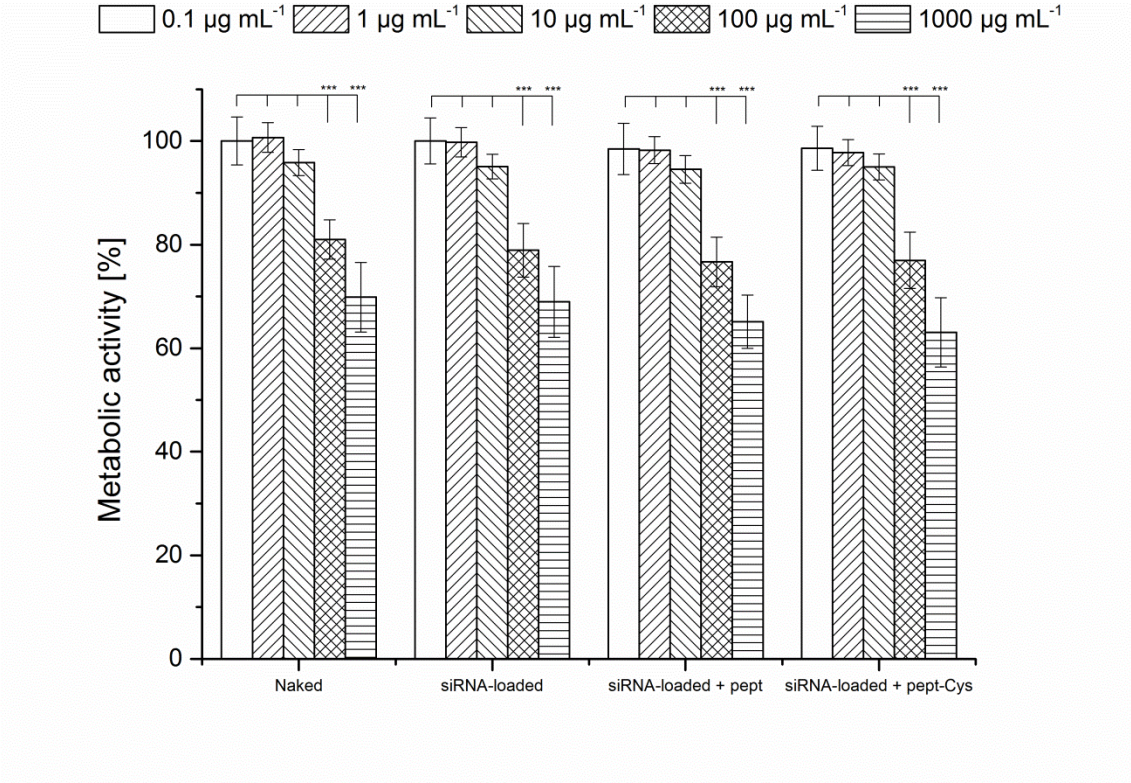

Figure 4.5. Metabolic activity of brain endothelial cells (hCMEC/D3) when incubated with different concentrations of Witepsol E85:Stearylamine(99:1) nanoparticles during 24h. Nanoparticles concentrations were calculated based on lipids concentrations. Naked nanoparticles were unloaded and non-functionalized; siRNA-loaded were loaded and non-functionalized; siRNA-loaded + peptide were loaded and functionalized with pept or pept-Cys.

Polymeric nanoparticles are known as biocompatible carriers that circumvent free-drug toxicity by encapsulation. Copolymers are non-toxic materials as well, as Guo and colleagues also evaluated through the biocompatibility assessment of nanoparticles made of polyethylene glycol-poly L-lysine-poly lactic-co-glycolic acid (PEG-PLL-PLGA) copolymer (Guo *et al.*, 2015). They observed low *in vitro* cytotoxicity of these nanoparticles on mouse fibroblast L929 cells, through MTT assay. Neves and colleagues observed SLN made of cetyl palmitate as safe carriers for hCMEC/D3 cell line at concentrations up to 1500 µg mL^{-1}, not compromising the cell metabolic activity (Neves *et al.*, 2015). This concentration is much higher than the maximum observed by us as safe when using lipid nanoparticles (10 µg mL^{-1}). The main reason for that could be the presence of stearylamine, which is an already described potentially toxic lipid (Hung *et al.*, 2005). Accordingly, a study where nanoemulsions containing cholesterol and amphotericin B were assessed, the influence of stearylamine was evaluated. Authors observed that loaded and unloaded nanoemulsions without stearylamine were approximately 40-fold less toxic to J774 macrophages than the

nanoemulsions containing 0.1% stearylamine. That scenario was further highlighted when stearylamine was used at 0.2%, which emphasized this cationic lipid-related enhanced toxicity (Caldeira *et al.*, 2015).

4.6. Cell-nanoparticle interaction

To verify whether the used cell line (hCMEC/D3) was expressing the receptor against which the nanoparticles were functionalized, a simple test where cells were immuno-labeled was performed. Two dilutions of the primary antibody (antibody against transferrin receptor) were assessed (**Figure 4.6**). The most concentrated condition (primary antibody at 1:50) showed a significant expression of 2.9-fold of the TfR-related signal intensity, compared to the unstained control. Negative control was also performed when only the labeled secondary antibody was added to the cells, to verify the inexistence of unspecific bindings and false positives results.

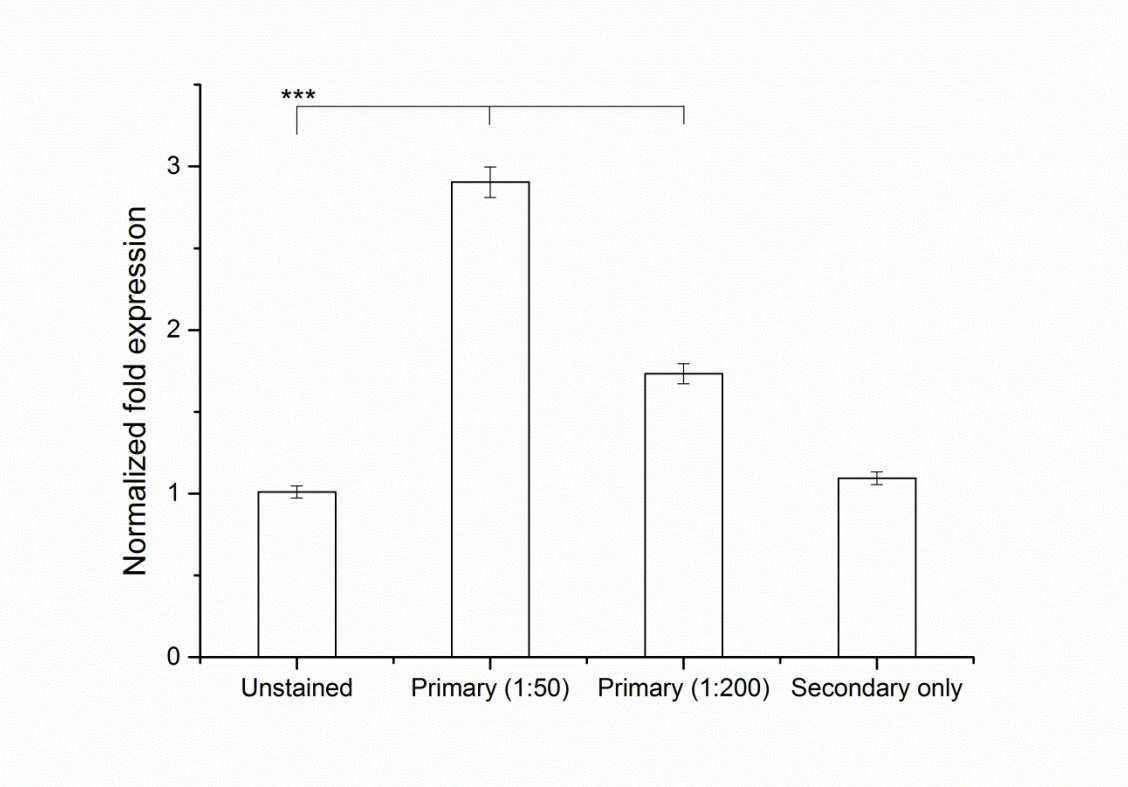

Figure 4.6. Transferrin receptor labeling expression by the hCMEC/D3 cell line. Different conditions and controls were tested: unstained cells, with primary and secondary-labeled antibody, with secondary-labeled antibody only. All the samples were normalized to the unstained control.

This result testified the transferrin receptor expression on this cell line. Therefore, experiments proceeded to evaluate the interaction between cells and nanoparticles, mainly through transferrin receptor.

The interaction between non-functionalized/functionalized nanoparticles and human brain endothelial cells was studied over time through fluorescence microscopy and cytometry (fluorescence-activated cell sorting, FACS). Fluorescence microscopy study was performed as a qualitative and visual analysis, using the same protocol as FACS experiments. Nanoparticles (labeled in green) were incubated with human brain endothelial cells (labeled in red) for 15 min, 1h and 4h, and their interaction was assessed. It was possible to observe that polymeric nanoparticles interacted with human brain endothelial cells in higher extent after functionalization (**Figure 4.7**), since they were observed in the close vicinity of the cell membranes. This difference was detected on both functionalized with pept and pept-Cys polymeric nanoparticles, meaning that both functionalization approaches were successful.

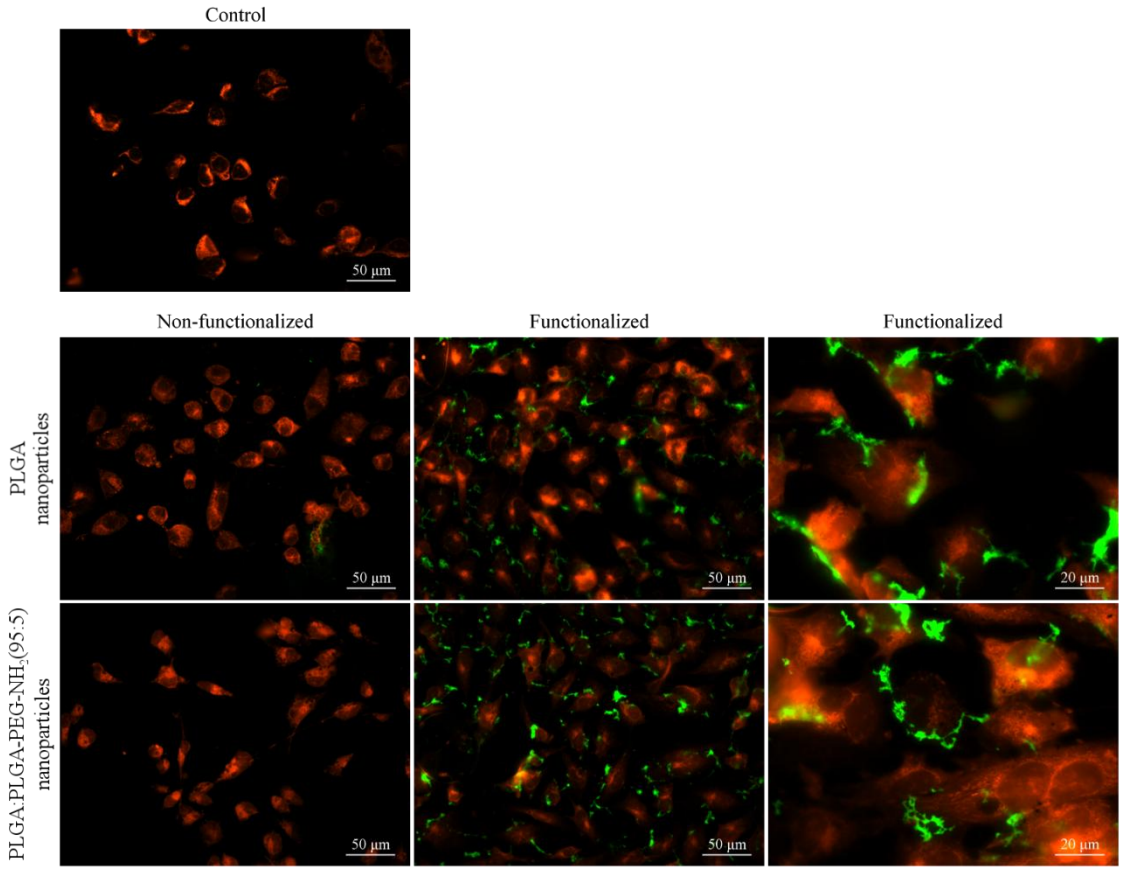

Figure 4.7. Fluorescence microscope images representative of the interaction between polymeric nanoparticles (non-functionalized and functionalized) and human brain endothelial cells, after an incubation period of 4h. Cells were stained in red, nanoparticles in green. The control group was cells without nanoparticles.

For lipid systems this difference was not evident (data not shown), which may indicate an inefficient functionalization either due to a low yield binding chemistry process itself, or due to the lack of correct peptide availability for its receptor. Significant differences over time were also not observed, which is probably related to the lack of precision and accuracy of this technique, reason why it was used just to give a general view of what was happening. Nonetheless, these qualitative data suggest that functionalization processes reached their goals on polymeric nanoparticles, by increasing nanoparticles interaction with blood-brain barrier cells.

To validate NMR and fluorescence microscope data, flow cytometry analysis was performed as a quantitative test. As a direct result, histograms were obtained and consequently the fold increase of the fluorescence geometric mean of all samples when compared to the control (cells without nanoparticles) was determined (**Table 4.4**). Correspondent histograms from polymeric nanoparticles with hCMEC/D3 cell line are present on **Figure 4.8**.

Table 4.4. Flow cytometry quantification of the interaction between labeled nanoparticles and hCMEC/D3 cells over time. The fold increase was related to the fluorescence comparison with unstained control (cells without nanoparticles), meaning the fold increase of the percentage of cells interacting with the nanoparticles.

NP system	Fold increase		
	t = 15 min	t = 1 h	t = 4 h
PLGA	2.34 ± 0.37 *** ###	5.44 ± 0.16 *** ###	9.29 ± 0.48 *** ###
PLGA with pept	13.98 ± 0.87 ***	16.35 ± 0.47 ***	32.73 ± 2.04 *** ###
PLGA:PLGA-PEG-NH_2 (95:5)	2.58 ± 0.42 *** #	4.27 ± 0.34 ***	5.63 ± 0.88 ***
PLGA:PLGA-PEG-NH_2 (95:5) with pept-Cys	9.77 ± 0.19 ***	12.33 ± 0.32 ***	21.26 ± 2.51 *** ##
Witepsol E85:Stearylamine (99:1)	1.10 ± 0.12 **	1.11 ± 0.11 ***	1.42 ± 0.39 **
Witepsol E85:Stearylamine (99:1) with pept	2.48 ± 0.27 ** #	3.30 ± 0.24 *** #	4.17 ± 0.17 ** ##
Witepsol E85:Stearylamine (99:1)	1.10 ± 0.12 **	1.11 ± 0.11 ***	1.42 ± 0.39 **
Witepsol E85:Stearylamine (99:1) with pept-Cys	2.34 ± 0.30 ** #	3.13 ± 0.11 *** #	4.37 ± 0.47 ** ##

** $p < 0.01$, *** $p < 0.001$ – For the comparison within the same time point
# $p < 0.05$, ## $p < 0.01$, ### $p < 0.001$ – For the comparison within the same NP system

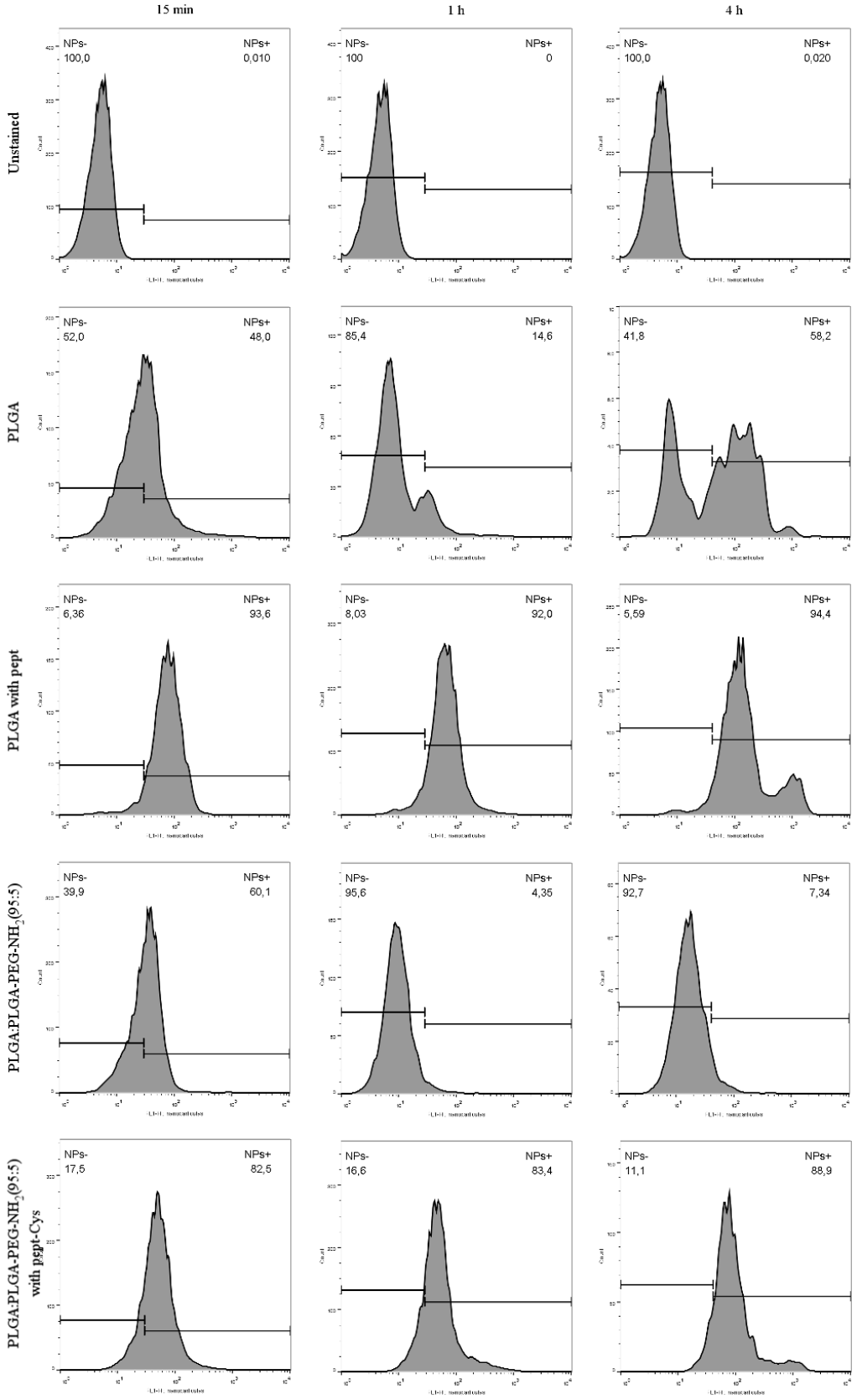

Figure 4.8. Representative flow cytometry histograms of polymeric nanoparticles (non-functionalized and functionalized) with human brain endothelial cells over time. The control was the unstained line (cells without nanoparticles).

For all the studied labeled systems, when incubated with hCMEC/D3 cells, an increase of fluorescence over time was observed due to an increased interaction and further binding to the surface and/or internalization of nanoparticles into cells, as expected but not detected on fluorescence microscope analysis. This increment was even higher for nanoparticles with the peptide at their surface, reaching significantly higher values of fluorescence fold increase after 4h. By comparison between non-functionalized and functionalized nanoparticles, FACS results corroborate NMR and fluorescence microscope evidences. Polymeric nanoparticles were successful functionalized, since fluorescence was significantly higher when functionalized nanoparticles were used rather than non-functionalized, meaning that functionalized nanoparticles interacted more with cell membranes. On histograms, these differences were detected by the observation of peak shifts to the right (increased fluorescence direction) between samples over time and between non-functionalized and functionalized nanoparticles. From these representative histograms shown on **Figure 4.8**, it was possible to quantify that, after 4h of incubation with fluorescent nanoparticles, 94.4% of cells were attached to functionalized PLGA nanoparticles, while 58.2% of cells were attached to non-modified PLGA nanoparticles. As well, 88.9% of cells were interacting with functionalized PLGA:PLGA-PEG-NH_2(95:5) nanoparticles, while only 7.34% interacted with non-functionalized PLGA:PLGA-PEG-NH_2(95:5) nanoparticles. This means that the proper attachment between nanoparticles and BBB cells was significantly increased when these systems were functionalized. Moreover, the same trend was observed for lipid systems. However, the fluorescence obtained for these lipid functionalized particles after 4h of incubation with cells, although much higher than the obtained for non-functionalized ones, corresponded to low values of fluorescence after all (much lower than the ones obtained for polymeric nanoparticles), which explains why differences were not detected through the fluorescence microscope. This may suggest that the functionalization process on lipid nanoparticles may not have been as successful as for polymeric systems. As it was mentioned before, a functionalization process has several critical steps, such the spatial peptide orientation on these lipid systems that could made it unavailable for the receptor or the possible low functionalization yield for these carriers. Furthermore, non-functionalized polymeric nanoparticles interacted more with cells than non-functionalized lipid ones did, which could indicate that even before functionalization the ability of these lipid nanoparticles to interact with cells is not that promising. Therefore, besides functionalization and targeting success, nanoparticles matrix composition could also influence their interaction with cells.

Functionalization process improved the potential efficacy of nanoparticles, mainly the polymeric ones, since they became more attracted and capable to interact with their target

cells, being more bonded to their surface and/or internalized compared to non-functionalized ones. Both peptides, using both chemistries, resulted on a significantly higher interaction with BBB cells compared to non-functionalized nanoparticles, 3.5-fold with pept and 3.8-fold with pept-Cys, after 4h in contact with cells. For lipid systems, lipid nanoparticles with pept improve the interaction with cells by 2.9-fold while lipid nanoparticles with pept-Cys 3.1-fold, compared to respective non-functionalized nanoparticles. Therefore, FACS results complement NMR spectra and fluorescence microscope images, confirming the presence of peptides on nanoparticles surface and the increased nanoparticle-cell interaction after functionalization.

Araújo and co-workers assessed the interaction of PLGA nanoparticles modified with chitosan and a cell penetrating peptide with Caco-2 and HT29-MTX cells (Araújo *et al.*, 2015). They observed by confocal microscopy no significant interaction for both unmodified nanoparticles. However, when nanoparticles were further functionalized with cell penetrating peptide, cell-nanoparticle interactions were higher, as more particles were associated and internalized by the cells. In the same study, quantitative flow cytometry experiments demonstrated that functionalized nanoparticles presented a 5.6-fold increase in the interaction with the intestinal cells, compared to the unmodified nanoparticles (Araújo *et al.*, 2015). These values are similar to the ones obtained by our functionalized polymeric nanoparticles.

Kang and his group developed a nanosystem aimed to treat glioblastoma. For that, to achieve BBB, polymeric nanoparticles (PLGA-PEG) were functionalized with a cyclic nine amino acid peptide (named as CRT peptide), an iron-mimic moiety targeting the transferrin-receptor (TfR). The main aim of this study was to compare this CRT functionalization with Tf-modified nanoparticles and unmodified ones. Cell-nanoparticle interactions were assessed using brain capillary endothelial cell line (BCEC) and rat C6 glioma cell line over expressing TfR. Fluorescence microscope images showed an increased fluorescence intensity of CRT-nanoparticles compared to unmodified nanoparticles, in BCEC cells and C6 cells. Additionally, quantitative experiments determined that, in BCEC cells, the fluorescence signal related to CRT-nanoparticles was 1.9-fold higher than for unmodified particles, which is a value significantly lower than the obtained in the present study. As well, the fluorescence signal of Tf-nanoparticles was 1.6-fold and 1.8-fold higher than on unmodified particles after 1 and 4h, respectively. Similar data were obtained for C6 cells, highlighting the advantages of CRT and Tf functionalization over unmodified nanoparticles on cell-nanoparticle interaction (Kang *et al.*, 2015).

Additionally, it is important to highlight how functionalization is a delicate issue. Nanoparticles surface, either charge, coating or conjugated molecules, have an impact on their behavior, namely on cellular interaction and uptake. Increased ligand concentrations on nanoparticle surfaces can result in serum protein binding and enhance rapid clearance or diminish the ability of the ligands to interact with their target receptors. Therefore, the number, density, and orientation of targeting ligands on the surface of nanoparticles are important factors for an effective targeting (Amin *et al.*, 2015). Specifically, the active site of the ligand must be available in the correct three-dimensional arrangement to correctly bind to the receptor. In this study, the possibility to have a side-oriented covalent link of transferrin-receptor peptide needs to be considered, since it is correlated with further cell interaction and, therefore, could be critical for nanoparticles efficacy. This could be the reason why lipid nanoparticles had low binding values to BBB cells.

5. Conclusions

Worldwide spread brain disorders are an actual problem that our society faces nowadays. Surpass BBB is the main common key for all brain disorders, which could in the future lead to improved therapies and maybe cures. Regarding that, this work aimed to develop a nanosystem able to transport siRNA against P-gp towards the brain endothelial cells. Basic lipid and polymeric nanoparticles were produced and, as a first step, functional groups were added *via* the addition of a new lipid/polymer to regular systems in order to promote the functionalization process, namely the peptide binding to nanoparticles surface. siRNA was loaded and its association efficiency reached 50% on PLGA:PLGA-PEG-NH_2(95:5) nanoparticles. These systems enabled a prolonged release of siRNA from their matrices, reaching around 60% after 24h. Two peptides against transferrin-receptor were tested through two chemically distinct approaches (carbodiimide and maleimide), planning to further choose the one that attains better results after the functionalization procedure. Obtained functionalized nanoparticles had an increased size and NMR new peaks when compared to non-functionalized samples, which suggest the successful presence of peptides on all developed systems. Nanoparticles (unloaded, siRNA-loaded, siRNA-loaded and functionalized) were found to have no cytotoxicity on a cell line generally utilized as a BBB model, once used up to concentrations of 1000 μg mL^{-1} for polymeric systems and 10 μg mL^{-1} for lipid ones. Again, cell-nanoparticle interaction data suggest that both functionalization processes achieved their goals on polymeric nanoparticles, by making these modified

systems more attracted and capable to interact (3.5 to 3.8-fold more) with targeted TfR-expressing BBB cells than non-functionalized ones.

Therefore, this study focused on nanoparticles improvement and highlighted the importance of carriers, namely correctly functionalized carriers, to obtain better outcomes. The best systems obtained through these experiments were polymeric nanoparticles (PLGA and PLGA:PLGA-PEG-NH_2 (95:5)), which were effectively functionalized with TfR-peptides. This great achievement supports and encourages their promising potential. By interacting more and more specifically with their target cells, this nanoparticles approach will further improve their ability to successfully permeate and deliver siRNA on these cells, ending with a likely more permeable BBB needed to reach drug therapeutic concentrations in brain.

6. Acknowledgements

The authors would like to acknowledge all the help of Victória Leiro with the NMR experiments. Carlos Fernandes would like to thank to FCT for financial support (SFRH/BD/98519/2013).

7. References

Abbott, N.J., Patabendige, A.A., Dolman, D.E., Yusof, S.R. and Begley, D.J. 2010. Structure and function of the blood-brain barrier. Neurobiol Dis. 37 (1): 13-25.

Amin, M.L., Joo, J.Y., Yi, D.K. and An, S.S. 2015. Surface modification and local orientations of surface molecules in nanotherapeutics. J Control Release. 207: 131-142.

Araújo, F., Shrestha, N., Shahbazi, M.A., Liu, D., Herranz-Blanco, B., Mäkilä, E.M., Salonen, J.J., Hirvonen, J.T., Granja, P.L., Sarmento, B. and Santos, H.A. 2015. Microfluidic assembly of a multifunctional tailorable composite system designed for site specific combined oral delivery of peptide drugs. ACS Nano. 9 (8): 8291-8302.

Bagwe, R.P., Hilliard, L.R. and Tan, W. 2006. Surface modification of silica nanoparticles to reduce aggregation and non-specific binding. Langmuir. 22 (9): 4357-4362.

Bataineh, H., Pestovsky, O. and Bakac, A. 2012. pH-induced mechanistic changeover from hydroxyl radicals to iron(iv) in the Fenton reaction. Chem Sci. 3 (5): 1594-1599.

Bauer, B., Hartz, A.M.S., Fricker, G. and Miller, D.S. 2005. Modulation of P-glycoprotein transport function at the blood-brain barrier. Exp Biol Med. 230 (2): 118-127.

Bhaskar, S., Tian, F., Stoeger, T., Kreyling, W., de la Fuente, J.M., Grazu, V., Borm, P., Estrada, G., Ntziachristos, V. and Razansky, D. 2010. Multifunctional nanocarriers for diagnostics, drug delivery and targeted treatment across blood-brain barrier: perspectives on tracking and neuroimaging. Part Fibre Toxicol. 7 (3): 1-25.

Caldeira, L.R., Fernandes, F.R., Costa, D.F., Frezard, F., Afonso, L.C. and Ferreira, L.A. 2015. Nanoemulsions loaded with amphotericin B: a new approach for the treatment of leishmaniasis. Eur J Pharm Sci. 70: 125-131.

Campbell, M.L., Guerra, F.D., Dhulekar, J., Alexis, F. and Whitehead, D.C. 2015. Target-specific capture of environmentally relevant gaseous aldehydes and carboxylic acids with functional nanoparticles. Chemistry. 21 (42): 14834-14842.

Cruz, L.J., Tacken, P.J., Fokkink, R., Joosten, B., Stuart, M.C., Albericio, F., Torensma, R. and Figdor, C.G. 2010. Targeted PLGA nano- but not microparticles specifically deliver antigen to human dendritic cells via DC-SIGN in vitro. J Control Release. 144 (2): 118-126.

Cui, Z.K., Fan, J., Kim, S., Bezouglaia, O., Fartash, A., Wu, B.M., Aghaloo, T. and Lee, M. 2015. Delivery of siRNA via cationic Sterosomes to enhance osteogenic differentiation of mesenchymal stem cells. J Control Release. 217: 42-52.

das Neves, J., Michiels, J., Arien, K.K., Vanham, G., Amiji, M., Bahia, M.F. and Sarmento, B. 2012. Polymeric nanoparticles affect the intracellular delivery, antiretroviral activity and cytotoxicity of the microbicide drug candidate dapivirine. Pharm Res. 29 (6): 1468-1484.

Esfandyari-Manesh, M., Mostafavi, S.H., Majidi, R.F., Koopaei, M.N., Ravari, N.S., Amini, M., Darvishi, B., Ostad, S.N., Atyabi, F. and Dinarvand, R. 2015. Improved anticancer delivery of paclitaxel by albumin surface modification of PLGA nanoparticles. Daru. 23 (28): 1-8.

Fisher, M., Abramov, M., Van Aerschot, A., Xu, D., Juliano, R.L. and Herdewijn, P. 2007. Inhibition of MDR1 expression with altritol-modified siRNAs. Nucleic Acids Res. 35 (4): 1064-1074.

Fonte, P., Soares, S., Sousa, F., Costa, A., Seabra, V., Reis, S. and Sarmento, B. 2014. Stability study perspective of the effect of freeze-drying using cryoprotectants on the structure of insulin loaded into PLGA nanoparticles. Biomacromolecules. 15 (10): 3753-3765.

Gabathuler, R. 2010. Approaches to transport therapeutic drugs across the blood-brain barrier to treat brain diseases. Neurobiol Dis. 37 (1): 48-57.

Gilmore, J.L., Yi, X., Quan, L. and Kabanov, A.V. 2008. Novel nanomaterials for clinical neuroscience. J Neuroimmune Pharmacol. 3 (2): 83-94.

Gomes, M.J., Martins, S. and Sarmento, B. 2015. siRNA as a tool to improve the treatment of brain diseases: mechanism, targets and delivery. Ageing Res Rev. 21: 43-54.

Guo, L., Chen, B., Liu, R., Liu, P., Xia, G., Wang, Y., Li, X., Chen, W., Wang, X. and Jiang, H. 2015. Biocompatibility assessment of polyethylene glycol-poly L-lysine-poly lactic-co-glycolic acid nanoparticles in vitro and in vivo. J Nanosci Nanotechno. 15 (5): 3710-3719.

Hong, W., Chen, D., Jia, L., Gu, J., Hu, H., Zhao, X. and Qiao, M. 2014. Thermo- and pH-responsive copolymers based on PLGA-PEG-PLGA and poly(l-histidine): Synthesis and in vitro characterization of copolymer micelles. Acta Biomater. 10 (3): 1259-1271.

Huang, R.Q., Qu, Y.H., Ke, W.L., Zhu, J.H., Pei, Y.Y. and Jiang, C. 2007. Efficient gene delivery targeted to the brain using a transferrin-conjugated polyethyleneglycol-modified polyamidoamine dendrimer. Faseb J. 21: 1117-1125.

Hung, C.F., Hwang, T.L., Chang, C.C. and Fang, J.Y. 2005. Physicochemical characterization and gene transfection efficiency of lipid emulsions with various co-emulsifiers. Int J Pharm. 289 (1-2): 197-208.

Jain, P.P., Leber, R., Nagaraj, C., Leitinger, G., Lehofer, B., Olschewski, H., Olschewski, A., Prassl, R. and Marsh, L.M. 2014. Liposomal nanoparticles encapsulating iloprost exhibit enhanced vasodilation in pulmonary arteries. Int J Nanomedicine. 9: 3249-3261.

Kang, T., Jiang, M., Jiang, D., Feng, X., Yao, J., Song, Q., Chen, H., Gao, X. and Chen, J. 2015. Enhancing glioblastoma-specific penetration by functionalization of nanoparticles with an iron-mimic peptide targeting transferrin/transferrin receptor complex. Mol Pharm. 12 (8): 2947-2961.

Kikwai, L., Babu, R.J., Prado, R., Kolot, A., Armstrong, C.A., Ansel, J.C. and Singh, M. 2005. In vitro and in vivo evaluation of topical formulations of Spantide II. AAPS PharmSciTech. 6 (4): 565-572.

Kuo, Y.C. and Chen, H.H. 2010. Effect of electromagnetic field on endocytosis of cationic solid lipid nanoparticles by human brain-microvascular endothelial cells. J Drug Target. 18 (6): 447-456.

Lamichhane, S.P., Arya, N., Ojha, N., Kohler, E. and Shastri, V.P. 2015. Glycosaminoglycan-functionalized poly-lactide-co-glycolide nanoparticles: synthesis, characterization, cytocompatibility, and cellular uptake. Int J Nanomedicine. 10: 775-789.

Li, T.S., Yawata, T. and Honke, K. 2014. Efficient siRNA delivery and tumor accumulation mediated by ionically cross-linked folic acid-poly(ethylene glycol)-chitosan oligosaccharide lactate nanoparticles: for the potential targeted ovarian cancer gene therapy. Eur J Pharm Sci. 52: 48-61.

Mahringer, A., Ott, M., Reimold, I., Reichel, V. and Fricker, G. 2011. The ABC of the blood-brain barrier - regulation of drug efflux pumps. Curr Pharm Design. 17: 2762-2770.

Martin-Banderas, L., Munoz-Rubio, I., Prados, J., Alvarez-Fuentes, J., Calderon-Montano, J.M., Lopez-Lazaro, M., Arias, J.L., Leiva, M.C., Holgado, M.A. and Fernandez-Arevalo, M. 2015. In vitro and in vivo evaluation of Delta(9)-tetrahidrocannabinol/PLGA nanoparticles for cancer chemotherapy. Int J Pharm. 487 (1-2): 205-212.

Moos, T. and Morgan, E.H. 2000. Transferrin and transferrin receptor function in brain barrier systems. Cell Mol Neurobiol. 20 (1): 77-95.

Murthy, S.K. 2007. Nanoparticles in modern medicine: State of the art and future challenges. Int J Nanomedicine. 2 (2): 129-141.

Neves, A.R., Queiroz, J.F., Weksler, B., Romero, I.A., Couraud, P.O. and Reis, S. 2015. Solid lipid nanoparticles as a vehicle for brain-targeted drug delivery: two new strategies of functionalization with apolipoprotein E. Nanotechnology. 26 (49): 1-11.

Platzer, G., Okon, M. and McIntosh, L. 2014. pH-dependent random coil 1H, 13C, and 15N chemical shifts of the ionizable amino acids: a guide for protein pK a measurements. J Biomol NMR. 60 (2-3): 109-129.

Qi, L., Lu, Y. and Wu, W. 2012. Absorption, disposition and pharmacokinetics of solid lipid nanoparticles. Curr Drug Metab. 13 (4): 418-428.

ResearchAndMarkets 2007. Drug delivery technology - revolutionizing CNS therapies. (PharmaVision).

Soares, S., Fonte, P., Costa, A., Andrade, J., Seabra, V., Ferreira, D., Reis, S. and Sarmento, B. 2013. Effect of freeze-drying, cryoprotectants and storage conditions on the stability of secondary structure of insulin-loaded solid lipid nanoparticles. Int J Pharm. 456 (2): 370-381.

Thamake, S.I., Raut, S.L., Ranjan, A.P., Gryczynski, Z. and Vishwanatha, J.K. 2011. Surface functionalization of PLGA nanoparticles by non-covalent insertion of a homo-bifunctional spacer for active targeting in cancer therapy. Nanotechnology. 22: 1-10.

Venkateswarlu, V. and Manjunath, K. 2004. Preparation, characterization and in vitro release kinetics of clozapine solid lipid nanoparticles. J Control Release. 95 (3): 627-638.

Wang, C.F., Sarparanta, M.P., Makila, E.M., Hyvonen, M.L., Laakkonen, P.M., Salonen, J.J., Hirvonen, J.T., Airaksinen, A.J. and Santos, H.A. 2015. Multifunctional porous silicon nanoparticles for cancer theranostics. Biomaterials. 48: 108-118.

Weksler, B., Romero, I.A. and Couraud, P.O. 2013. The hCMEC/D3 cell line as a model of the human blood brain barrier. Fluids Barriers CNS. 10 (16): 1-10.

Zhang, Q., Wang, A., Meng, Y., Ning, T., Yang, H., Ding, L., Xiao, X. and Li, X. 2015. NMR Method for Accurate Quantification of Polysorbate 80 Copolymer Composition. Anal Chem. 87 (19): 9810-9816.

Zimmermann, J.L., Nicolaus, T., Neuert, G. and Blank, K. 2010. Thiol-based, site-specific and covalent immobilization of biomolecules for single-molecule experiments. Nat Protoc. 5 (6): 975-985.

CHAPTER V

Delivery of siRNA silencing P-glycoprotein in peptide-functionalized nanoparticles causes efflux modulation at a human blood-brain barrier model

This chapter was based on the following submitted paper:

- **Gomes, M.J.**, Kennedy, P.J., Martins, S. and Sarmento, B. 2017. Delivery of siRNA silencing P-glycoprotein in peptide-functionalized nanoparticles causes efflux modulation at a human blood-brain barrier model. Submitted.

1. Abstract

As a tightly organized layer of endothelial cells, blood-brain barrier (BBB) has distinctive features that limit the capacity of drugs to enter the brain and reach therapeutic targets. One of the most effective BBB-related obstacles is the P-glycoprotein (P-gp), which acts as an efflux pump. Silencing this protein expression *via* siRNA constitutes a potential way to triumph over BBB blockade, improving delivery of drugs to the brain. In this work, new functionalized nanoparticles *via* different peptide linkage bridges, targeted to transferrin receptor, were developed to deliver P-gp silencing siRNA to brain endothelial cells. Both carbodiimide and maleimide approaches were used to anchor a peptide to the surface of PLGA-COOH and PLGA-PEG-NH_2 materials, respectively, assuring target effect and prolonged blood circulation of siRNA-containing nanoparticles. Beyond their ability to improve siRNA permeability through the BBB by 2-fold, it was shown that, 96h post transfection, maleimide functionalized PLGA:PLGA-PEG-NH_2 nanoparticles successfully induced reduction of P-gp mRNA expression up to 52%, compared to non-functionalized systems. Subsequently, increase on rhodamine 123 permeability through the human BBB model up to 27% was detected. In this fashion, such values reveal the brightness of this approach to possibly enable drugs to reach brain in higher and therapeutic concentrations.

KEYWORDS: Blood-brain barrier; P-glycoprotein; siRNA; Targeted nanoparticles; Transferrin-receptor binding peptide

2. Introduction

The incidence of central nervous system (CNS) related diseases is continuously increasing due to ageing population along with an increased average life expectancy (Gomes *et al.*, 2015). Therefore, CNS disorders are a worldwide concern to individuals, their families and societies in general. Existing therapies for CNS diseases are mainly blocked by BBB related obstacles, which hampers more than 98% of candidate drugs, presenting a major challenge for the pharmaceutical industry (Anand *et al.*, 2015). As a result, current treatments are failing their meaningful purpose, which creates an opportunity for nanomedicine to arise as an alternative pathway to circumvent BBB handicaps.

BBB, as a tightly packed layer of endothelial cells surrounded by pericytes, astrocytes and microglial cells, presents molecular and receptor structures able to mediate the transport of substances in and out of the brain. In a first approach, BBB restricts the passage of foreign substances into the brain. Additionally, efflux transporters like P-gp are one of the main contributors for brain penetration limitations, pumping drugs back to the blood stream (Abbott *et al.*, 2010; Bhaskar *et al.*, 2010). P-gp is a phosphorylated glycoprotein expressed in multiple cell types with relevant activity at the luminal plasma membrane of the capillary brain endothelium (Mahringer *et al.*, 2011). This efflux pump is often over-expressed in tumor cells which contributes to the multi-drug resistant phenotype commonly observed in cancer cells (Fisher *et al.*, 2007).

Nanoparticle-based drug delivery systems have a potentially customized surface that promotes not only their targeting but also their cellular uptake by endogenous transport systems acting as “Trojan horse” (Gao *et al.*, 2017). Thus, nanoparticles (NPs) should act as biocompatible and biodegradable materials with surface functional groups where targeting ligands could be anchored, directing these systems to specific cells or tissues and decreasing their off-targets effects.

Efflux transporters are considered attractive targets to be inhibited and improve drug passage across the BBB (Mahringer *et al.*, 2011). Nanoparticles, on the other hand, have shown their ability to be addressed to the BBB (Gomes *et al.*, 2016). Therefore, by combining these concepts with the ability of specific small interfering RNA (siRNA) sequences to transient and reversibly silence P-gp, this arises as a possible solution to surpass BBB. Gene silencing through siRNA offers a specific deactivation of genes since it specifically binds to complementary messenger RNA (mRNA) sequences, leading to degradation of the target mRNA, and following down-regulation of protein synthesis (Malmo *et al.*, 2013). Hence,

siRNA against P-gp is capable to specific and directly down-regulate P-gp expression and subsequent transport activity, helping to improve its substrates permeability through the BBB. Simultaneously, nanoparticles protect the siRNA from enzymatic degradation and may direct it to brain endothelial cells through surface functionalization, thus improving siRNA cellular delivery.

This study proposes a peptide-functionalized nanomaterial to transport siRNA against human P-gp (P-gp-siRNA) specifically to the BBB, temporarily reducing drug efflux, and increasing drug permeability kinetics in the CNS. This system, based on merging poly(lactic-co-glycolic acid) (PLGA) and PEGylated PLGA, was firstly directed to the BBB through surface modification in a site-oriented manner with a peptide against transferrin receptor (TfR) over expressed at the BBB (Gabathuler, 2010), derivative of transferrin itself (Gomes *et al.*, 2016). In addition, a BBB monolayer model was created with human brain endothelial cells, hCMEC/D3 (Weksler *et al.*, 2013), in order to assess permeability kinetics of siRNA itself. The same cell line was treated with siRNA-loaded nanoparticles to further evaluation of their effect on P-gp expression. Moreover, the permeability of a model P-gp substrate (rhodamine 123) was also assessed, after P-gp down-regulation, to understand its influence on drug efflux.

3. Materials and Methods

3.1. Materials

PLGA 5004A, was purchased from Corbion – Purac, PLGA-PEG-NH_2 from PolySciTech. Ethyl acetate was purchased from VWR, siRNA-FITC against P-gp, siRNA against P-gp and scrambled siRNA from Santa Cruz Biotechnology, TfR-peptide from AnaSpec, TfR-peptide-Cys from Eurogentec, and SM$(PEG)_{24}$ was from Thermo Scientific. EBM-2 medium from Lonza, 12-well plate PET inserts 0.4 µm from Corning BD, Vectashield and DAPI from Vector Laboratories Inc, and ScreenFectA from InCella. Several materials were purchased from Sigma: Tween 80, EDC (1-ethyl-3-(3-dimethylaminopropyl)carbodiimide), NHS (N-hydroxysuccinimide), MES (2-(N-morpholino)ethanesulfonic acid), hydrocortisone, ascorbic acid, HEPES, bFGF (basic fibroblast growth factor), verapamil hydrochloride and paraformaldehyde. Others were purchased from Invitrogen: Rhodamine 123, WGA Alexa Fluor 594, P-gp and YWHAZ

primers. From Gibco it was purchased FBS, penicillin-streptomycin, chemically defined lipid concentrate, HBSS, collagen I rat protein and trypsin-EDTA.

3.2. Methods

3.2.1. Nanoparticles production

Polymeric nanoparticles were prepared through a modified solvent emulsification evaporation method based on the water-in-oil-in-water (w/o/w) double emulsion technique (Fonte *et al.*, 2014; Soares *et al.*, 2013), already described by us (Gomes *et al.*, 2016). Briefly, twenty milligrams of polymer (PLGA and/or PLGA-PEG-NH_2) were dissolved in ethyl acetate, siRNA (13.55 ng μL^{-1}) was added, and the solution was homogenized using a Vibra-Cell™ ultrasonic processor. The primary formed emulsion (w/o) was then added into the surfactant solution, 2% of Tween 80, and homogenized again for 60s. The second formed emulsion (w/o/w) was finally added to another solution of the same surfactant, and was left under magnetic stirring at 300 rpm for at least 3h for ethyl acetate evaporation. In the end, two types of systems were obtained: PLGA and PLGA:PLGA-PEG-NH_2 (95:5) (% w/w).

To conjugate the peptide to nanoparticles surface, two approaches were followed: (1) the carbodiimide chemistry, to link an amine group to a carboxyl group (Araújo *et al.*, 2015; Wang *et al.*, 2015), using a 12 amino acid peptide (Thr-His-Arg-Pro-Pro-Met-Trp-Ser-Pro-Val-Trp-Pro, named here as pept); or (2) the maleimide chemistry, to link an amine group to a sulfhydryl group (Esfandyari-Manesh *et al.*, 2015; Zimmermann *et al.*, 2010), using a 13 amino acid peptide (the same pept with an extra cysteine on the carboxyl termination; Thr-His-Arg-Pro-Pro-Met-Trp-Ser-Pro-Val-Trp-Pro-Cys, named here as pept-Cys).

The peptide was conjugated to the surface of the nanoparticles following our previous described method (Gomes *et al.*, 2016). In brief, for the amide formation, the EDC/NHS coupling chemistry method was used. Carboxyl groups from PLGA nanoparticles diluted on a MES solution (10 mM, pH~5.5) were activated by EDC (3.14 µL, 17 mM) and NHS (1.2 mg), during 30 min. The pept (100 µL, 1 mg mL^{-1}) was then added and pH adjusted to 7.5. Finally, the mixture was kept stirring (300 rpm) at room temperature for 3h30. Process described was performed in the dark. Meanwhile, for the maleimide conjugation chemistry, PLGA:PLGA-PEG-NH_2 (95:5) nanoparticles were diluted on a PB solution (0.1 M, pH~7). The cross linker SM$(PEG)_{24}$ was added (2 µL, 250 mM) and the mixture was stirred in the dark, at 300 rpm for

4h. Then, pept-Cys was added (50 µL, 6.2 mg mL^{-1}) and the mixture was stirred for another 4h.

Afterwards, nanoparticles were collected by centrifugation at 20,000 × g, 4°C for 20 min and washed with MilliQ-water. Functionalized nanoparticles were then analyzed by Zetasizer and fluorescence.

3.2.2. Nanoparticles characterization

After production, nanoparticles were characterized for their average particle size, polydispersity index (PdI) and average zeta potential by electrophorethic light scattering using a Malvern Zetasizer Nano ZS instrument (Malvern Instruments Ltd). For these measurements, samples were diluted in MilliQ-water. To determine the association efficiency (AE) of the developed nanosystems, the amount of siRNA-FITC associated to the nanoparticles was calculated by a fluorescent assay (ex. 494 nm, em. 517 nm). AE was determined indirectly by the difference between the total amount of siRNA used to prepare the systems and the amount that remained in the aqueous phase after nanoparticles isolation by centrifugation (20,000 × g, 4°C for 20 min), according to the following equation:

$$\text{AE}\ [\%] = \frac{\text{Initial mass of siRNA} - \text{Mass of siRNA in supernatant}}{\text{Total mass of siRNA}} \times 100$$

3.2.3. Cell culture

Immortalized human Cerebral Microvascular Endothelial Cell Line (hCMEC/D3 cell line) was purchased from Cedarlane (Canada). The cells (passage 35-41) were grown in tissue culture flasks (Orange Scientific), in EBM-2 medium supplemented with FBS (5%, v/v), penicillin-streptomycin (1%, v/v), hydrocortisone (1.4 µM), ascorbic acid (5 µg mL^{-1}), chemically defined lipid concentrate (1/100, v/v), HEPES (10 mM) and bFGF (1 ng mL^{-1}). This last supplement was added extemporaneously in the culture medium. Cells were maintained in an incubator (Binder) at 37°C with 5% CO_2 in water saturated atmosphere. Cells were subcultured every 3-4 days using trypsin-EDTA to detach them from the flasks. The culture medium was replaced every other day.

3.2.4. Blood-brain barrier *in vitro* model setup and characterization

The BBB *in vitro* model was based on a previous work from our group (Mendes *et al.*, 2015) with some minor modifications. Briefly, the membrane of a 12-well plate Transwell® system was coated with rat tail collagen type I (50 µg mL^{-1}) for 1h at 37°C before seeding the cells. hCMEC/D3 cells were then cultured at the desired density on the apical side (500 µL) of the semi-permeable filter (insert), and the well was filled with 1.5 mL of medium. The system was maintained in the incubator at 37°C with 5% CO_2 during 8 or 12 days. Cell culture medium was changed on days 2, 4, 6, 8 and 10. Cell monolayer integrity was periodically monitored by determining the transendothelial electrical resistance (TEER) using an endothelial volt-ohm meter (Millicell® ERS-2 (Millipore, USA)). The resistance value (Ω cm^2) of an empty filter was subtracted from each measurement.

To assess the development of a BBB monoculture membrane, at culture day 8 a staining was performed on the Transwell® adherent cells. Briefly, cells were fixed with 4% paraformaldehyde at room temperature. Upon washing, cells were maintained in the dark and labeled with WGA Alexa Fluor 594 (for cell membranes, 5 µg mL^{-1}) during 10 min at room temperature. After washing with PBS, DAPI was added (for nuclei, 1 µg mL^{-1}), incubated 3 min at room temperature, and the excess was removed. Labeled membrane was moved to a microscope slide using the mounting medium Vectashield and photographed using an inverted fluorescence microscope (Axiovert 200M from Zeiss).

3.2.5. siRNA permeability

When the BBB membrane was established (day 8), siRNA permeability was determined either as a free compound or loaded in nanoparticles. First, medium was removed from inserts and wells which were then washed with PBS, and HBSS (1.5 mL) was added to the receptor chamber (basolateral side). On the apical side, siRNA (free or loaded in nanoparticles) solution in HBSS (40.5 nM; 500 µL) was added, and the Transwell® systems were moved to an orbital shaker kept at 100 rpm and 37°C during 3h. Samples (200 µL) were taken from all wells to a microtiter plate (Microplate Costar 96) at predetermined time points (15 min, 30 min, 45 min, 1h, 1h30, 2h and 3h), and the same volume of fresh buffer was added. siRNA-FITC that crossed the membrane over time was quantified through fluorescence with a plate reader (ex. 494 nm, em. 517 nm). The apparent permeability (Papp) of siRNA was calculated by the following equation:

$$\mathrm{Papp}\ [\mathrm{cm\ s^{-1}}] = \frac{\mathrm{dm}}{\mathrm{dt}} \times \frac{1}{c_0 \times A}$$

where dm/dt is the permeated mass over time, c_0 the initial concentration at the apical compartment, and A the surface area of the membrane (0.9 cm^2). The percentage of siRNA permeated mass was calculated based on the relation between mass that crossed and the total initial theoretical mass at the apical side.

Cell-seeded inserts with HBSS only were also used as permeability blanks. TEER was measured at the beginning and at the end of this assay to check membrane integrity.

To evaluate the effectiveness of receptor-mediated endocytosis, siRNA-loaded functionalized nanoparticles permeability was also tested after blocking transferrin receptor. An excess of the peptide used on those functionalized nanoparticles (50× molar excess relative to the peptide on nanoparticles surface (Pridgen *et al.*, 2013)) was used during 30 min to block the receptor.

3.2.6. hCMEC/D3 cells transfection

Cells were seeded (0.1×10^6 cells/well) on a 24-well plate and allowed to attach overnight. Then, medium was removed and siRNA (50 nM) complexed with a transfection agent or loaded in nanoparticles was added (500 μL). For the controls, same calculations and protocol were performed, but without siRNA. Transfection was kept during 6h. After that time, cells were gently washed with PBS and fresh medium was added. At different time points (24, 48 and 96h) RNA was extracted and analyzed.

ScreenFectA was the transfection agent used as a control cationic lipid able to form liposomes and act as liposomal vector for oligonucleotides transfection (Enlund *et al.*, 2014; Li *et al.*, 2015). siRNA complexes were produced following manufacturer's instructions.

3.2.7. P-gp mRNA expression in hCMEC/D3 cells

RNA was extracted, isolated and purified from previously transfected hCMEC/D3 samples using the Quick-RNA MicroPrep kit (R1050, Zymo Research) according to the manufacturer's instructions. Total purified RNA was quantified by Nanodrop (ND1000). P-gp mRNA expression was analyzed by quantitative reverse transcription polymerase chain reaction (qRT-PCR) using the SYBR Green One Step qPCR kit (B25002, Biotool) according to manufacturer's instructions. Primers for P-gp (forward: 5'-CCCATCATTGCAATAGCAGG-3', reverse: 5'-GTTCAAACTTCTGCTCCTGA-3' (Kim *et al.*, 2008)) and reference gene YWHAZ (forward: 5'–GATGAAGCCATTGCTGAACTTG-3', reverse: 5'-

GTCTCCTTGGGTATCCGATGTC-3' (Nelissen *et al.*, 2010)) were used at 250 nM final concentration. Around 50 ng of RNA was mixed with the SYBR green and enzyme mixes in a 20 µL total reaction volume in 96-well plate format and fluorescence was monitored with the iQ5 real time PCR detection system (Bio-Rad). Quality control measures (e.g. melt curve analysis and no template controls) were always implemented. The iQ5 optical system software (Bio-Rad) was used to evaluate the relative expression levels (ddCt algorithm) incorporating the efficiency of the reaction as determined by a 3 log-fold dilution series standard curve. The unloaded ScreenFectA or nanoparticles from the 24h time point was implemented as the expression control.

3.2.8. Functional assay through rhodamine 123 permeability

At day 8 of the developed BBB membrane, medium on the apical and basolateral compartments was removed and the cells were treated with the nanoparticles (unloaded, siRNA-loaded and siRNA-loaded functionalized). In order to have a siRNA final concentration of 50 nM, nanoparticles in medium were added. For the controls, same calculations and protocol were performed, but without siRNA or nanoparticles. After 6h, both compartments were washed and fresh medium was added. At a predetermined time point (96h, day 12) rhodamine 123 permeability was assessed.

At day 12, inserts with non-previously treated BBB membranes were used to chemically inhibit P-gp using verapamil (Jahne *et al.*, 2016), as a positive control. Medium on the apical and basolateral compartments was removed and replaced by verapamil solution (50 µM, in HBSS). Transwell® systems were incubated 1h at 37°C. Then, both compartments were washed and rhodamine 123 permeability was tested.

For the rhodamine 123 permeability study at day 12, the protocol performed was the same used for siRNA permeability already described here, except for the following details. The tested solution was rhodamine 123 at 2.5 µM in HBSS. To quantify rhodamine 123 a fluorescence plate reader was used (ex. 507 nm, em. 529 nm).

3.2.9. Statistical analysis

For the data analysis one-way analysis of variance (ANOVA) was performed to compare multiple groups. Differences between groups were compared with a post hoc test (Tukey's honestly significant difference). Results are reported as mean ± standard deviation

from a minimum of three independent experiments. Differences were considered significant at * $p < 0.05$, ** $p < 0.01$, or *** $p < 0.001$. All statistical analyses were performed with the software PASW Statistics 20 (IBM Corporation).

4. Results and Discussion

4.1. Nanoparticles characterization

Polymeric nanoparticles have been demonstrate to load gene material as siRNA and engineered for a straightforward BBB targeting, with specificity and reduced toxicity to surrounding tissues (Tam *et al.*, 2016). In this work, new ligands based on transferrin-mimetic peptides were selected to be anchored to the surface of PLGA and PLGA:PLGA-PEG nanoparticles and target the BBB.

PLGA-based nanoparticles with different bulk compositions (regular PLGA and a co-polymer mixture PLGA:PLGA-PEG-NH_2) were produced aiming to surface modification through different functionalization chemistries and peptides. Both peptides (pept and pept-Cys) were used according the functional groups available at the surface of nanoparticles and bound by two distinct approaches, carbodiimide and maleimide, respectively, as previously described (Gomes *et al.*, 2016). Nanoparticles were evaluated regarding mean size, PdI, surface charge and siRNA association efficiency (**Table 5.1**).

Table 5.1. Physicochemical characteristics of polymeric nanoparticles: unloaded and siRNA-loaded, non-functionalized and functionalized with pept or pept-Cys.

NP system	Mean Size [nm]	PdI	Zeta Potential [mV]	Association Efficiency [%]
Unloaded-PLGA	116.3 ± 1.0	0.262 ± 0.013	-31.3 ± 1.6	-
siRNA-PLGA	113.3 ± 1.9	0.238 ± 0.014	-33.8 ± 1.6	49.1 ± 1.1
siRNA-PLGA-pept	313.1 ± 17.5 ***	0.464 ± 0.076 **	-23.4 ± 7.3	48.4 ± 1.5
Unloaded-PLGA:PLGA-PEG-NH_2 (95:5)	115.0 ± 4.6	0.274 ± 0.020	-29.6 ± 1.3	-
siRNA-PLGA:PLGA-PEG-NH_2 (95:5)	116.9 ± 2.9	0.259 ± 0.026	-29.0 ± 1.4	49.6 ± 1.1
siRNA-PLGA:PLGA-PEG-NH_2 (95:5)-pept-Cys	482.4 ± 33.0 ***	0.607 ± 0.042 ***	-41.2 ± 2.7 **	50.7 ± 2.0

PdI, polydispersity index; ** $p < 0.01$, *** $p < 0.001$

The loading of siRNA did not change the physicochemical properties of bare PLGA and PLGA:PLGA-PEG nanoparticles, resulting in mean particle size around 115 nm and charge of -30 mV. The association efficiency of siRNA was close to 50%, a satisfying value considering the hydrophilic nature of the siRNA molecule. The functionalization increased the mean particle size of nanoparticles, in agreement with our previous findings (Gomes *et al.*, 2016), although surface charge and association efficiency were retained. Functionalized PLGA:PLGA-PEG nanoparticles were larger than functionalized PLGA nanoparticles (mean sizes around 482.4 nm and 313.1 nm, respectively), which may be related with the chemistry used for binding the peptide. The maleimide approach applied to the co-polymer systems used a cross-linker that has a PEG chain of 95.4 Å, enhancing particle hydrodynamic radius. The particle size enlargement has been observed in different nanosystems surface-functionalized with peptides (Englert *et al.*, 2016). Moreover, the large size and PdI could have to do with some nanoparticles aggregation probably promoted by the amine groups (Bagwe *et al.*, 2006).

4.2. Blood-brain barrier model

The BBB is a tightly packed layer of endothelial cells commonly modeled *in vitro* by the human brain endothelial capillary cell line hCMEC/D3 (Poller *et al.*, 2008). Here, several endothelial cell concentrations on the apical side of the semi-permeable filter were tested, namely 1.25, 2.5, 5, 10 and 15 $\times$ 10^4 cells/cm^2 (D1 to D5, respectively) and their integrity was tracked by TEER measurements, until day 12 in culture. An increase in TEER values would indicate a superior monolayer confluence and, thus, integrity. High initial densities (D3 to D5) led to faster confluence, which could probably be the reason why relatively high resistance values were achieved in early stages (day 4, **Figure 5.1**). However, after being maintained during a short period, these values started to decrease over time (**Figure 5.1**). On the other hand, the two lowest initial cell densities (D1 and D2) developed membranes which resistance increased more until day 8, reaching the most high values, and then slightly decreased or stabilized. Furthermore, as initial cell density increased, the monolayer was less straight and thin (data not shown), due to cells growing on top of each other. It is believed that the number of cells surpassed the available area for a confluent monolayer, starting to detach and decreasing transendothelial resistance and cell membrane integrity. The highest TEER value (29.4 ± 2.3 Ωcm^2) was achieved with an initial endothelial cell density of 2.5 $\times$ 10^4 cells/cm^2 (D2) and after 8 days in monoculture on a Transwell® (**Figure 5.1**). Therefore, since a stable membrane of human brain endothelial cells was obtained on these conditions, they were used in the following procedures.

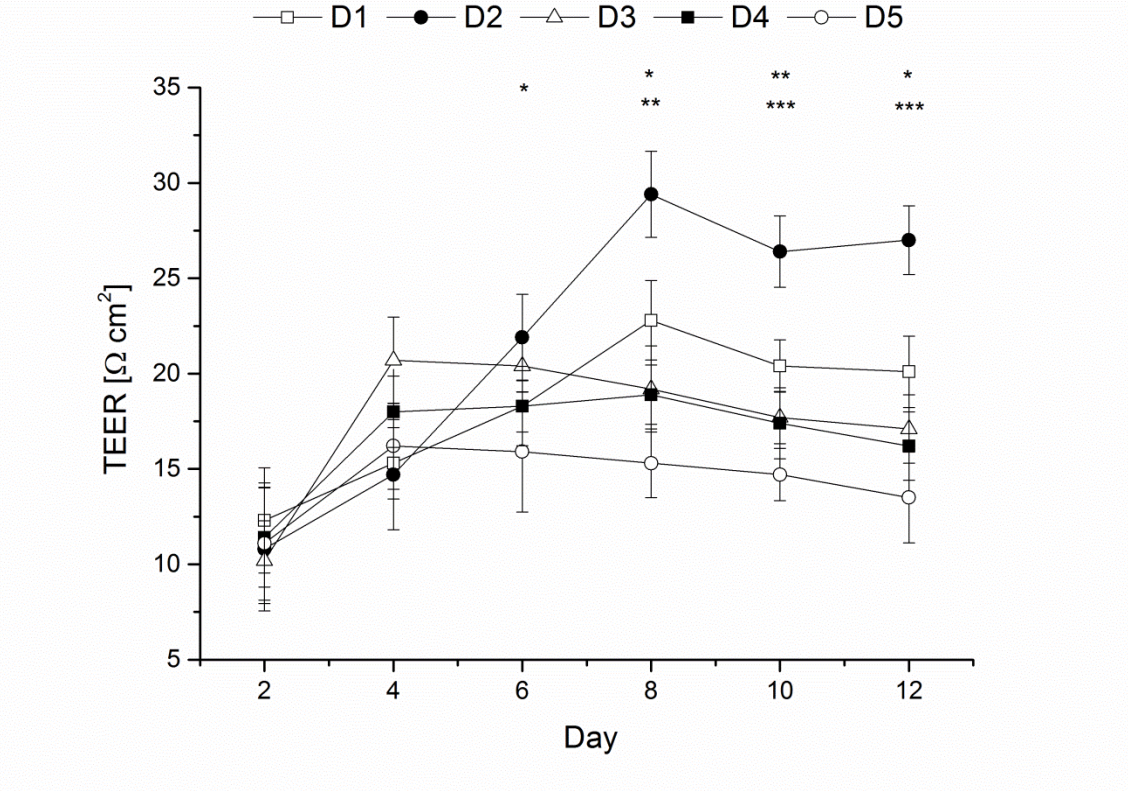

Figure 5.1. TEER measurements for all membranes developed with different initial cell densities (1.25 × 10^4 cells/cm^2 D1, 2.5 × 10^4 cells/cm^2 D2, 5 × 10^4 cells/cm^2 D3, 10 × 10^4 cells/cm^2 D4, 15 × 10^4 cells/cm^2 D5), over 12 days in culture on Transwell®. TEER values of D1 are significantly different from D5 at days 8 (**), 10 (**) and 12 (*). D2 is significantly different from D5 at day 6 (*). At days 8, 10 and 12, D2 is significantly different from D1 (*, **, *, respectively) and from all the other densities (**, ***, ***, respectively).

Choosing these cell density and time based on obtained TEER values is also related to what is known from literature. Previous work from our group already showed 33 Ωcm^2 as the highest TEER value achieved after seven days in monoculture, which is similar to selected conditions (Mendes *et al.*, 2015). Moreover, it is commonly accepted that mammalian systems show high BBB *in vivo* TEER values, above 1,000 Ωcm^2 (Weksler *et al.*, 2013). However, such values are difficult to achieve with *in vitro* models. hCMEC/D3 monolayers usually obtain TEER around 30-50 Ωcm^2, as several studies report (Qosa *et al.*, 2014; Ragnaill *et al.*, 2011; Weksler *et al.*, 2013). To complement TEER results, BBB monoculture membrane was labeled and visualized at the microscope to verify the development of a robust monolayer through the selected conditions. Long cells with parallel growth creating a whole and confluent membrane at culture day 8 were visualized (**Figure 5.2**).

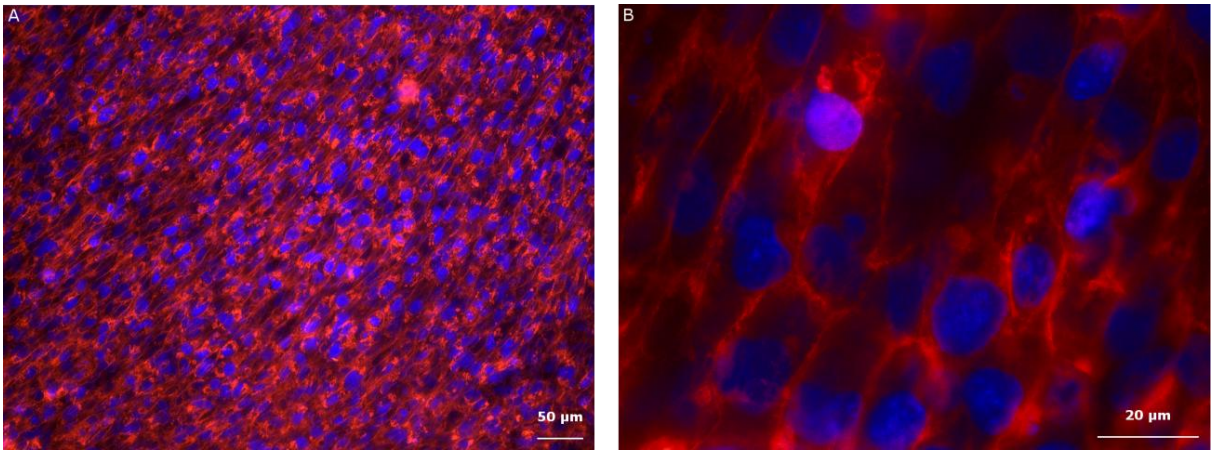

Figure 5.2. Fluorescence microscope images of human brain endothelial cell monolayer, after 8 days in culture on Transwell®; scale bar of 50 µm for (**A**) and 20 µm for (**B**). Cell membranes were stained in red, and nuclei in blue.

4.3. siRNA permeability

Permeability studies were performed in order to evaluate the influence of nanoparticles to promote the crossing of siRNA through a human BBB cell-based model. TfR-targeted nanoparticles resulted in a two-fold increase of siRNA permeability compared to non-functionalized nanoparticles, either for PLGA or PLGA:PLGA-PEG-NH_2 nanosystems (**Figure 5.3 A**). Interestingly, siRNA permeability was 1.3-fold higher for siRNA-PLGA:PLGA-PEG-NH_2-pept-Cys compared to siRNA-PLGA-pept nanoparticles, which may indicate that selected peptide orientation achieved through the maleimide binding approach is more effective to improve cellular interaction than the carbodiimide chemistry used for PLGA nanoparticles. In a similar approach, Park and colleagues developed a targeted polyethylenimine-based system to deliver siRNA against beta-secretase 1 through the BBB (Park *et al.*, 2015). The permeability of functionalized siRNA complexes was 2.2-fold higher than non-functionalized ones, indicating the efficacy of surface modification on the BBB permeability.

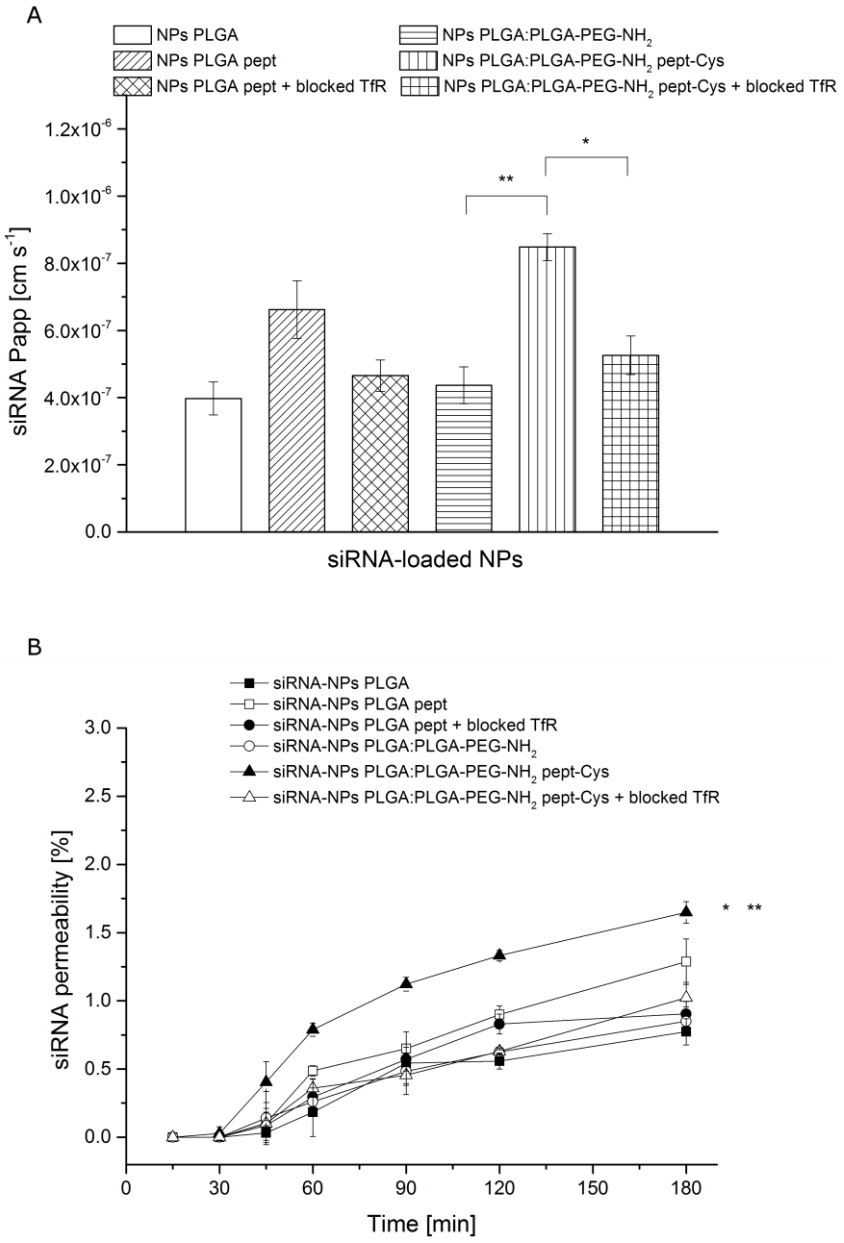

Figure 5.3. (**A**) siRNA apparent permeability values obtained 3h after the siRNA-loaded in the different systems have crossed the BBB membrane. (**B**) Percentage of siRNA mass permeated through the BBB membrane using siRNA-loaded in all studied nanoparticles (with and without blocked transferrin receptor), during 3h.

On the other hand, by blocking the transferrin receptor with the peptide 30 minutes prior the permeability assay, it was clear a decrease on the amount of siRNA that reached the basolateral side. Hence, for TfR-targeted nanoparticles without receptor blockage, siRNA permeability was 1.4 to 1.6-fold higher than when receptor was blocked. These results endorse the active role of the receptor on the active transport mechanism. It is known that

transferrin receptor involves clathrin-mediated endocytosis (Damm *et al.*, 2005; Fekri *et al.*, 2016). Thus, functionalized nanoparticles get in the cells through transferrin receptor, which is initiated with ligand binding and receptor activation. This complex diffuses through the plasma membrane and is captured by a forming clathrin-coated pit that then forms a clathrin-coated vesicle which will fuse to an early endosome. After this, the endocytosed cargo will be sorted to lysosomes, recycling, or other cellular pathways (Fekri *et al.*, 2016). Several other works also demonstrate nanoparticles internalization through receptor blocking assays. Park and co-workers observed a 65% significant reduced permeability of modified complexes when the receptor was blocked by the used peptide (Park *et al.*, 2015). Moreover, and also in accordance with our results, Pridgen et al studied nanoparticles targeted to the neonatal Fc receptor (Pridgen *et al.*, 2013). They observed that the enhanced transport achieved through targeted nanoparticles was significantly reduced when the Fc receptor was blocked, meaning that it was largely mediated by this receptor. Although only a modest increase in targeting was observed in the *in vitro* model, this translated to significant *in vivo* function (Pridgen *et al.*, 2013). As such, this suggests that our NPs could also yield promising results *in vivo* as well.

When comparing the permeability of siRNA loaded into different nanoparticles (mean values ranging between 4.0 – 8.5 $\times$ 10^{-7} cm s^{-1}) and in solution (2.7 $\times$ 10^{-6} ± 2.3 $\times$ 10^{-7} cm s^{-1}), the free siRNA was able to cross the BBB more extensively than loaded into non-functionalized or even functionalized nanoparticles. Differences in free and loaded siRNA might be expected, as the size and low flexibility of nanocarriers are against the physical barrier that BBB provides. Also, we previously demonstrated that siRNA releases slowly from nanoparticles (Chapter IV from this thesis), which is in agreement with the overall siRNA that reaches the basolateral compartment. Moreover, in an *in vivo* situation, free siRNA would not be able to reach BBB due to harsh *in vivo* conditions such as enzymatic degradation (Choi *et al.*, 2014) and absence of targeting moiety for the BBB.

Regarding the siRNA permeation profile (**Figure 5.3 B**), the permeability kinetics was very similar among all used systems: initially, on the first hour, it increased faster than during later time points, which could probably be associated with the slow release profile of siRNA from nanoparticles (Chapter IV from this thesis). After 3h, the siRNA permeability from siRNA-PLGA:PLGA-PEG-NH_2-pept-Cys nanoparticles was significantly higher than from the non-functionalized and functionalized nanoparticles with previous blocked receptor. These results are in accordance with apparent permeability values (**Figure 5.3 A**).

Overall, PLGA:PLGA-PEG nanoparticles obtained more promising results than regular PLGA systems. When TfR-targeted, they significantly improve their capability to

interact with human brain endothelial cells, and consequently siRNA permeability. This may be related to the presence of PEG on the surface of nanoparticles, as it not only enhances biocompatibility by inhibiting interaction with serum proteins (Rahme *et al.*, 2015; Tam *et al.*, 2016), but also makes the bounded peptide to be more spatially available to its receptor. As well, the maleimide chemistry used to bind the peptide to the nanoparticle surface could also have some influence on these greater results, as already mentioned. This chemical method improved specificity and correct peptide orientation when compared to carbodiimide used approach from regular PLGA functionalization system (Gomes *et al.*, 2016). Thus, siRNA-PLGA:PLGA-PEG-NH_2-pept-Cys formulation was selected for further experiments. Still, the rational for this approach is to retain the siRNA inside brain endothelial cells, where it is desired to act by silencing P-gp, and not to cross the BBB. Consequently and according to latest data, in general, siRNA low permeability through the human BBB model was achieved and confirmed considering that only less than 2% crossed the membrane, which hints that siRNA was being retained on cells.

4.4. P-gp mRNA expression in hCMEC/D3 cells

In order to check the silencing efficiency of the siRNA sequence used in this work, human BBB cells were transfected with siRNA against P-gp (P-gp-siRNA) by using a transfection agent, ScreenFectA. This agent is known to boost up siRNA silence effect, acting as a siRNA-specific positive control (Enlund *et al.*, 2014), along with high transfection efficiency and low cytotoxicity (Li *et al.*, 2015).

Down-regulation was quantified at the mRNA level through qRT-PCR at different time points after transfection (**Figure 5.4**). It was found that, 24h post transfection, P-gp-siRNA significantly decreased P-gp mRNA expression levels on 45% compared to the treatment with transfection agent only. On the other hand, treatment with non-targeted siRNA (scrambled-siRNA) did not induce any silencing effect, eliminating non-specific effects from nanoparticles. Additionally, following time points (48h and 96h) did not reveal any difference between cell treatments, meaning that the P-gp-siRNA knockdown action was only noticed at 24h post transfection. This probably occurred due to the fast siRNA ability to enter in the cells and transfect them, which could be promoted by the transfection agent features already mentioned, and further cell recovery over a transient oligonucleotide silencing effect.

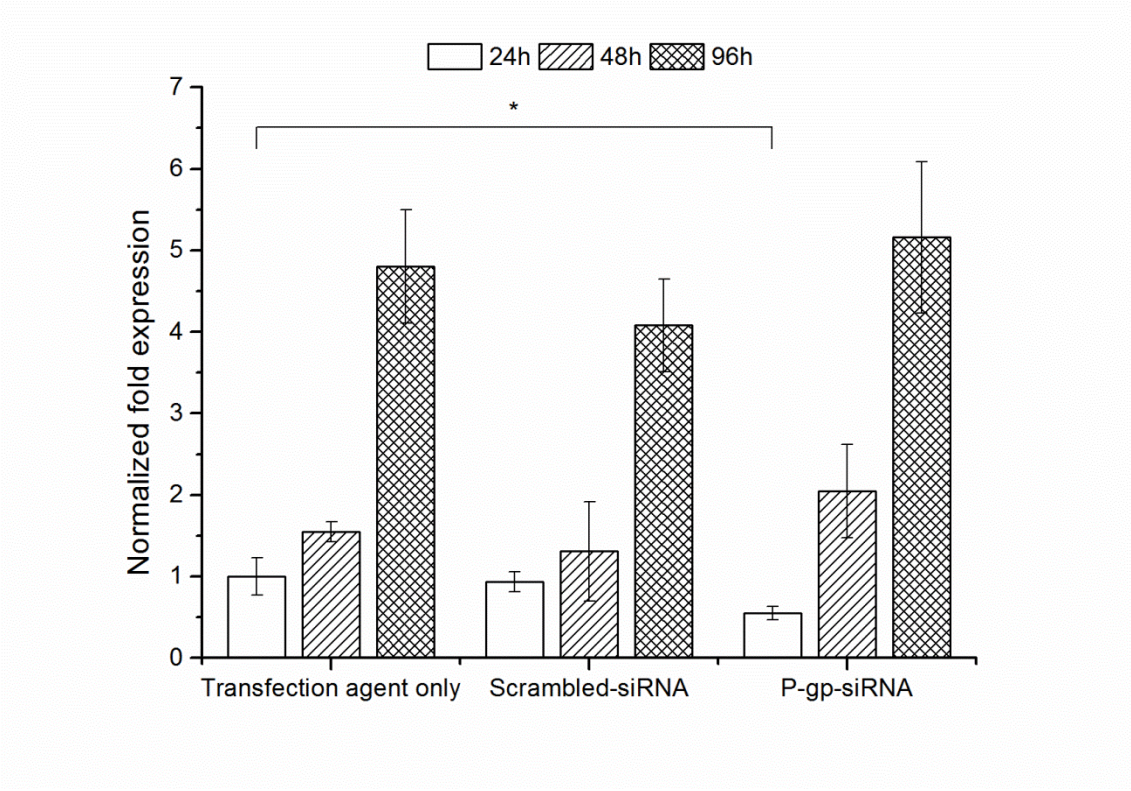

Figure 5.4. Expression of P-gp mRNA at several time points, after hCMEC/D3 cells transfection with different type of transfection agent combinations: transfection agent only (negative control), scrambled-siRNA transfection agent (negative control), and P-gp-siRNA transfection agent. Fold expression was normalized to the transfection agent only control at 24h.

P-gp mRNA expression data stressed up the already studied increased expression of P-gp on higher cell densities, related with the increased P-gp half-life detected under this condition (Muller *et al.*, 1995; Stierle *et al.*, 2004), which is the reason why P-gp mRNA levels increased over time, within the same transfection type.

Previous works also studied siRNA-mediated gene down-regulation in BBB cells. For example, the organic cation/carnitine transporter (OCTN2) knockdown was evaluated in hCMEC/D3 cells (Higuchi *et al.*, 2015). Authors reported that OCTN2-siRNA (5 nM) treatment decreased OCTN2 mRNA expression by 90%, 48h after transfection using Lipofectamine RNAiMAX (Higuchi *et al.*, 2015). Another study was performed to understand the interaction between caveolin-1 (Cav-1) and P-gp transport activity in a rat brain endothelial cell line (Barakat *et al.*, 2007). Authors found that Cav-1-siRNA (50 nM) transfection induced a strong 90% of Cav-1 down-regulation, 48h post transfection using HiPerFect transfection agent. Interestingly, accumulation of P-gp substrates were reduced up to 40% in transfected cells, suggesting that down-regulation of Cav-1 enhanced P-gp

transport activity (Barakat *et al.*, 2007). Although these preceding examples stated higher silenced expressions when using commercially available transfection agents than the one obtained here (90% *versus* 45%), as well as at a different time point (48h *versus* 24h post transfection), that does not depreciate P-gp-siRNA knockdown results. Maximum silencing efficiency depends on several factors like the target protein half-life, cell line used, cell health, viability and confluency, as well as the media, serum presence, antibiotics, transfection agent and method, and siRNA sequence itself (Gu *et al.*, 2016).

To verify siRNA-loaded nanoparticles ability to silence P-gp from human brain endothelial cells, cells were transfected with unloaded nanoparticles (negative control), P-gp-siRNA-loaded nanoparticles, and P-gp-siRNA-loaded nanoparticles functionalized with a peptide toward the BBB. At different time points post transfection (24h, 48h and 96h) P-gp mRNA expression was evaluated (**Figure 5.5**).

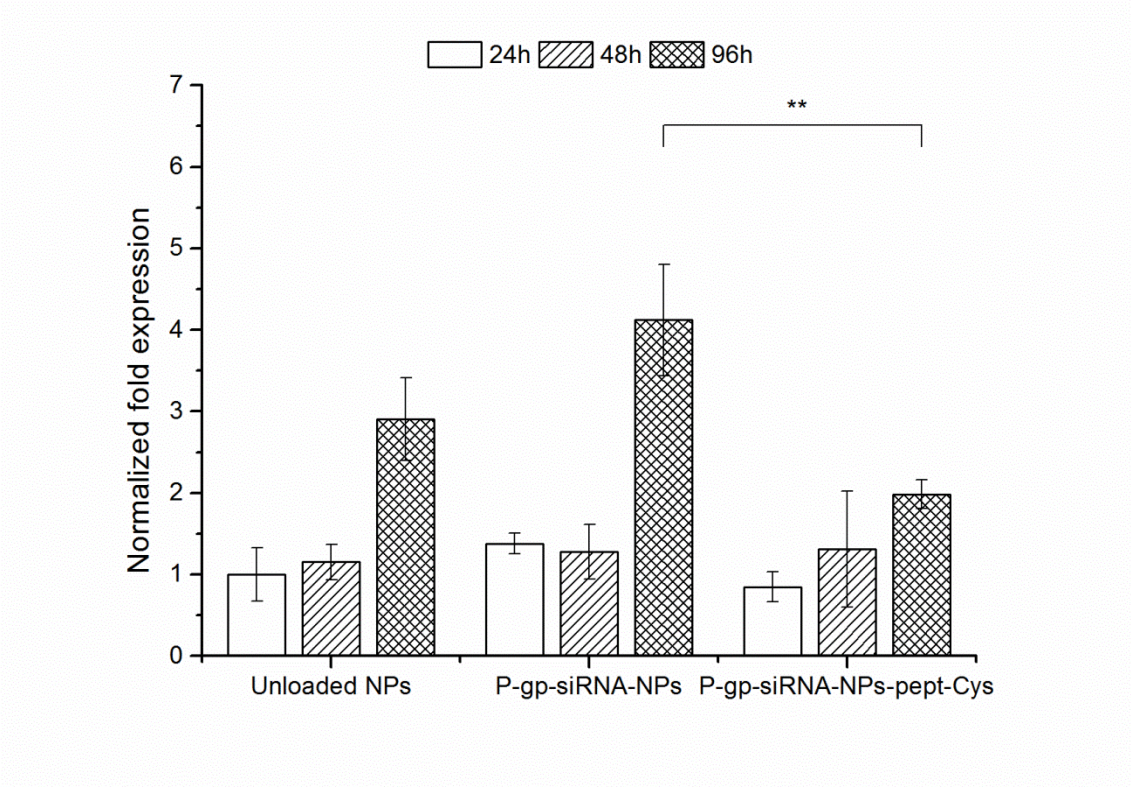

Figure 5.5. Expression of P-gp mRNA at different time points, after cell transfection with different type of nanoparticles (unloaded, P-gp-siRNA-loaded and P-gp-siRNA-loaded targeting BBB). Fold expression was normalized to the unloaded nanoparticles control at 24h.

At 24h post transfection, functionalized nanoparticles induced a P-gp mRNA expression 15% inferior than unloaded nanoparticles did. This value is much lower than the

45% observed for P-gp-siRNA on the transfection agent experiment (**Figure 5.4**), which could be justified through the improved transfection enabled by the commercial transfection agent, plus the more controlled release of siRNA by the nanoparticles that avoided its burst silencing effect.

In order to compare nanoparticle's and transfection agent's efficiency, a study where polyethylenimine-PEG nanoparticles were developed to evaluate their DNA transfection ability for mammalian cells was performed (Nimesh *et al.*, 2006). These particles were compared to lipofectin (transfection agent) on the transfection of luciferase gene (150 mM). 48h post transfection, authors claimed that co-polymer nanoparticles were found to be the most efficient on luciferase transfection, yielding 11-fold higher levels of luciferase activity (Nimesh *et al.*, 2006). Another group assessed the ability of cationic multi-shell calcium phosphate nanoparticles and the transfection agent Lipofectamine to transfect DNA encoding GFP (0.2-0.3 µg per well) on several cell lines (Neuhaus *et al.*, 2016). Researchers stated Lipofectamine as the most efficient transfection agent (Neuhaus *et al.*, 2016). Gathering all these published data, it is possible to verify that transfection efficiency of nanoparticles *versus* commercial transfection agents does not follow a rationale trend, as it depends on numerous factors; inclusively, it has been related to the size of transfection polymer and its cytotoxicity. Usually, high molecular weight polymers reported superior transfection efficiency (Nimesh *et al.*, 2006), which in turn is often correlated with low cell viability (Neuhaus *et al.*, 2016). Furthermore, nanoparticles aggregation has been associated with decreased transfection efficiency (Ota *et al.*, 2013), which could be affecting the developed system as Zetasizer results might suggest.

At 48h post transfection, no differences were detected (**Figure 5.5**). As well, no significant differences were observed between mRNA levels when cells were treated with unloaded and siRNA-loaded nanoparticles. This could be associated with the diminished ability of these non-functionalized particles to interact with brain endothelial cells (Gomes *et al.*, 2016), and resulting reduced siRNA capacity to get in the cells and silence its target protein on a quantifiable extension.

P-gp mRNA quantification results (**Figure 5.5**) showed that 96h after transfection, when siRNA-loaded TfR-targeted nanoparticles were used, the P-gp mRNA expression was reduced. Such down-regulation corresponded to an expression 32 to 52% lower compared to unloaded nanoparticles and siRNA-loaded nanoparticles, respectively. Therefore, although P-gp mRNA expression increased over time while cell density also increased (Muller *et al.*, 1995; Stierle *et al.*, 2004), there was a P-gp silencing effect when siRNA-loaded

functionalized nanoparticles were used, which was highlighted at 96h. Consequently, this was the selected time point for the functional assay permeability experiment.

A delayed P-gp down-regulation was observed, from 24h post transfection when a commercial transfection agent was used to 96h post transfection when the produced nanosystem was applied. This time gap could be justified due to nanoparticles-related siRNA more controlled release, which extend and retard its effect.

To study drug resistance on breast cancer cells, P-gp-siRNA complexed with polyethylenimine substituted with lipids was tested by Aliabadi and colleagues (Aliabadi *et al.*, 2013). 48h post transfection (54 nM siRNA), the P-gp mRNA levels decreased around 50% compared to values obtained for scrambled-siRNA control (Aliabadi *et al.*, 2013). PLGA has also been utilized to conquer tumor drug resistance as P-gp-siRNA carrier functionalized with biotin for active tumor targeting (Patil *et al.*, 2010). Adenocarcinoma cells were transfected with siRNA-loaded PLGA nanoparticles (0.2 nM siRNA), resulting in about 50% decrease of P-gp mRNA expression levels 72h post transfection, when compared with control treatments (Patil *et al.*, 2010). Moreover, chitosan nanoparticles complexed with P-gp-siRNA were used to transfect a rat BBB model cell line (Malmo *et al.*, 2013). 48h post transfection (100 nM siRNA), P-gp mRNA levels were 20% reduced compared to the untreated cells. From the transfection with chitosan only or scrambled-siRNA, no significant change in mRNA expression was detected, indicating absence of non-specific effects from chitosan or nanoparticles, respectively (Malmo *et al.*, 2013).

These P-gp knockdown values and respective post transfection selected times are mostly in accordance with the obtained results, but none of them were performed on human brain endothelial cells, highlighting this work novelty with the hCMEC/D3 cell line. Additionally, P-gp-siRNA transfection, targeted to these cells through a specific peptide-oriented chemistry, constitutes an innovative application of such functionalization method. Furthermore, down-regulation percentages and times depend on nanoparticles composition and siRNA release profile, in addition to the already mentioned factors.

4.5. Functional assay through rhodamine 123 permeability

To quantify the effects of siRNA-mediated silencing on P-gp function, the permeability of a well-established P-gp substrate (rhodamine 123 (Lee *et al.*, 2013)) was tested on a human BBB *in vitro* membrane 96h after cells treatment. BBB models were subjected to

different treatments: no transfection/inhibition; transfection with unloaded nanoparticles, siRNA-loaded nanoparticles and siRNA-loaded TfR-targeted nanoparticles; and P-gp chemical inhibition. Rhodamine 123 apparent permeability was calculated (**Figure 5.6 A**), as well as the permeation profile (**Figure 5.6 B**).

No cellular treatment and treatment with unloaded nanoparticles induced similar rhodamine 123 permeability values through the BBB model, indicating that these systems by themselves did not interfere with cellular efflux. However, P-gp-siRNA-loaded nanoparticles treatment brought an increased rhodamine permeability of 11 to 12% compared to no treatment and unloaded nanoparticles treatment, respectively. This slight increase was not predicted by the P-gp mRNA expression assay, although siRNA silencing action was noticed by this functional experiment. Following this, cells treated with P-gp-siRNA-loaded functionalized nanoparticles enabled a significant increase on rhodamine permeability – 26, 27 and 17% higher than values obtained for non-treated cells, unloaded nanoparticles and siRNA-loaded nanoparticles treatments, respectively. Those differences have a close relation with the reduced P-gp mRNA expression obtained for these nanosystems 96h post transfection. When P-gp as an ABC transporter is down-regulated, a weaker efflux made by this protein is reached, and thus also an increased uptake/permeability of its substrates such as rhodamine 123 is attained.

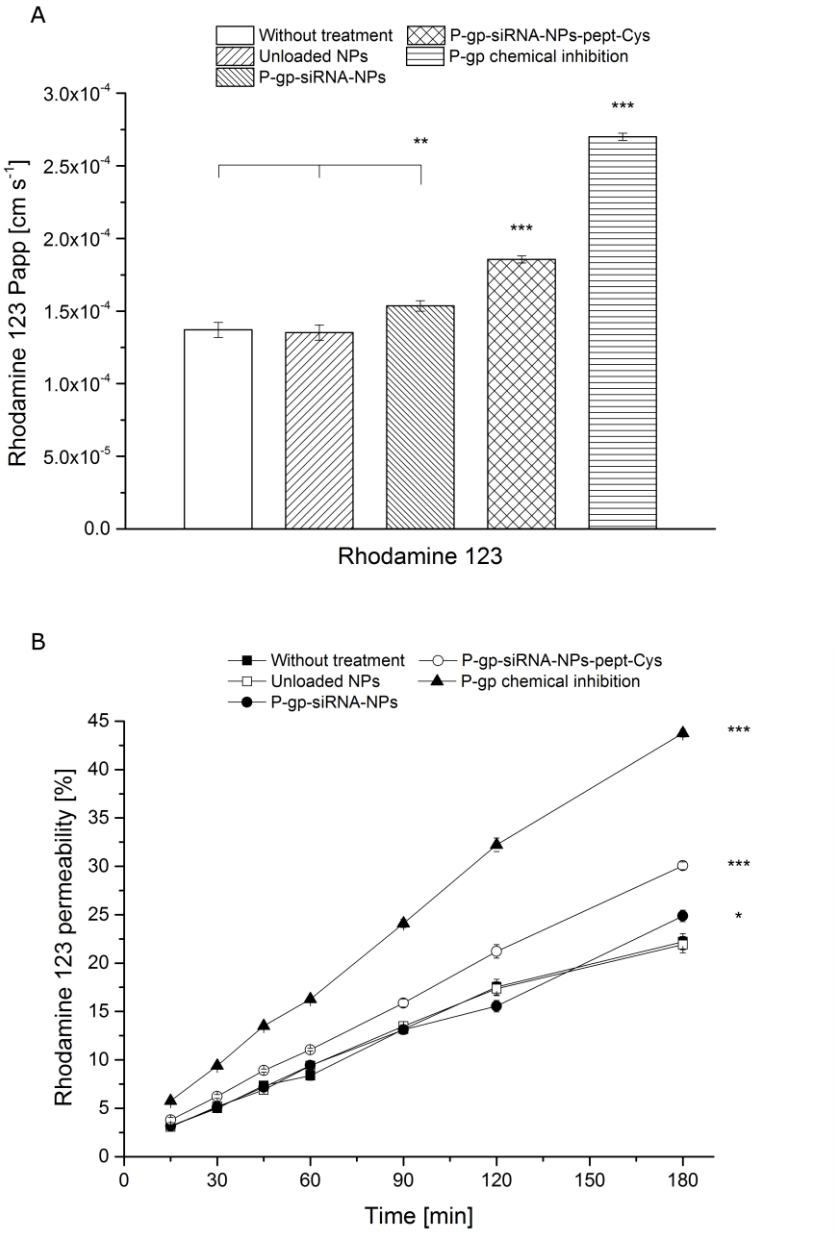

Figure 5.6. (**A**) Rhodamine 123 apparent permeability values obtained 3h after crossing through a BBB model membrane previously treated with: any transfection/inhibition, unloaded nanoparticles, P-gp-siRNA-loaded nanoparticles, P-gp-siRNA-loaded TfR-targeted nanoparticles, and P-gp chemical inhibitor (verapamil). (**B**) Percentage of rhodamine 123 mass permeated through the previously treated BBB membrane, over 3h.

Since TfR-targeted, P-gp siRNA-loaded nanoparticles caused a decrease on P-gp mRNA expression between 32 and 52%, as already discussed. Therefore, an equivalent increase on rhodamine 123 permeability could be expected. However, P-gp efflux kinetics has a maximum transport rate related with its saturation nature and substrate-concentration

dependence (Sjostedt *et al.*, 2014). Hence, although rhodamine permeability had, in fact, increased after functionalized nanoparticles treatment, it is not feasible or correct to quantitatively correlate P-gp expression with P-gp substrates permeability.

Rhodamine permeability rose even more significantly when P-gp was inhibited through a chemical way – it was 49, 50, 43 and 31% higher than permeability obtained when cells were treated without any agent, with unloaded nanoparticles, siRNA-loaded nanoparticles, and siRNA-loaded functionalized nanoparticles, respectively. This was expected since chemical inhibition tends to be more powerful than a transfection dependent on siRNA silencing capacity (Duan *et al.*, 2004). Still, siRNA has several advantages such as a transient and reversible action, reduced toxicity towards non-specific tissues (which is related to the TfR-targeting of used nanoparticles), and high specificity (Navarro *et al.*, 2012). On the other hand, chemical inhibitors as verapamil could easily promote side effects related to interactions with the second drug that would be further administered to cross the barrier (Navarro *et al.*, 2012).

In a previous study, to investigate the effects of drugs on the function and expression of P-gp, rhodamine 123 efflux assays were performed in Caco-2 cells (Abbasi *et al.*, 2016). After verapamil (300 μM) and posterior rhodamine 123 (5 μM) incubation, authors found the mean intracellular concentration of rhodamine 123 on the verapamil-treated cells to be 2-fold higher than on non-treated cells (Abbasi *et al.*, 2016). These results highlighted the already known P-gp inhibitors capacity.

In accordance with apparent permeability values, rhodamine permeated mass through a cellular membrane pre-treated with P-gp-siRNA-loaded functionalized nanoparticles was significantly higher from all other particles over all time points (**Figure 5.6 B**). As well, verapamil treatment led to the same conclusion, with a more noticeable effect. At the 3h time point, the P-gp-siRNA-loaded nanoparticles treatment also significantly enhanced the rhodamine permeated mass.

In a study where P-gp-siRNA-loaded chitosan nanoparticles were investigated as a potential way to silence P-gp in a rat BBB model, doxorubicin (50 μM) was used for a functional assay as a P-gp substrate (Malmo *et al.*, 2013). In addition to the effective P-gp knockdown observed after P-gp-siRNA (100 nM) transfection, authors described a decrease in doxorubicin efflux, and subsequent 60% metabolic activity reduction caused by this drug action. These results meant increased cellular delivery and efficacy of P-gp model substrate when this transporter was silenced (Malmo *et al.*, 2013). In another previous study, after a single P-gp-siRNA (200 nM) transfection, Caco-2 cells expressed lower amounts of P-gp mRNA (Lee *et al.*, 2013). Subsequently, rhodamine 123 efflux decreased, increasing its

intracellular accumulation. Authors obtained consistent results through both P-gp-siRNA and a well established P-gp inhibitor, LY335979 (Lee *et al.*, 2013). Caco-2 cell line used by Lee had also been used by Klein with the same purpose. However, Klein treated cells with both silicon quantum dots complexed with P-gp-siRNA and P-gp-siRNA-Lipofectamine 2000 (Klein *et al.*, 2009). After that, cells were incubated with rhodamine 123 (0.1 mM) and results stated that, from day 0 to day 8 post transfection, the P-gp transporter efficiency for the rhodamine 123 dropped continuously for both type of transfection carriers, revealing the siRNA silencing capacity (Klein *et al.*, 2009).

In agreement with obtained rhodamine 123 permeability results, previously published works, as discussed, also state the significant increase of this P-gp substrate permeability when P-gp is down-regulated. However, again, the present study stands out from all the others already performed in the P-gp-siRNA and P-gp substrate permeability field by the use of targeted systems to a human brain endothelial cell line. This cell line, hCMEC/D3, is being nowadays the most commonly selected for the development of *in vitro* BBB models (Weksler *et al.*, 2013).

It is important to highlight that TEER was kept constant from culture day 8 (cell treatment) until day 12 (permeability experiment 96h later), meaning that membrane integrity was not lost (data not shown).

Overall, results from this work suggest that developed anti-P-gp siRNA-loaded TfR-targeted co-polymer carriers could be a promising strategy to circumvent a human BBB huge obstacle like drug efflux transport, improving drugs ability to cross this biological barrier.

5. Conclusions

Surpassing the BBB is the main common trick for brain therapies success due to its physiological restrictive features that creates a CNS unique environment. Therefore, this work focused on establishing a new platform to silence P-gp, facilitating P-gp substrates transport across this biological membrane. Hence, siRNA against P-gp was used and targeted to human brain endothelial cells through TfR-targeted peptide-functionalized polymeric nanoparticles. Maleimide functionalized PLGA:PLGA-PEG-NH_2 (95:5) nanoparticles successfully targeted the BBB and led to a significant 2-fold increase on the siRNA permeability through the BBB model, compared to the non-functionalized systems. When transferrin receptor was previously blocked, the permeability of siRNA-loaded

functionalized nanoparticles decreased to values similar to the ones obtained for non-functionalized nanoparticles. This emphasized the transcellular pathway that TfR-targeted particles also took to cross the membrane, proving the existence of receptor-mediated endocytosis through transferrin receptor. Beyond their ability to improve siRNA permeability, functionalized nanoparticles also decreased P-gp mRNA expression in endothelial cells. 96h post transfection, the expression of P-gp mRNA was 52% reduced when cells were treated with functionalized compared to non-functionalized siRNA-loaded nanoparticles. Subsequently, the permeability of rhodamine 123, a P-gp substrate, across a cell-based BBB model was 17% higher after 6h treatment with functionalized siRNA-loaded nanoparticles. Instead of siRNA, verapamil, a P-gp chemical inhibitor, was also tested, which drove rhodamine permeability to increase 31% more than the values achieved when siRNA-loaded functionalized nanoparticles were used. Still, chemical inhibitors are not as specific as siRNA and have potential side effects problems related to drug-drug interactions when the drug that needs to cross the BBB is also administered (Navarro *et al.*, 2012).

TfR-targeted siRNA-loaded co-polymer nanoparticles had been underlined during this work since they profitably induced P-gp silencing and consequent rhodamine 123 permeability enhancement through a human BBB model. Therefore, these results suggest that developed anti-P-gp siRNA-loaded functionalized carriers could be a promising approach to temporarily disrupt the human BBB to enable drugs to reach the CNS in therapeutic concentrations. Concurrently, by adjusting the targeting ligands attached to the nanoparticles surface, this siRNA against P-gp system could be translated to other fields as cancer, by addressing drug-resistance in tumors characterized as P-gp over expressing tissues.

6. Acknowledgements

This work was supported by the Programa Operacional Potencial Humano (POCH), specifically by the BiotechHealth Programme (Doctoral Programme on Cellular and Molecular Biotechnology Applied to Health Sciences). Patrick J. Kennedy would like to thank to BiotechHealth Doctoral Programme and FCT for financial support (SFRH/BD/99036/2013).

7. References

Abbasi, M.M., Valizadeh, H., Hamishehkar, H. and ZakeriMilani, P. 2016. Inhibition of P-glycoprotein expression and function by antidiabetic drugs gliclazide, metformin, and pioglitazone in vitro and in situ. Res Pharm Sci. 11 (3): 177-186.

Abbott, N.J., Patabendige, A.A., Dolman, D.E., Yusof, S.R. and Begley, D.J. 2010. Structure and function of the blood-brain barrier. Neurobiol Dis. 37 (1): 13-25.

Aliabadi, H.M., Mahdipoor, P. and Uludag, H. 2013. Polymeric delivery of siRNA for dual silencing of Mcl-1 and P-glycoprotein and apoptosis induction in drug-resistant breast cancer cells. Cancer Gene Ther. 20 (3): 169-177.

Anand, P., O'Neil, A., Lin, E., Douglas, T. and Holford, M. 2015. Tailored delivery of analgesic ziconotide across a blood brain barrier model using viral nanocontainers. Sci Rep. 5 (12497): 1-10.

Araújo, F., Shrestha, N., Shahbazi, M.A., Liu, D., Herranz-Blanco, B., Mäkilä, E.M., Salonen, J.J., Hirvonen, J.T., Granja, P.L., Sarmento, B. and Santos, H.A. 2015. Microfluidic assembly of a multifunctional tailorable composite system designed for site specific combined oral delivery of peptide drugs. ACS Nano. 9 (8): 8291-8302.

Bagwe, R.P., Hilliard, L.R. and Tan, W. 2006. Surface modification of silica nanoparticles to reduce aggregation and non-specific binding. Langmuir. 22 (9): 4357-4362.

Barakat, S., Demeule, M., Pilorget, A., Regina, A., Gingras, D., Baggetto, L.G. and Beliveau, R. 2007. Modulation of p-glycoprotein function by caveolin-1 phosphorylation. J Neurochem. 101 (1): 1-8.

Bhaskar, S., Tian, F., Stoeger, T., Kreyling, W., de la Fuente, J.M., Grazu, V., Borm, P., Estrada, G., Ntziachristos, V. and Razansky, D. 2010. Multifunctional nanocarriers for diagnostics, drug delivery and targeted treatment across blood-brain barrier: perspectives on tracking and neuroimaging. Part Fibre Toxicol. 7 (3): 1-25.

Choi, K.M., Jang, M., Kim, J.H. and Ahn, H.J. 2014. Tumor-specific delivery of siRNA using supramolecular assembly of hyaluronic acid nanoparticles and 2b RNA-binding protein/siRNA complexes. Biomaterials. 35 (25): 7121-7132.

Damm, E.M., Pelkmans, L., Kartenbeck, J., Mezzacasa, A., Kurzchalia, T. and Helenius, A. 2005. Clathrin- and caveolin-1-independent endocytosis: entry of simian virus 40 into cells devoid of caveolae. J Cell Biol. 168 (3): 477-488.

Duan, Z., Brakora, K.A. and Seiden, M.V. 2004. Inhibition of ABCB1 (MDR1) and ABCB4 (MDR3) expression by small interfering RNA and reversal of paclitaxel resistance in human ovarian cancer cells. Mol Cancer Ther. 3 (7): 833-838.

Englert, C., Trutzschler, A.K., Raasch, M., Bus, T., Borchers, P., Mosig, A.S., Traeger, A. and Schubert, U.S. 2016. Crossing the blood-brain barrier: glutathione-conjugated poly(ethylene imine) for gene delivery. J Control Release. 241: 1-14.

Enlund, E., Fischer, S., Handrick, R., Otte, K., Debatin, K.M., Wabitsch, M. and Fischer-Posovszky, P. 2014. Establishment of lipofection for studying miRNA function in human adipocytes. PLoS One. 9 (5): 1-8.

Esfandyari-Manesh, M., Mostafavi, S.H., Majidi, R.F., Koopaei, M.N., Ravari, N.S., Amini, M., Darvishi, B., Ostad, S.N., Atyabi, F. and Dinarvand, R. 2015. Improved anticancer delivery of paclitaxel by albumin surface modification of PLGA nanoparticles. Daru. 23 (28): 1-8.

Fekri, F., Delos Santos, R.C., Karshafian, R. and Antonescu, C.N. 2016. Ultrasound microbubble treatment enhances clathrin-mediated endocytosis and fluid-phase uptake through distinct mechanisms. PLoS One. 11 (6): 1-22.

Fisher, M., Abramov, M., Van Aerschot, A., Xu, D., Juliano, R.L. and Herdewijn, P. 2007. Inhibition of MDR1 expression with altritol-modified siRNAs. Nucleic Acids Res. 35 (4): 1064-1074.

Fonte, P., Soares, S., Sousa, F., Costa, A., Seabra, V., Reis, S. and Sarmento, B. 2014. Stability study perspective of the effect of freeze-drying using cryoprotectants on the structure of insulin loaded into PLGA nanoparticles. Biomacromolecules. 15 (10): 3753-3765.

Gabathuler, R. 2010. Approaches to transport therapeutic drugs across the blood-brain barrier to treat brain diseases. Neurobiol Dis. 37 (1): 48-57.

Gao, W., Liu, Y., Jing, G., Li, K., Zhao, Y., Sha, B., Wang, Q. and Wu, D. 2017. Rapid and efficient crossing blood-brain barrier: hydrophobic drug delivery system based on propionylated amylose helix nanoclusters. Biomaterials. 113: 133-144.

Gomes, M.J., Fernandes, C., Martins, S., Borges, F. and Sarmento, B. 2016. Tailoring lipid and polymeric nanoparticles as siRNA carriers towards the blood-brain barrier - from targeting to safe administration. J Neuroimmune Pharmacol. doi: 10.1007/s11481-016-9685-6.

Gomes, M.J., Martins, S. and Sarmento, B. 2015. siRNA as a tool to improve the treatment of brain diseases: mechanism, targets and delivery. Ageing Res Rev. 21: 43-54.

Gu, J., Hao, J., Fang, X. and Sha, X. 2016. Factors influencing the transfection efficiency and cellular uptake mechanisms of pluronic P123-modified polypropyleneimine/pDNA polyplexes in multidrug resistant breast cancer cells. Colloid Surface B. 140: 83-93.

Higuchi, K., Kitamura, A., Okura, T. and Deguchi, Y. 2015. Memantine transport by a proton-coupled organic cation antiporter in hCMEC/D3 cells, an in vitro human blood-brain barrier model. Drug Metab Pharmacokinet. 30 (2): 182-187.

Jahne, E.A., Eigenmann, D.E., Moradi-Afrapoli, F., Verjee, S., Butterweck, V., Hebeisen, S., Hettich, T., Schlotterbeck, G., Smiesko, M., Hamburger, M. and Oufir, M. 2016. Caco-2 permeability studies and in vitro hERG liability assessment of tryptanthrin and indolinone. Planta Med. 82 (13): 1192-1201.

Kim, Y.K., Kim, N.H., Hwang, J.W., Song, Y.J., Park, Y.S., Seo, D.W., Lee, H.Y., Choi, W.S., Han, J.W. and Kim, S.N. 2008. Histone deacetylase inhibitor apicidin-mediated drug resistance: involvement of P-glycoprotein. Biochem Bioph Res Co. 368 (4): 959-964.

Klein, S., Zolk, O., Fromm, M.F., Schrodl, F., Neuhuber, W. and Kryschi, C. 2009. Functionalized silicon quantum dots tailored for targeted siRNA delivery. Biochem Bioph Res Co. 387 (1): 164-168.

Lee, S.D., Osei-Twum, J.A. and Wasan, K.M. 2013. Dose-dependent targeted suppression of P-glycoprotein expression and function in Caco-2 cells. Mol Pharm. 10 (6): 2323-2330.

Li, L.M., Ruan, G.X., HuangFu, M.Y., Chen, Z.L., Liu, H.N., Li, L.X., Hu, Y.L., Han, M., Davidson, G., Levkin, P.A. and Gao, J.Q. 2015. ScreenFect A: an efficient and low toxic liposome for gene delivery to mesenchymal stem cells. Int J Pharm. 488: 1-11.

Mahringer, A., Ott, M., Reimold, I., Reichel, V. and Fricker, G. 2011. The ABC of the blood-brain barrier - regulation of drug efflux pumps. Curr Pharm Design. 17: 2762-2770.

Malmo, J., Sandvig, A., Varum, K.M. and Strand, S.P. 2013. Nanoparticle mediated P-glycoprotein silencing for improved drug delivery across the blood-brain barrier: a siRNA-chitosan approach. PLoS One. 8 (1): 1-8.

Mendes, B., Marques, C., Carvalho, I., Costa, P., Martins, S., Ferreira, D. and Sarmento, B. 2015. Influence of glioma cells on a new co-culture in vitro blood-brain barrier model for characterization and validation of permeability. Int J Pharm. 490: 94-101.

Muller, C., Laurent, G. and Ling, V. 1995. P-glycoprotein stability is affected by serum deprivation and high cell density in multidrug-resistant cells. J Cell Physiol. 163: 538-544.

Navarro, G., Sawant, R.R., Biswas, S., Essex, S., Tros de Ilarduya, C. and Torchilin, V.P. 2012. P-glycoprotein silencing with siRNA delivered by DOPE-modified PEI overcomes doxorubicin resistance in breast cancer cells. Nanomedicine (Lond). 7 (1): 65-78.

Nelissen, K., Smeets, K., Mulder, M., Hendriks, J.J. and Ameloot, M. 2010. Selection of reference genes for gene expression studies in rat oligodendrocytes using quantitative real time PCR. J Neurosci Methods. 187 (1): 78-83.

Neuhaus, B., Tosun, B., Rotan, O., Frede, A., Westendorfb, A.M. and Epple, M. 2016. Nanoparticles as transfection agents: a comprehensive study with ten different cell lines. RSC Adv. 6: 18102-18112.

Nimesh, S., Goyal, A., Pawar, V., Jayaraman, S., Kumar, P., Chandra, R., Singh, Y. and Gupta, K.C. 2006. Polyethylenimine nanoparticles as efficient transfecting agents for mammalian cells. J Control Release. 110 (2): 457-468.

Ota, S., Takahashi, Y., Tomitaka, A., Yamada, T., Kami, D., Watanabe, M. and Takemura, Y. 2013. Transfection efficiency influenced by aggregation of DNA/polyethylenimine max/magnetic nanoparticle complexes. J Nanopart Res. 15 (1653): 1-12.

Park, T.E., Singh, B., Li, H., Lee, J.Y., Kang, S.K., Choi, Y.J. and Cho, C.S. 2015. Enhanced BBB permeability of osmotically active poly(mannitol-co-PEI) modified with rabies virus glycoprotein via selective stimulation of caveolar endocytosis for RNAi therapeutics in Alzheimer's disease. Biomaterials. 38: 61-71.

Patil, Y.B., Swaminathan, S.K., Sadhukha, T., Ma, L. and Panyam, J. 2010. The use of nanoparticle-mediated targeted gene silencing and drug delivery to overcome tumor drug resistance. Biomaterials. 31 (2): 358-365.

Poller, B., Gutmann, H., Krähenbühl, S., Weksler, B., Romero, I.A., Couraud, P.O., Tuffin, G., Drewe, J. and Huwyler, J. 2008. The human brain endothelial cell line hCMEC/D3 as a human blood-brain barrier model for drug transport studies. J Neurochem. 107 (5): 1358-1368.

Pridgen, E.M., Alexis, F., Kuo, T.T., Levy-Nissenbaum, E., Karnik, R., Blumberg, R.S., Langer, R. and Farokhzad, O.C. 2013. Transepithelial transport of Fc-targeted nanoparticles by the neonatal fc receptor for oral delivery. Sci Transl Med. 5 (213): 1-8.

Qosa, H., LeVine, H., 3rd, Keller, J.N. and Kaddoumi, A. 2014. Mixed oligomers and monomeric amyloid-beta disrupts endothelial cells integrity and reduces monomeric amyloid-beta transport across hCMEC/D3 cell line as an in vitro blood-brain barrier model. Biochim Biophys Acta. 1842 (9): 1806-1815.

Ragnaill, M.N., Brown, M., Ye, D., Bramini, M., Callanan, S., Lynch, I. and Dawson, K.A. 2011. Internal benchmarking of a human blood-brain barrier cell model for screening of nanoparticle uptake and transcytosis. Eur J Pharm Biopharm. 77 (3): 360-367.

Rahme, K., Guo, J., Holmes, J.D. and O'Driscoll, C.M. 2015. Evaluation of the physicochemical properties and the biocompatibility of polyethylene glycol-conjugated gold nanoparticles: a formulation strategy for siRNA delivery. Colloid Surface B. 135: 604-612.

Sjostedt, N., Kortejarvi, H., Kidron, H., Vellonen, K.S., Urtti, A. and Yliperttula, M. 2014. Challenges of using in vitro data for modeling P-glycoprotein efflux in the blood-brain barrier. Pharm Res. 31 (1): 1-19.

Soares, S., Fonte, P., Costa, A., Andrade, J., Seabra, V., Ferreira, D., Reis, S. and Sarmento, B. 2013. Effect of freeze-drying, cryoprotectants and storage conditions on

the stability of secondary structure of insulin-loaded solid lipid nanoparticles. Int J Pharm. 456 (2): 370-381.

Stierle, V., Laigle, A. and Jolles, B. 2004. The reduction of P-glycoprotein expression by small interfering RNAs is improved in exponentially growing cells. Oligonucleotides. 14: 191-198.

Tam, V.H., Sosa, C., Liu, R., Yao, N. and Priestley, R.D. 2016. Nanomedicine as a non-invasive strategy for drug delivery across the blood brain barrier. Int J Pharm. 515: 331-342.

Wang, C.F., Sarparanta, M.P., Makila, E.M., Hyvonen, M.L., Laakkonen, P.M., Salonen, J.J., Hirvonen, J.T., Airaksinen, A.J. and Santos, H.A. 2015. Multifunctional porous silicon nanoparticles for cancer theranostics. Biomaterials. 48: 108-118.

Weksler, B., Romero, I.A. and Couraud, P.O. 2013. The hCMEC/D3 cell line as a model of the human blood brain barrier. Fluids Barriers CNS. 10 (16): 1-10.

Zimmermann, J.L., Nicolaus, T., Neuert, G. and Blank, K. 2010. Thiol-based, site-specific and covalent immobilization of biomolecules for single-molecule experiments. Nat Protoc. 5 (6): 975-985.

CHAPTER VI

General discussion, conclusions and future perspectives

1. General discussion and conclusions

Bioengineering, as a functional, innovative and trendy field, has been of growing importance for the pharmaceutical and biomedical research. Along with the progress of more fundamental fields, such as biology and biochemistry, which promote a deeper knowledge of human body function, the evolution of biotechnology is enticing modern society to believe in an improved efficiency of treatments. Indeed, drug and gene delivery systems, engineered to specifically target desired cells or tissues, are diamonds ready to be polished, that could become meaningful for the increasing incidence of central nervous system (CNS) disorders. Similarly, the development of membranes mimicking biological barriers, as blood-brain barrier (BBB), is of topmost significance to predict the *in vivo* behavior of delivery systems. Therefore, the rational of this thesis work followed a compromise between nanotechnology, BBB models and their interaction, in order to end up by achieving a successful optimized system for the modulation of drug efflux at the human BBB.

As discussed in this thesis work, nanoparticles based on lipid or polymeric matrices, already known for their ability to carry oligonucleotides, were implemented as an anti P-glycoprotein (P-gp) small interfering RNA (siRNA) protective and delivery system. These carriers were further surface-modified, through polyethylene glycol coating (PEGylation) and receptor-targeted functionalization, to upgrade their functional characteristics. Simultaneously, the development of BBB models, phospholipid- and cell-based ones, enabled the assessment of nanoparticles feasibility and potential, as well as their ability to interact with human brain endothelial cells and inflect brain-to-blood drug efflux.

Therefore, firstly, a new BBB phospholipid-based model was implemented through a phospholipid vesicle-based permeability assay (PVPA) method. BBB-PVPA, made of a phosphatidylcholine and phosphatidylethanolamine mixture, only addressed passive transcellular-like diffusion and intended to be an alternative and/or complement to cellular models. Membranes produced through this method were easy to develop by a short-time consuming protocol, leading to similar permeability data as other *in vitro* BBB models. These advantages light up this model as an excellent way for high throughput screening of permeability properties. Thus, potential drug/nanosystem candidates, early in the development process, could be screened using this model, inspiring a pre-selection of the best drug/nanosystem before continue to *in vitro* and *in vivo* studies. One of the main objectives of the barrier developed through this method was to enable results extrapolation and prediction. Consequently, it was used to test the permeability of siRNA, as a free

biomolecule and loaded in simple lipid (Witepsol E85) and polymeric (poly(lactic-co-glycolic acid); PLGA) nanoparticles.

To promote BBB crossing, it is often argued that the ideal size for a non-targeted system is up to 200 nm (Chen *et al.*, 2004). Thus, rapidly uptake by the reticuloendothelial system is avoided and, therefore, blood circulation time and nanoparticles contact time with the BBB are increased (Chen *et al.*, 2004; Kaur *et al.*, 2008). Developed siRNA-loaded nanoparticles accomplished this prerequisite since they had a mean size of 140 nm and were slightly negative (-10 mV). In general, nanocarriers, especially solid lipid nanoparticles (SLN), improved the siRNA transport across the non-cellular barrier. Their hydrophobic composition with high affinity to lipid membranes made of liposomes enabled siRNA permeability to increase from 10% (free-siRNA) to 14 and 19% (siRNA-loaded polymeric and lipid nanoparticles, respectively). Therefore, nanoparticles were found to be able to interact with BBB-PVPA liposomes, passively crossing the barrier, revealing capability to interact with BBB-like cellular membranes. Afterwards, nanoparticles were improved by changing the surfactant and combining an additional lipid/polymer envisioning further functionalization processes. siRNA reached association efficiency (AE) of 50% for the polymeric systems and 31% for the selected SLN, while retaining a prolonged release from nanoparticles matrices (60% released after 24h). Two distinct chemical approaches, carbodiimide and maleimide, promoted surface modification with a peptide against transferrin-receptor (TfR), which was physicochemical confirmed by the increase of mean particles size and by nuclear magnetic resonance peptide-related new peaks. Most importantly, the interaction between human brain endothelial cells and non-cytotoxic nanoparticles, evaluated through fluorescence microscopy and flow cytometry, revealed that functionalization improved 4-fold the capability of polymeric nanoparticles to interact with cells. Hence, polymeric nanocarriers have proved to be crucial to potentiate siRNA efficiency, by promoting its targeted brain delivery and subsequent uptake. More specifically, the maleimide functionalization of a polymeric system, developed with both PLGA and PLGA-PEG amine terminated, improved siRNA permeability (2-fold) through a BBB cell-based model, compared to non-functionalized systems. This same system led to 52% reduction of P-gp messenger RNA (mRNA) expression in human brain endothelial cells 96h post transfection, which drove to a 17% increase of rhodamine 123, as a P-gp substrate, permeability.

As siRNA permeability was tested in two distinct BBB models, the final comparison between obtained results is imperative. On one hand, permeability of free-siRNA was similar for BBB-PVPA and cell-based model, indicating that PVPA was a good method to predict the permeability of a biomolecule as siRNA and, potentially, other biopharmaceutical hydrophilic drugs. On the other hand, the same trend was not observed for siRNA when loaded in

nanoparticles. When BBB-PVPA was used, siRNA-PLGA nanoparticles had apparent permeability values around 5.5×10^{-6} cm s^{-1}, which were higher than the ones obtained for the cell-based model, $4.0 – 8.5 \times 10^{-7}$ cm s^{-1}. Among the factors that could explain this difference are the BBB-PVPA membrane hydrophobicity and the biochemistry complexity of BBB cells. Since BBB-PVPA consisted of liposomes, lacking any hydrophilic structure as cytoplasm or extracellular matrix, this membrane was more hydrophobic than the cell-based one, which could cause an increased affinity and interaction with apolar nanoparticles, leading to higher siRNA-loaded permeability. Although the selected BBB-PVPA barrier reached transendothelial electrical resistance values above 2,000 Ωcm^2 on the same day of production, these also highly decreased on 50% during the permeability experiment, meaning that tested drugs/molecules may open some spaces within the membrane. That may actually caused an augment of the paracellular permeability of molecules and justify the difference obtained for siRNA-loaded nanoparticles on BBB-PVPA *versus* BBB cell-based model. Moreover, other possible reason is related to the difference of tested nanoparticles on both models. Developed systems were improved along the project, by changing the surfactant and surface functionalization, which led them to become larger and that could have reduced their ability to permeate the membrane. Finally, as a biologic system, cell-based membrane addressed both passive and active transports. As so, it also had other obstacles (missing on the BBB-PVPA model) that nanoparticles needed to overcome, which may have hampered their crossing ability.

Through functionalization, nanoparticles were targeted to the TfR which is over expressed at the BBB. This receptor is both temperature and energy dependent (Harding *et al.*, 1983). When uptaking transferrin, as well as other possible ligands such functionalized nanoparticles, TfR is also internalized. It is well known that TfR involves clathrin-mediated endocytosis (Damm *et al.*, 2005; Fekri *et al.*, 2016). Thus, functionalized nanoparticles get in the cells through binding and receptor activation. The complex TfR plus nanoparticles diffuses through the plasma membrane and is captured by a forming clathrin-coated pit that then forms a clathrin-coated vesicle which will fuse to an early endosome. After this, the receptor is recycled back to the plasma membrane, which normally requires previous passage through early endosomes and recycling endosomes (Harding *et al.*, 1983; Sheff *et al.*, 2002; van Dam *et al.*, 2002). Consequently, TfR recycling enables the continuous internalization of functionalized nanoparticles.

Subsequently, after a successful siRNA transport until reach the brain endothelial cells due to nanoparticles engineering, siRNA is released from its biodegradable carriers. This stage is a key step for the oligonucleotide since, during its intracellular trafficking into the cytoplasm, it has to escape from endosomes and avoid lysosomes to be able to silence its

target protein (Ma, 2014). However, since clathrin-mediated endocytosis commonly directs the entry agent to lysosomal compartments (Rejman *et al.*, 2005), most likely, some of P-gp-siRNA was degraded by the lysosomal content, where various nucleases within an acidic environment are located. The efficient and successful siRNA, that circumvented these vesicles and went to the cytosol, can then associate with the RNA-induced silencing complex (RISC), directing the cleavage of mRNA complementary sequences (Fountaine *et al.*, 2005; Martinez and Tuschl, 2004).

When loaded in functionalized polymeric nanoparticles, P-gp-siRNA has silenced 52% of P-gp mRNA expression in human brain endothelial cells, 96h post transfection. Therefore, it is hypothesized that P-gp production was not completely depleted. Although not being the presumed theoretical goal of such assay, it was somehow a plus. Indeed, normal cell trafficking, as metabolites excretion, involves P-gp transport (Thiebaut *et al.*, 1987). Moreover, P-gp-siRNA treatments promote a transient P-gp down-regulation. After treatment interruption and according to P-gp turnover, the silencing effect is discontinued and P-gp production comes back to normal (Gomes *et al.*, 2015).

Overall, this project ended up with an efficient TfR-targeted anti-P-gp siRNA-loaded nanosystem whose promising results pointed out that it could be the trigger to down-regulate P-gp at the BBB, ending with numerous drug reaching brain advantages. Consequently, any P-gp substrate drug that is desired to achieve the CNS in therapeutic concentrations would benefit from this transient opportunity. Concomitantly, the giant power of this siRNA against P-gp system could be translated to other fields as cancer, by addressing drug-resistance in tumors characterized as P-gp over expressing tissues, through simply adjusting the targeting ligands attached to the nanoparticles surface.

2. Future perspectives

Nanoparticles developed to carry siRNA to a specific location arise through the convergence of bioengineering, technology and pharmaceutical fields to fill medicine needs. This was exactly the great goal of this thesis work, achieved by the refinement of a siRNA delivery system designed to surpass BBB obstacles. Nonetheless, when caught by the scientific research area, the possibilities for “what you can do next” are endless. The continuous knowledge evolution does not allow future perspectives to decline.

siRNA-loaded carriers may still be improved by enhancing its AE and refining its release profile. Through siRNA association with natural polyamines (like spermidine and putrescine), which are small positive charged molecules that strongly bind to negative phosphate groups from nucleic acids, the oligonucleotide become more stable and robust. Hence, complexed siRNA association to nanoparticles happens to be stronger and its release from them harder to attain. As demonstrated on previous studies (Woodrow *et al.*, 2009), we have already obtained promising preliminary results where PLGA nanoparticles with higher AE were produced after complex siRNA with polyamines. siRNA AE increased, from 50% to 55% and 67%, when spermidine and putrescine were used, respectively. Accordingly, these systems attained an interesting siRNA release profile, mainly characterized by a diminished initial burst release. Complexed siRNA could be advantageous in different ways, however, due to these molecules amine composition, toxicity arises as a serious possible problem. Therefore, assays regarding their cytotoxicity and further transfection efficiency should be performed.

Unlike clathrin-mediated endocytosis, the caveolae-dependent endocytosis could bypass lysosomes, avoiding entry molecules degradation (Kou *et al.*, 2013). Therefore, a topic that could be further explored is the nanoparticles targeting mechanism. Using a ligand that targets a caveolae-dependent receptor, the siRNA early degradation would be circumvented. At the BBB, low density lipoprotein receptors are proposed to operate through the caveolar mechanism (Georgieva *et al.*, 2014), which makes apolipoprotein E a great promising ligand for nanoparticles surface.

Still regarding nanosystems production, an interest aspect that could be optimized is adapting the production method to smooth the progress of its scale-up to an industrial level. Replacing double emulsion conventional method with microfluidics technique could be a great bottom line to also reduce the production time.

Furthermore, anti-P-gp siRNA silencing efficiency evaluation may be deeper assessed, besides the P-gp mRNA expression. Following the transcription and translation path, P-gp levels should also be determined through Western Blot analysis. Thus, the functional assay timing could be updated regarding the post transfection time when the protein itself is silenced and less expressed.

Moreover, translate this approach to an *in vivo* study would be the icing on the cake. Healthy adult male Wistar rats would be intravenously administered with free-siRNA or siRNA-loaded nanoparticles prior to a P-gp substrate (as paclitaxel or rhodamine 123) administration. Afterwards, rats would be euthanized at different time points, followed by brain removal, P-gp substrate detection, mRNA and protein extraction and quantification.

Immunohistochemistry on brain histological slides would also monitor P-gp expression reduction. As reported by *in vitro* results, drug accumulation in the brain is expected to increase in rats injected with TfR-targeted siRNA-loaded nanoparticles. After the *in vivo* proof of concept, the therapeutic relevance of modulating the BBB efflux with developed siRNA carriers could, in the future, be determined through simultaneous administration of these nanoparticles with anticancer compounds in rats with induced brain tumors, or neuroprotective agents in rats with induced stress.

Finally, regarding cancer as one of the most central research fields nowadays, the developed siRNA against P-gp system may be applied to cancer-related therapy. This could have great advantages due to the known drug-resistance in tumors characterized as P-gp over expressing tissues. By adjusting the targeting ligands attached to the nanoparticles surface, different targets could be addressed.

As hereby described, several aspects are ready to be optimized pursuing successful and effective targeted anti-P-gp siRNA delivery systems.

3. References

Chen, Y., Dalwadi, G. and Benson, H.A. 2004. Drug delivery across the blood-brain barrier. Curr Drug Deliv. 1 (4): 361-376.

Damm, E.M., Pelkmans, L., Kartenbeck, J., Mezzacasa, A., Kurzchalia, T. and Helenius, A. 2005. Clathrin- and caveolin-1-independent endocytosis: entry of simian virus 40 into cells devoid of caveolae. J Cell Biol. 168 (3): 477-488.

Fekri, F., Delos Santos, R.C., Karshafian, R. and Antonescu, C.N. 2016. Ultrasound microbubble treatment enhances clathrin-mediated endocytosis and fluid-phase uptake through distinct mechanisms. PLoS One. 11 (6): 1-22.

Fountaine, T.M., Wood, M.J.A. and Wade-Martins, R. 2005. Delivering RNA interference to the mammalian brain. Curr Gene Ther. 5: 399-410.

Georgieva, J.V., Hoekstra, D. and Zuhorn, I.S. 2014. Smuggling drugs into the brain: an overview of ligands targeting transcytosis for drug delivery across the blood-brain barrier. Pharmaceutics. 6: 557-583.

Gomes, M.J., Martins, S. and Sarmento, B. 2015. siRNA as a tool to improve the treatment of brain diseases: mechanism, targets and delivery. Ageing Res Rev. 21: 43-54.

Harding, C., Heuser, J. and Stahl, P. 1983. Receptor-mediated endocytosis of transferrin and recycling of the transferrin receptor in rat reticulocytes. J Cell Biol. 97 (2): 329-339.

Kaur, I.P., Bhandari, R., Bhandari, S. and Kakkar, V. 2008. Potential of solid lipid nanoparticles in brain targeting. J Control Release. 127 (2): 97-109.

Kou, L., Sun, J., Zhai, Y. and He, Z. 2013. The endocytosis and intracellular fate of nanomedicines: implication for rational design. Asian J Pharm Sci. 8 (1): 1-10.

Ma, D. 2014. Enhancing endosomal escape for nanoparticle mediated siRNA delivery. Nanoscale. 6 (12): 6415-6425.

Martinez, J. and Tuschl, T. 2004. RISC is a 5' phosphomonoester-producing RNA endonuclease. Genes Dev. 18: 975-980.

Rejman, J., Bragonzi, A. and Conese, M. 2005. Role of clathrin- and caveolae-mediated endocytosis in gene transfer mediated by lipo- and polyplexes. Mol Ther. 12 (3): 468-474.

Sheff, D., Pelletier, L., O'Connell, C.B., Warren, G. and Mellman, I. 2002. Transferrin receptor recycling in the absence of perinuclear recycling endosomes. J Cell Biol. 156 (5): 797-804.

Thiebaut, F., Tsuruo, T., Hamada, H., Gottesman, M.M., Pastan, I. and Willingham, M.C. 1987. Cellular localization of the multidrug-resistance gene product P-glycoprotein in normal human tissues. Proc Natl Acad Sci USA. 84: 7735-7738.

van Dam, E.M., Ten Broeke, T., Jansen, K., Spijkers, P. and Stoorvogel, W. 2002. Endocytosed transferrin receptors recycle via distinct dynamin and phosphatidylinositol 3-kinase-dependent pathways. J Biol Chem. 277 (50): 48876-48883.

Woodrow, K.A., Cu, Y., Booth, C.J., Saucier-Sawyer, J.K., Wood, M.J. and Saltzman, W.M. 2009. Intravaginal gene silencing using biodegradable polymer nanoparticles densely loaded with small-interfering RNA. Nat Mater. 8: 526-533.